



UNIVERSITÀ DEGLI STUDI DI
FIRENZE

Facoltà di Scienze Matematiche, Fisiche e Naturali
Dipartimento di Matematica e Informatica “Ulisse Dini”

Dottorato di Ricerca in Matematica

**Grid Homology in Lens
Spaces**

Candidato:
Daniele Celoria

Tutor:
Prof. Graziano Gentili

Relatore:
Prof. Paolo Lisca

Ciclo XXVIII, Settore Scientifico Disciplinare MAT/03

Introduction

Ozsváth and Szabó's Heegaard Floer homology [41] is undoubtedly one of the most powerful tools of recent discovery in low dimensional topology. It has far reaching consequences and has been used to solve long standing conjectures (for a survey of some results see [43]).

It associates¹ a graded group to a closed and oriented 3-manifold Y , the *Heegaard Floer homology* of Y , by applying a variant of Lagrangian Floer theory in a high dimensional manifold determined by an Heegaard decomposition of Y .

Soon after its definition, it was realized independently in [39] and [49] that a knot $K \subset Y$ induces a filtration on the complex whose homology is the Heegaard Floer homology of Y . Furthermore the filtered quasi isomorphism type is an invariant of the couple (Y, K) , denoted by $HFK(Y, K)$.

The major computational drawback of these theories lies in the differential, which is defined through a count of pseudo-holomorphic disks with appropriate boundary conditions.

Nonetheless, a result of Sarkar and Wang [53] ensures that, after a choice of a suitable doubly pointed Heegaard diagram \mathcal{H} for (Y, K) , the differential can be computed directly from the combinatorics of \mathcal{H} . If moreover Y is a rational homology 3-sphere such that $g(Y) = 1$ (*i.e.* $Y = S^3$ or $L(p, q)$), the whole complex $HFK(Y, K)$ admits a neat combinatorial definition, known as *Grid homology*.

Grid homology in S^3 was pioneered by Manolescu, Ozsváth and Sarkar in [29], and for lens spaces by Baker, Hedden and Grigsby in [4]. It is denoted by $GH(Y, K)$ where Y is either S^3 or a lens space, and K is a knot in Y . As the name suggests both the ambient manifold and the knot K are encoded in a grid, from which complex and differential for the grid homology can be extracted by simple combinatorial computations.

¹There are actually many different variants of the theory, which we ignore presently; in the following Sections we will define some variants which will be relevant throughout the discussion.

The aim of this Thesis is threefold: first we are going to generalize the existing theory of grid homology for links in lens spaces through a coefficient extension; we are then going to describe a `soige` program capable of computing such sign refined extension. Finally we are going to detail several instances where the grid homology for links in lens spaces provides new insight, or is used to produce combinatorial proofs of known results.

The thesis is structured as follows:

Chapter 1 gives an introduction on some properties of links in lens spaces, and shows how to obtain a diagrammatic representation through the use of *grid diagrams*. This chapter contains also the definitions of Heegaard decomposition, $Spin^c$ structures and some polynomial invariants, which will be used extensively throughout the thesis.

Chapter 2 gives the relevant definitions of Heegaard Floer and Knot Floer homology, and shows how grid homology can be interpreted as its combinatorial counterpart. It provides an entirely combinatorial and (almost) self-contained introduction to grid homology for knots in lens spaces, for the *hat*, *minus* and *tilde* graded versions. We also present here some structure results for the grid homology of certain classes of knots, together with the behaviour of $GH(L(p, q), K)$ under orientation reversal of K (Proposition 2.27).

Chapter 3 presents the combinatorial extension for the coefficients of the ground ring from \mathbb{F}_2 to \mathbb{Z} . This part is drawn from the author's preprint [12]. Here we show how to employ the $Spin$ central extension of the permutation group to prove existence and uniqueness of the sign refined theory (Theorem 3.2), and compute it on a small example.

Chapter 4 displays the interplay between several aspects of the theory and 4-dimensional notions. We define concordances between knots in lens spaces and a related notion of genus. Then, after introducing an action of concordances of knots in the 3-sphere on concordances in arbitrary lens spaces, we define *almost-concordances* of knots and *genuine* knots. We prove that all knots in lens spaces are concordant to genuine knots (Theorem 4.7) and introduce the τ -invariants. In Section 4.2 we prove that these τ -invariants provide a lower bound on the genus of cobordism between knots in lens spaces (Theorem 4.14); furthermore, we introduce a move on mixed diagrams, the *snatch*, and propose a way in which these invariants might be used to provide new bounds on the slice genus of knots in S^3 . In Section 4.3 we show that

the equivalence relation given by almost-concordance is nontrivial, by showing how to distinguish some classes using modified versions of the τ invariant, the τ -shifted invariant. The contents of this Chapter have been subsequently generalized in my paper [13].

In **Chapter 5** we discuss three other situations in which grid homology can give some useful insight. We start by introducing two analogues of the Seifert genus for rationally nullhomologous knots in rational homology spheres, and use the detection of these genera by the grid homology to compute the values of the Θ function introduced in [56] by Turaev for the lens spaces $L(p, 1)$.

We then study the decategorification(s) χ_t of \widehat{GH} and show some of its properties (Proposition 5.22) which are analogous to the ones exhibited by the classical Alexander polynomial for knots in the 3-sphere. We define a family of invariants for links in lens spaces introduced by Cornwell in [10], which generalize the classical HOMFLYPT polynomial. Then we show (Theorem 5.26) that, after the choice of a suitable normalization, the polynomials χ_t coincide with a specialization of this HOMFLYPT polynomial, hence they provide the same generalization of the Alexander polynomial to links in lens spaces.

Finally we present the reformulation of the Berge conjecture in terms of grid homology of knots in lens spaces, due to Hedden and Rasmussen. We show how to prove (Propositions 5.35 and 5.41) that no counterexamples to the conjecture can originate from grid number 2 knots, and from *generalized torus knots*, introduced in Definition 5.39.

Lastly, in **Chapter 6**, we are going to present some programs developed by the author during the course of the Phd, which compute the grid homology of knots and links in lens spaces. These tools allowed us to prove, analogously to what was done in [16], that knots with small parameters have torsion-free knot Floer homologies. We display some sample computations for small knots in Subsection 6.2.1.

Acknowledgements. I would like to warmly thank my advisor Paolo Lisca for the constant support and András Stipsicz for suggesting this interesting topic. I also want to thank Marco Golla for teaching me everything I always wanted to know about Floer Homology, and Paolo Aceto, Francesco Lin, Stefano Riolo, Leone Slavich and Enrico Manfredi for stimulating conversations. A special mention goes to Agnese Barbensi and my family, who helped and encouraged me during the

writing of this thesis. I also acknowledge the Mathematics Department of Pisa for the computational time.

Contents

Introduction	3
Chapter 1. Preliminaries	9
1.1. Knot theory and Lens spaces	9
1.2. Representing links with grids	17
Chapter 2. Grid homology	23
2.1. Heegaard Floer homology	23
2.2. Knot Floer homology	28
2.3. From holomorphic to combinatorial	34
2.4. Grid homology in lens spaces	36
Chapter 3. Sign refined theory	51
Chapter 4. 4-dimensional aspects	61
4.1. Definitions	61
4.2. Genus bounds	66
4.3. Related constructions	72
Chapter 5. Applications	81
5.1. Turaev's Θ function for $L(p, q)$	81
5.2. Cornwell's polynomial and decategorification	88
5.3. Some restrictions on the Berge Conjecture	95
Chapter 6. Computations	105
6.1. The programs	105
6.2. Examples	108
Bibliography	111

CHAPTER 1

Preliminaries

1.1. Knot theory and Lens spaces

In the following, if not otherwise specified, Y will always denote a closed, oriented and connected 3-manifold. Furthermore we are going to require that $H_*(Y; \mathbb{Q}) \cong H_*(S^3; \mathbb{Q})$ as graded rings; we will often refer to such a Y as a *rational homology 3-sphere*, or $\mathbb{Q}HS^3$ for brevity.

It is a classical result in low dimensional topology, that all 3-manifolds can be obtained by gluing two genus g handlebodies H_1, H_2 along their boundary Σ_g by a diffeomorphism $\phi : \Sigma_g \rightarrow \Sigma_g$. This decomposition is known as *Heegaard decomposition*. It can be shown that the result of the attachment is uniquely determined once we know the image of a set of g disjoint simple curves on Σ_g under the map ϕ , provided that these curves are independent in $H_1(\Sigma_g; \mathbb{Z})$.

Equivalently we can represent a 3-manifold as a genus g surface with two sets of g simple disjoint closed curves α and β , as shown in Figure 1.1. We require that $\alpha_i \cap \alpha_j = \beta_i \cap \beta_j = \emptyset$ for $i \neq j$, and that all intersections are transversal. We obtain a 3-manifold from such a picture by taking the product $\Sigma_g \times [0, 1]$, and gluing thickened disks $\mathbb{D}^2 \times \mathbb{D}^1$ to the curves α along $\Sigma_g \times \{0\}$, and to the β curves along $\Sigma_g \times \{1\}$. The gluing of the disks identifies $S^1 \times \{0\}$ with each α/β curve. After this process we obtain a 3-manifold with S^2 boundary components, which can be uniquely filled with \mathbb{D}^3 s to obtain a closed 3-manifold. The triple $(\Sigma_g, \alpha, \beta)$ is known as *an Heegaard diagram* for the 3-manifold it represents.

Clearly a fixed 3-manifold admits infinitely many distinct Heegaard diagrams; however it can be proved that two Heegaard diagrams representing the same 3-manifold are connected by a finite sequence of elementary moves¹. The minimal genus of a splitting surface among all Heegaard diagrams for Y is called the *genus* of Y .

There is a particular class of $\mathbb{Q}HS^3$ s which is particularly simple from the point of view of Heegaard splittings; these are the *lens spaces*, denoted by $L(p, q)$. These are the only $\mathbb{Q}HS^3$ which can be obtained

¹See [41] for a complete list of these moves in a slightly more general context.

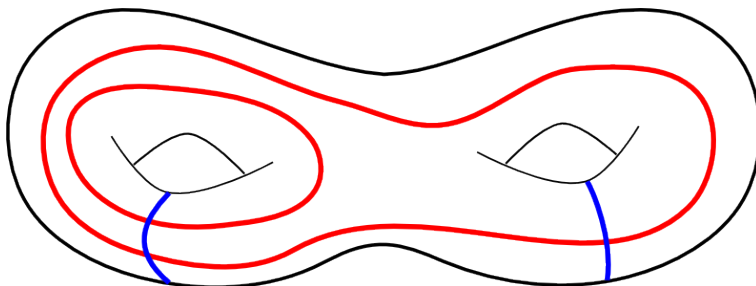


FIGURE 1.1. An Heegaard decomposition, described by two sets of handle attachments to a genus 2 surface.

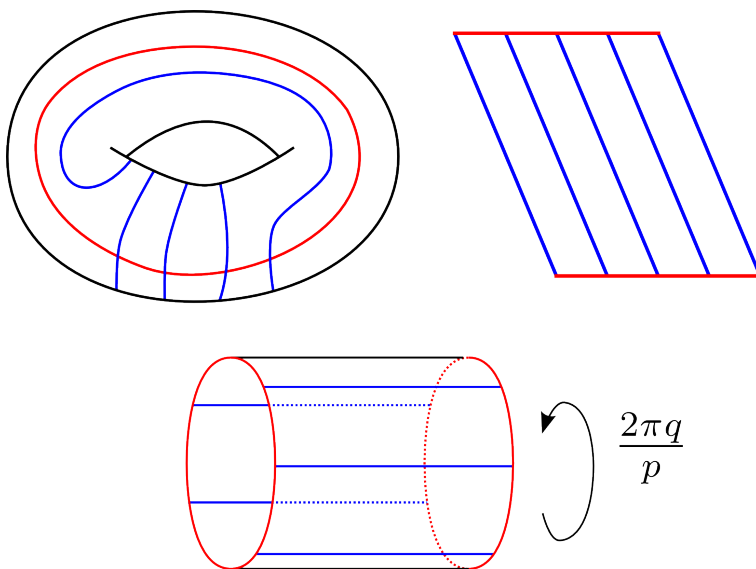


FIGURE 1.2. Three presentations for the minimal (with respect to the number of curves and intersections) Heegaard diagram of lens spaces; on the top-left the genus 1 splitting, on the top-right a planar representation (the slope of the blue lines for $L(p, q)$ is $-\frac{p}{q}$), and in the lower part another way to look at the identifications.

by a genus 1 Heegaard decomposition. Choose two coprime integers $p > q > 0$, and define $L(p, q)$ as the 3-manifold described by the Heegaard diagram of Figure 1.2.

The diagram is a torus $S^1 \times S^1$ with a meridian α and a longitude β which intersects α p times. In terms of the standard² basis $\{\mu, \lambda\}$ the longitude is the $-p\mu + q\lambda$ simple closed curve.

In particular when $p = 1$ and $q = 0$ we get a Heegaard diagram for S^3 . Since the complement of an unknotted solid torus in S^3 is diffeomorphic to another unknotted solid torus, it is immediate to see that all lens spaces can be obtained by Dehn surgery on the unknot $\bigcirc \subset S^3$. According to the convention we choose, $L(p, q) = S^3_{-\frac{p}{q}}(\bigcirc)$.

The only interesting homology of a lens space sits in degree 1:

$$H_1(L(p, q); \mathbb{Z}) \cong \mathbb{Z}/p\mathbb{Z}$$

so lens spaces with different p parameters are automatically not homotopy equivalent. However given two lens spaces $L(p, q)$ and $L(p, q')$ with $q \neq q'$, these might be homeomorphic. The classification of homeomorphism/homotopy classes of lens spaces was first carried out by Reidemeister in 1935, and more recently with elementary techniques by Przytycki and Yasukhara in [48].

THEOREM 1.1. *Two lens spaces $L(p, q)$ and $L(p, q')$ are:*

- *homotopy equivalent* iff $qq' \equiv \pm n^2 \pmod{p}$ for some³ $n \in \mathbb{N}$
- *homeomorphic* iff $q' \equiv \pm q^{\pm 1} \pmod{p}$

An alternative description of lens spaces is as quotients of $S^3 = |z_1|^2 + |z_2|^2 = 1 \subset \mathbb{C}^2$ under the action of the map

$$(1) \quad \pi_{p,q} : (z_1, z_2) \mapsto \left(e^{\frac{2\pi i}{p}} z_1, e^{\frac{2\pi i q}{p}} z_2 \right)$$

In the next chapters we are going to use the inverse of this map to lift links from $L(p, q)$ back to S^3 .

There is yet another way to describe lens spaces, this time as boundaries of compact 4-manifolds. Given the coprime integers p and q there is a unique way of representing the rational number $\frac{p}{q}$ as a *continued fraction*:

$$\frac{p}{q} = a_0 - \frac{1}{a_1 - \frac{1}{a_2 - \frac{1}{a_3 - \dots - \frac{1}{a_m}}}}$$

²Where λ here stands for the Seifert longitude of the embedded splitting torus, seen as the boundary of a neighborhood of the unknot.

³Notational remark: unless otherwise specified, $m \pmod{p}$ will denote the minimal positive representative.

with $a_i > 1$ for all $i > 0$. In this case we will write $\frac{p}{q} = [a_0, \dots, a_m]$. Then the lens space $L(p, q)$ is the boundary of the four manifold $W_{p,q}$ obtained by adding m 2-handles to the 4-ball along the framed link in $S^3 = \partial\mathbb{D}^4$ shown in Figure 1.3.

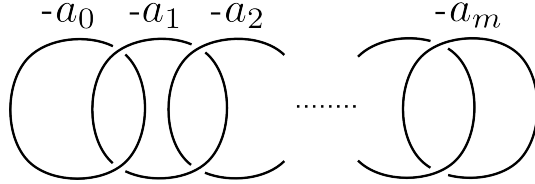


FIGURE 1.3. A Kirby diagram for the 4-manifold $W_{p,q}$.

In particular $W_{p,1}$ can be represented by a Kirby diagram⁴ composed by only one unknot with framing $-p$. Other alternative descriptions of lens spaces can be found *e.g.* in [51].

We briefly introduce spin^c structures, which will be useful in the next chapters. The approach we are going to adopt relies on Turaev's definition [55] of $\text{spin}^c(Y)$ for a closed 3-manifold Y .

DEFINITION 1.2. *Two nowhere vanishing vector fields on a closed 3-manifold Y are homologous if they are homotopic outside a 3-ball, through nowhere vanishing vector fields. A spin^c structure on Y is given by the homology class of a non-singular vector field.*

Note that the existence of non singular vector fields on an arbitrary 3-manifold Y is a consequence of the fact that $\chi(Y) = 0$. There is an action of $H^2(Y; \mathbb{Z})$ on the set of spin^c structures on Y which will be useful later on: fix a trivialization τ of the tangent bundle TY , so that non-singular vector fields v are in correspondence with maps $f_v : Y \rightarrow S^2$. Now define $\delta^\tau(v) = f_v^*([S^2]) \in H^2(Y; \mathbb{Z})$, where $[S^2]$ is the fundamental class of the sphere. δ^τ gives a bijection $\text{Spin}^c(Y) \leftrightarrow H^2(Y; \mathbb{Z})$; moreover if $H^2(Y; \mathbb{Z})$ contains no 2-torsion, δ^τ is independent of the trivialization, and in all cases the difference $\delta(v_1, v_2) = \delta^\tau(v_1) - \delta^\tau(v_2)$ does not depend on τ . There is a natural involution on $\text{spin}^c(Y)$, denoted by J , which sends the homology class of a non-singular vector field v to the class of its opposite $-v$. We also briefly mention that we can define the evaluation of the first Chern class c_1 on $\mathfrak{s} \in \text{spin}^c(Y)$ as $c_1(\mathfrak{s}) = \mathfrak{s} - J\mathfrak{s} \in H^2(Y; \mathbb{Z})$. We will say that $\mathfrak{s} \in \text{spin}^c(Y)$ is *torsion* if the image under c_1 is a torsion element of $H^2(Y; \mathbb{Z})$.

We are going to adopt the conventions of [36], and thus often identify

⁴For the relevant definitions an excellent source is [19].

$\text{spin}^c(L(p, q))$ with \mathbb{Z}_p in a fixed manner (cf. also Definition (15)).

We can now introduce a class of submanifolds of lens spaces which will be the main protagonist of this dissertation, that is links.

A m -component link $L \subset L(p, q)$ is just going to be the isotopy class of an embedding

$$\iota : \bigsqcup^m S^1 \longrightarrow L(p, q)$$

If $m = 1$ we will call L a *knot* (and usually will denote it by K to remark the difference). To avoid confusion, a knot in a 3-manifold Y will be usually denoted by (Y, K) ; a tubular neighborhood of K in Y will be denoted by $\nu(K)$. We are also going to denote by $\mathcal{L}(Y)$ and $\mathcal{K}(Y)$ the set of (respectively) oriented links and knots in Y .

The main difference with respect to links in S^3 is that a link in $L(p, q)$ can be non homologically trivial. In fact each link can be thought as a representative of its homology class. We will write $[L] = m \in H_1(L(p, q); \mathbb{Z})$ if L represents the class m . A link L representing the trivial class will be called *nullhomologous*; in this case L is the boundary of an embedded surface in $L(p, q)$. A particular class of nullhomologous knots is provided by *local knots*; this are knots which are contained in an embedded 3-ball inside $L(p, q)$. Clearly a local knot is nullhomologous, but the converse is false (even more than one might initially think, see example 4.13). A knot will be called *primitive* if its associated homology class generates $H_1(L(p, q); \mathbb{Z})$.

In each 3-manifold there is only one local knot which bounds an embedded disk; we will call it *trivial knot* and denote it by \bigcirc . In the case of lens spaces there is a generalization of the trivial knot to non-zero homology classes, the *simple knots*. Being homologically non trivial these knots, with the exception of \bigcirc , do not bound disks; as we will see in Section 2.4.3 however, they are in a precise sense the simplest knots in each homology class.

The first homology of the complement of an m -component link in S^3 is simply \mathbb{Z}^m ; for lens spaces there is an analogous result:

LEMMA 1.3 ([8]). *Let $L = \bigsqcup_{i=1}^m L_i \subset L(p, q)$ be an m -component link. Write $\delta_i = [L_i]$ for $i = 1, \dots, m$ and $d = \text{gcd}\{\delta_1, \dots, \delta_m, p\}$; then*

$$H_1(L(p, q) \setminus \nu(L); \mathbb{Z}) = \mathbb{Z}^m \oplus \mathbb{Z}/d\mathbb{Z}$$

In particular the complement of a primitive knot has torsion-free homology.

If a knot is not nullhomologous, call t the order of the homology class it represents in $H_1(L(p, q); \mathbb{Z})$. Push the knot on the boundary of

a tubular neighborhood and take t parallel copies of this pushoff. Then the resulting link is nullhomologous, and hence it bounds an embedded surface. This fact will be useful when giving a definition of genus for such knots in Chapter 4.

Apart from the homology class they represent, there is another natural invariant for links in $L(p, q)$, namely their preimage in S^3 under the map $\pi_{p,q}$ of Equation (1). Invariants that distinguish two knots with the same lift to S^3 are called *essential*. It is proved in [7] that the groups \widehat{GH} we will define later on are in fact essential.

Many operations which are naturally well defined for knots in the 3-sphere do not have counterparts for knots in lens spaces. Typical examples are the connected sum and disjoint union: if we take the connected sum⁵ of two knots $(L(p, q), K) \# (L(p', q'), K')$ the result is a knot inside $L(p, q) \# L(p', q')$ which is not a lens space, unless at least one of the summands is the three sphere. Similarly, if both the knots are not local, the notion of disjoint sum is ill defined, since there is no sphere which can separate them.

The study of knots and links in lens spaces, besides its intrinsic interest, can give insights into the classical theory: for example it is easily shown that rational Dehn surgery on a knot in the three sphere corresponds (after a suitable Rolfsen twist) to a Morse⁶ surgery on an induced knot in a lens space. The induced knot is the image of the original knot under the surgery. More precisely:

$$S_{\frac{p}{q}}^3(K) = L(q, r)_a(K')$$

with $a = \left\lfloor \frac{p}{q} \right\rfloor$ and $\frac{p}{q} = a + \frac{r}{q}$. In this case

$$(L(q, r), K') = (S^3, K) \# (L(q, r), T^{p,q})$$

where $T^{p,q}$ can be described as the knot induced by one component of the Hopf link, after performing a $\frac{r}{q}$ surgery on the other component.

In a somehow different vein, if one obtains a lens space upon performing surgery on $K \subset S^3$, the core of the filled torus gives an induced knot $\tilde{K} \subset L(p, q)$. Since lens spaces are the simplest 3-manifold, it is

⁵We will however define a restricted notion of connected sum in Chapter 4.

⁶That is, surgery with integer coefficient, which admits a straightforward 4-dimensional interpretation.

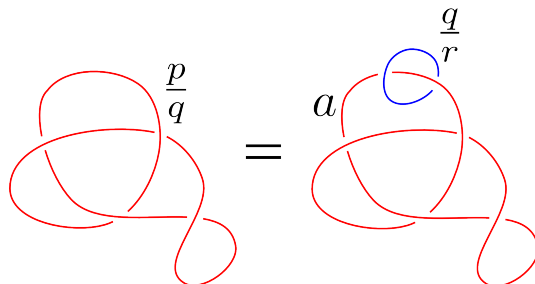


FIGURE 1.4. Conversion of a rational surgery on $K \subset S^3$ to Morse surgery on the induced knot $K' \subset L(a, b)$.

natural to ask whether there are restrictions on which knots can produce lens spaces in this way. In an unpublished manuscript John Berge gave a conjecturally complete list of knots in S^3 with this property.

We will return to some partial answers to this conjecture which can be proved using grid homology (defined in the next chapter) in Section 5.3.

The end of this section is devoted to a brief introduction to classical concepts of knot theory in the 3-sphere. Most of them will be generalized in the next chapters, so we take here the opportunity of establishing the notation.

The Alexander polynomial is one of the most versatile classical invariant for links in the 3-sphere. It has multiple ties with the topology and algebraic topology of 3 and 4 dimensional manifolds (for a survey of classical results and several equivalent definitions see [51]). It takes the form of a Laurent polynomial in $\mathbb{Z}[t^{\pm 1}]$, denoted by $\Delta_K(t)$.

The Alexander polynomial is known to satisfy a *skein relation*: if L_+ , L_- and L_0 are three oriented links differing only locally as shown in Figure 1.5, their polynomials satisfy the following relation:

$$(2) \quad \Delta_{L_+}(t) - \Delta_{L_-}(t) = \left(\sqrt{t} - \frac{1}{\sqrt{t}} \right) \Delta_{L_0}(t)$$

REMARK 1.4. The skein transformation $L_{\pm} \leftrightarrow L_0$ corresponds to an oriented *saddle move* (a.k.a. band attachment); we can think of this move as the attachment of an oriented band to the link.

A saddle move which decreases the number of components of the link will be called a *merge*, and a *split* otherwise.

Up to now we have only considered knots as equivalence classes of embeddings up to isotopy. There is however another weaker equivalence

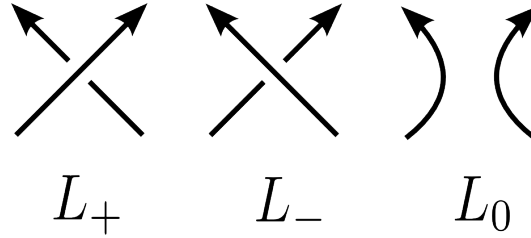


FIGURE 1.5. The diagram for the three links differ only locally as shown in Figure.

relation for knots in S^3 , known as *concordance*. We say that two knots K_0, K_1 are *concordant* if there exists a properly embedded annulus $A = S^1 \times [0, 1] \subset S^3 \times [0, 1]$ such that $A \cap S^3 \times \{i\} = K_i$, for $i = 0, 1$.

Call \mathcal{C} the set of concordance classes; we can endow it with a group operation by considering the (oriented) connected sum of knots. All isotopy classes of knots which are concordant to the unknot are called *slice knots*. Alternatively we can say that two knots $K_0, K_1 \subset S^3$ are concordant if $K_0 \# m(-K_1)$ is slice, with $m(K)$ denoting the mirror image of K .

If we consider general cobordisms, *i.e.* we use orientable surfaces with two boundary components instead of annuli, then there is only one equivalence class of knots. That is, every pair of knots in S^3 can be connected by a cobordism in $S^3 \times [0, 1]$. The proof of this fact follows easily by noting that every knot is equivalent to the unknot up to crossing changes, and a crossing change induces a genus-one cobordism.

We will denote by $K \sqcup \bigcirc^t$ the link obtained as disjoint union of K with t split trivial knots.

In [47, App. B4], it is shown how to put a cobordism between two knots in a *standard form*:

PROPOSITION 1.5. *Suppose two knots $K_0, K_1 \subset S^3$ are connected by a genus g cobordism Σ ; then there are two knots K'_0, K'_1 , and integers b, d such that*

- $K_0 \sqcup \bigcirc^b$ can be obtained from K'_0 by adding b oriented saddles.
- K'_0 and K'_1 are connected by $2g$ oriented saddles.
- $K_1 \sqcup \bigcirc^d$ can be obtained from K'_1 by adding d oriented saddles.

We will use this standard form in the case of cobordisms between knots in lens spaces in Chapter 4. We observe here that this standard form exists in a general 3-manifold (cf. [47, B4]).

Lastly, consider S^3 as the boundary of the 4-ball \mathbb{D}^4 ; then every knot $K \subset S^3$ bounds smooth properly embedded surfaces $(\Sigma, \partial\Sigma) \leftrightarrow$

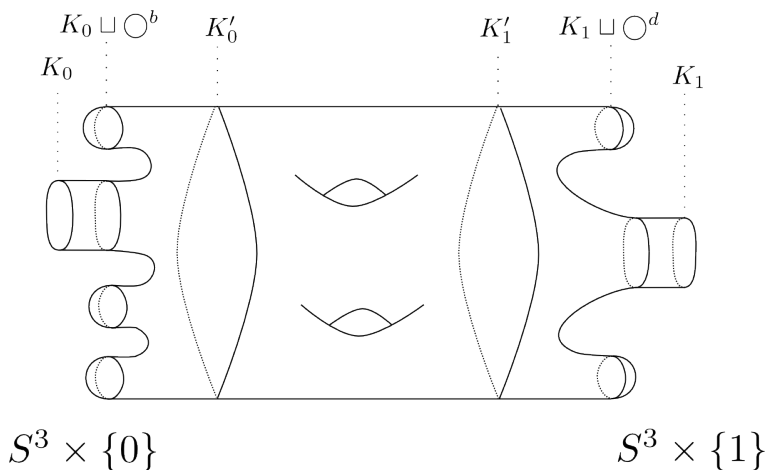


FIGURE 1.6. A schematic description of the standard form of a cobordism.

(\mathbb{D}^4, S^3) . The minimum of the genus among all these surfaces for a fixed K is called the *smooth 4-genus* of K , and denoted by $g_*(K)$.

Clearly⁷ $g(K) \geq g_*(K)$, and slice knots are the only ones with $g_* = 0$. We are going to generalize these notions to the case of knots in lens spaces in Chapter 4.

1.2. Representing links with grids

One of the features that make classical knot theory visual and provide several knot invariants is the possibility of drawing planar representations, *i.e.* diagrams. There is no straightforward generalization of the notion of diagrams for knots in 3-manifolds other than S^3 . Nonetheless a grid-diagrammatic approach (see [11]) can be carried out for lens spaces, providing us not only with some sort of diagrams, by also allowing one to combinatorially encode a couple $(L(p, q), L)$. This will be handy for the computations carried out in Chapter 6.

DEFINITION 1.6. Consider a $n \times pn$ grid in \mathbb{R}^2 , consisting of the segments $\tilde{\alpha}_i = (tnp, i)$ and $\tilde{\beta}_j = (j, tnp)$ with $i \in \{0, \dots, n\}$, $j \in \{0, \dots, np\}$ and $t \in [0, 1]$. A twisted grid for $L(p, q)$ is the grid on the torus given by identifying $\tilde{\beta}_0$ to $\tilde{\beta}_{pn}$, and then $\tilde{\alpha}_0$ to $\tilde{\alpha}_n$ with a twist depending on q (see Figure 1.7):

$$\alpha_n \ni (s, n) \sim (s - qn \pmod{pn}, 0) \in \alpha_0$$

Here $s \in [0, pn]$; the condition $(p, q) = 1$ guarantees that after the identifications the planar grid becomes a toroidal grid.

⁷ g denotes the usual Seifert genus of knots.

Call $\alpha = \{\alpha_i\}$ and $\beta = \{\beta_i\}$ $i \in \{1, \dots, n\}$ the n horizontal (resp. vertical) circles obtained after the identifications in the grid. Note that in a grid for $L(p, q)$ we have:

$$|\alpha_i \cap \beta_j| = p \quad \forall i, j \in \{1, \dots, n\}$$

We can encode a link L in $L(p, q)$ by placing a suitable version of the \mathbb{X} 's and \mathbb{O} 's for grid diagrams in S^3 : call $\mathbb{X} = \{\mathbb{X}_i\}$ and $\mathbb{O} = \{\mathbb{O}_i\}$, $i = 1, \dots, n$ two sets of markings. Put each one of them in the little squares⁸ of $G \setminus \alpha \cup \beta$ in such a way that each column⁹ and row contains exactly one element of \mathbb{X} and one of \mathbb{O} , and each square contains at most one marking.

Now join with a segment each \mathbb{X} to the \mathbb{O} which lies on the same row, and each \mathbb{O} to the \mathbb{X} which lies on the same column (keeping in mind the twisted identification). We adopt the orientation convention according to which vertical segments go from \mathbb{O} s to \mathbb{X} s¹⁰. To obtain L remove self intersections by resolving each crossing as an overcrossing¹¹ of the horizontal segments over the vertical ones (as in Figure 1.8).

The grid together with the markings is a multi-pointed Heegaard diagram¹² for $(L(p, q), L)$, called a *grid diagram*. Removing the markings produces a Heegaard diagram for $L(p, q)$, which can be obtained from the one described in the previous section by adding parallel copies of the attaching curves.

REMARK 1.7. There are two possible ways to connect each \mathbb{X}_i to the corresponding \mathbb{O} marking on the same row/column, but the isotopy class of the resulting link does not depend upon the possible choices. Indeed the two choices for each row/column are topologically related by a slide on a meridional disk of the Heegaard decomposition of $L(p, q)$, hence describe isotopic links.

The integers n, p and q will be called the *parameters* of the grid diagram G ; the p ($n \times n$) squares obtained by cutting the torus along α_1 and β_1 (in the planar representation of the grid) are called *boxes*.

We will often deliberately forget the distinction between planar and toroidal grids, according to the motto “draw on a plane, think on a

⁸For concreteness think of the markings as having half integral coordinates in the planar grid.

⁹Beware! In a twisted toroidal grid a column “wraps around” each row p times.

¹⁰Note that this convention is the opposite of the one used in [47], but agrees with the one of [4]; see also Remark 1.8.

¹¹Equivalently push horizontal/vertical segments in the solid torus determined by the α/β attaching curves respectively.

¹²See Section 2.2 for the definition.

torus". It is worth to point out that the case in which $p = 1$ and $q = 0$ gives as expected a usual grid diagram for a link in S^3 .

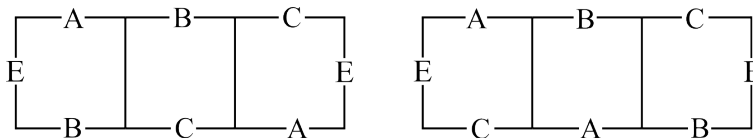


FIGURE 1.7. Top-bottom identifications for a 3 dimensional grid for $L(3, 1)$ (left) and $L(3, 2)$ (right).

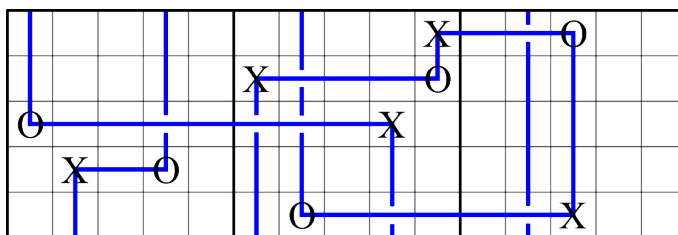


FIGURE 1.8. The link obtained by joining \mathbb{X} 's and \mathbb{O} 's in a grid for $L(3, 2)$ of grid dimension 5.

REMARK 1.8. Exchanging the two kinds of markings in a grid representing a knot K produces a grid diagram for the opposite knot $-K$. Note also that $[-K] = -[K] \pmod{p}$.

PROPOSITION 1.9 ([11],[4]). *Every link in $L(p, q)$ can be represented by a grid diagram; two different grid representations of a link differ by a finite number of grid moves analogous¹³ to Cromwell's for grid diagrams in S^3 :*

- *Translations: these are just vertical and horizontal integer shifts of the grid (keeping the twisted top/bottom identifications in mind).*
- *(non-interleaving) Commutations: if two adjacent row/columns c_1 and c_2 are such that the markings of c_1 are contained in a connected component of c_2 with the two squares containing the markings removed, then they can be exchanged.*
- *(de)Stabilizations: these are the only moves that change the dimension of the grid. There are 8 types of stabilizations, as shown in Figure 1.9. Destabilizations are just the inverse moves.*

¹³See [11].

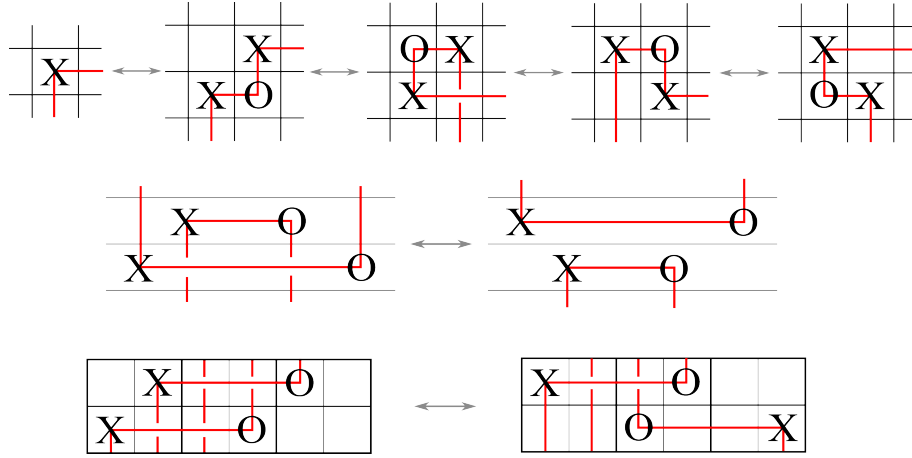


FIGURE 1.9. Some examples of grid moves; in the top there are four different kinds of stabilizations (there are other four where the roles of the markings are exchanged). In the middle a (non interleaving) row commutation. On the lower part an example of vertical translation in $L(3, 1)$.

REMARK 1.10. The homology class of a link $L \subset L(p, q)$ can be read directly from the grid (see also [10, Lemma 3.3]); we just need to keep track of the signed number of intersections of the link with a meridian of the torus. With the orientation conventions we have established (so that vertical arcs connect \mathbb{O} 's to \mathbb{X} 's):

$$H_1(L(p, q); \mathbb{Z}) \ni [L] = \#\{\alpha_1 \cap L\} \pmod{p}$$

The following Lemma gives an alternative way to compute the homology class of a link from the grid. It will be useful to prove a symmetry of grid homology.

LEMMA 1.11. *Suppose G is a grid of parameters (n, p, q) representing a link L in $L(p, q)$. Call $m = [L] \in H_1(L(p, q); \mathbb{Z})$ and denote by $a_i^{\mathbb{X}}$ and respectively $a_i^{\mathbb{O}}$ the number of the box (from the left) in which the i -th \mathbb{X}/\mathbb{O} marking lies. Then:*

$$(3) \quad \sum_{i=1}^n a_i^{\mathbb{O}} - a_i^{\mathbb{X}} \equiv qm \pmod{p}$$

PROOF. Construct a new grid \widehat{G} from G , by placing each \mathbb{X} marking in the same box of the \mathbb{O} marking in the same column, as in Figure 1.10. Call \widehat{L} the link represented by \widehat{G} ; now for \widehat{G} , by Remark 1.10 we

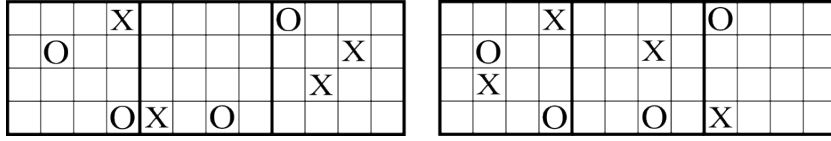


FIGURE 1.10. The grids G (on the left) and \widehat{G} , where each \mathbb{X} marking is moved close to the \mathbb{O} marking on the same column.

clearly have $[\widehat{L}] = \sum_{i=1}^n a_i^{\mathbb{O}} - a_i^{\mathbb{X}} \equiv 0 \pmod{p}$. We can get from \widehat{G} back to G by moving each \mathbb{X} marking back to its place.

The couple of markings on the i -th column of G provides a contribution of m_i to the homology class, and $m \equiv \sum_{i=1}^n m_i \pmod{p}$.

Note that moving the \mathbb{X} marking on the i -th column of \widehat{G} by k_i boxes to the left increases the homology class¹⁴ by $m_i \equiv k_i q^{-1} \pmod{p}$, and increases $a_i^{\mathbb{O}} - a_i^{\mathbb{X}}$ by k_i . So we can write

$$\sum_{i=1}^n a_i^{\mathbb{O}} - a_i^{\mathbb{X}} = \sum_{i=1}^n k_i$$

and

$$m \equiv \sum_{i=1}^n m_i \equiv \left(\sum_{i=1}^n k_i \right) q^{-1} \pmod{p}$$

And we are done. □

REMARK 1.12. If G is a grid of parameters (n, p, q) , we call n the dimension or *grid number* of G . The same term will also be used when referring to the isotopy class of a knot $(L(p, q), K)$; in this case we mean the quantity

$$GN(K) = \min\{n \mid G \text{ is a grid with parameters } (n, p, q) \text{ representing } K\}$$

Note that if $p, q = 1, 0$, then $GN(K)$ is the usual *arc index* (see [11]).

The skein moves described in Section 1.1 for the Alexander polynomial can be defined in the grid context too. They will be very useful in Chapter 4 and 5. They are described in Figure 1.11.

Note that G_0 and G'_0 are connected by a non-interleaving commutation, hence describe isotopic links. The change $G_{\pm} \leftrightarrow G_0$ is called an *interleaving* commutation (cf. [10] and Definition 1.9).

DEFINITION 1.13. *Two columns in a grid which comprise an interleaving commutation are called a positive/negative skein pair, according to whether they look like G_+ or G_- from Figure 1.11.*

¹⁴Seen as an element of $\mathbb{Z}/p\mathbb{Z}$.

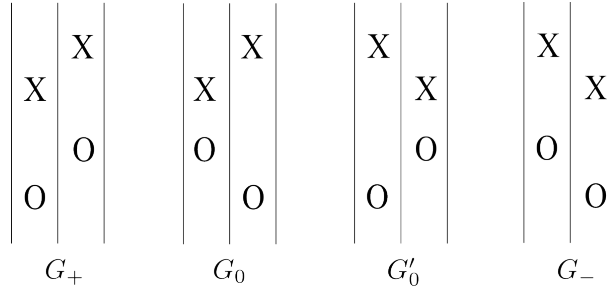


FIGURE 1.11. The column configurations for the skein moves in grid diagrams.

Note that if two grids differ by a skein change, then the links they represent differ by a crossing change.

REMARK 1.14. This convention is the same as the one in [47], and the opposite one of [10]; we adopt the former, since it works better with skein exact triangles (see Section 5.2).

There is a special class of knots in lens spaces, which in some regard can be considered the generalization of the trivial knot to non trivial homology classes. It is proved in [10] (see also Section 5.2), that up to crossing changes, every knot reduces to the unique simple knot in the same homology class (Proposition 5.16).

DEFINITION 1.15. A simple knot in $L(p, q)$ is a knot admitting a grid of dimension 1, (cf. also [24] and [4]). It is immediate to show that in each lens space $L(p, q)$ there is exactly one simple knot in each homology class; for $m \in H_1(L(p, q); \mathbb{Z})$ denote this knot by $T_m^{p,q}$.

Alternatively, using the fact that a 1-dimensional grid is the Heegaard splitting of $L(p, q)$ shown in Figure 1.2, these knots can be defined as those which are composed by one unknotted arc contained in each attaching disk of the decomposition.

LEMMA 1.16 ([50]). Simple knots are subject to the following relations¹⁵:

- (1) $T_m^{p,q} = -T_{-m}^{p,q}$
- (2) $T_{mq'}^{p,q} \cong T_m^{p,q'}$ if $qq' \equiv 1 \pmod{p}$
- (3) $T_{-m}^{p,p-q}$ is the mirror image of $T_m^{p,q} \in \overline{L(p, q)} = L(p, p - q)$

REMARK 1.17. Links in lens spaces can also be presented in another useful way, the *disk diagram form*. For a survey on the subject see [7].

¹⁵Note that the conventions and notations of [50] are different from ours.

CHAPTER 2

Grid homology

2.1. Heegaard Floer homology

In these first sections we are going to introduce Heegaard Floer homology for three manifolds, and its specialization to knots, the Knot Floer homology. Since the definitions are quite elaborate, we are not going to present a complete description; rather we are going to avoid most of the analytical aspects, and present a self contained definition along the lines of [43], aimed to better understand the source of the combinatorial counterparts we will introduce in Section 2.4.

In [41] Peter Ozsváth and Zoltán Szabó introduced a package of powerful invariants of spin^c 3-manifolds, known as *Heegaard Floer homologies*. There are many variations on these invariants, which we will denote collectively as $HF^\circ(Y, \mathfrak{s})$, where Y is a closed oriented 3-manifold, and $\mathfrak{s} \in \text{spin}^c(Y)$.

Here $\circ = +, -, \wedge, \infty$ stands for the possible variations, also known as *flavors*. In the following we will be mainly concerned with the *minus* and *hat* theories.

We sketch here the construction of the groups HF° , and we are going to restrict ourselves to $\mathbb{F} = \mathbb{F}_2$ coefficients. The details of the definition can be found in the original paper [41] from Ozsváth and Szabó.

Start with an Heegaard diagram for Y . In other terms choose a triple $\mathcal{H} = (\Sigma_g, \alpha, \beta)$, where Σ_g is a closed and oriented surface of genus g , and $\alpha = \bigcup_{i=1}^g \alpha_i, \beta = \bigcup_{i=1}^g \beta_i$ are two collections of g curves determining respectively the belt sphere of the 1-handles and the attaching spheres of the 2-handles, in the handle decomposition of Y induced by \mathcal{H} . So we will require that $\alpha_i \cap \alpha_j = \beta_i \cap \beta_j = \emptyset$ for $i \neq j$, that all the intersections are transverse, and that the curves of each type are independent in $H_1(\Sigma_g; \mathbb{Z})$.

It is also useful to reinterpret these data as induced by a self indexing Morse function $f : Y \rightarrow [0, 3]$ (after the choice of a suitable

Riemannian metric on Y): now the α and β curves are just the intersection between the stable/unstable submanifolds and Σ_g . We will also require that f has only one maximum and minimum.

To define the complexes we also need to add a point $z \in \Sigma_g \setminus \alpha \cup \beta$; the quadruple $(\Sigma_g, \alpha, \beta, z)$ is called a *pointed Heegaard diagram* for Y . There is a set of moves connecting any two pointed diagrams representing the same 3-manifold (see [41]). Given such a pointed diagram for Y consider the symmetric product

$$Sym^g(\Sigma_g) = \Sigma_g^{\times g} / \mathfrak{S}_g$$

It is not hard to show that $Sym^g(\Sigma_g)$ is a smooth manifold of dimension $2g$, which can be thought of as the set of unordered g -tuples of points in Σ_g . Moreover a complex structure on Σ_g endows $Sym^g(\Sigma_g)$ with an induced complex structure; there are two g -dimensional submanifolds contained in $Sym^g(\Sigma_g)$ which are totally real with respect to this structure.

These are the two tori $\mathbb{T}_\alpha = \prod_{i=1}^g \alpha_i$ and $\mathbb{T}_\beta = \prod_{i=1}^g \beta_i$. Note that since all the curves of each type were supposed to be disjoint, \mathbb{T}_α and \mathbb{T}_β are in fact embedded half dimensional submanifolds of $Sym^g(\Sigma_g)$, with finitely many transverse intersections.

The basepoint also induces a subspace $V_z = \{z\} \times Sym^{g-1}(\Sigma_g) \subset Sym^g(\Sigma_g)$, which is disjoint from $\mathbb{T}_\alpha \cup \mathbb{T}_\beta$. Regard the disk \mathbb{D}^2 as living in \mathbb{C} , and call $e_1 = \partial\mathbb{D}^2 \cap Re > 0$ and $e_2 = \partial\mathbb{D}^2 \cap Re < 0$.

Now, given two points $x, y \in \mathbb{T}_\alpha \cap \mathbb{T}_\beta$, denote by $\pi_2(x, y)$ the set of homotopy classes of continuous maps

$$\phi : \mathbb{D}^2 \longrightarrow Sym^g(\Sigma_g)$$

such that $\phi(-i) = x$, $\phi(i) = y$ and $\phi(e_1) \subset \mathbb{T}_\alpha$, $\phi(e_2) \subset \mathbb{T}_\beta$.

We can associate a spin^c structure to each intersection point by means of a map

$$\mathfrak{s}_z : \mathbb{T}_\alpha \cap \mathbb{T}_\beta \longrightarrow \text{spin}^c(Y)$$

The map is defined as follows: after the choice of the compatible Morse function f , each $x \in \mathbb{T}_\alpha \cap \mathbb{T}_\beta$ determines a g -tuple of trajectories connecting index 1 and index 2 critical points.

The basepoint z gives instead another trajectory connecting the maximum of f to the minimum. Deleting tubular neighborhoods of these trajectories gives a vector field by restricting ∇f , which is everywhere non zero. Moreover this vector field can be extended to the original manifold in a non singular manner. Now just denote by $\mathfrak{s}_z(x)$ the resulting homology class of this vector field.

After suitable perturbations (see [41] for the details), given a $\phi \in \pi_2(x, y)$ the moduli space $\mathcal{M}(\phi)$ of holomorphic representatives of ϕ is defined.

Composition of ϕ with an holomorphic map of the disk fixing $\pm i$ induces an \mathbb{R} action on $\mathcal{M}(\phi)$, so we can define $\widehat{\mathcal{M}}(\phi) = \mathcal{M}(\phi)/\mathbb{R}$.

It can be shown that if $x, y \in \mathbb{T}_\alpha \cap \mathbb{T}_\beta$, then $\mathfrak{s}_z(x) = \mathfrak{s}_z(y)$ iff $\pi_2(x, y) \neq \emptyset$.

Given a point $w \in \Sigma_g \setminus \alpha \cup \beta \cup z$ and two generators $x, y \in \mathbb{T}_\alpha \cap \mathbb{T}_\beta$, define the map

$$n_w : \pi_2(x, y) \longrightarrow \mathbb{Z}$$

as

$$n_w(\phi) = \#[\phi^{-1}(\{w\}) \times \text{Sym}^{g-1}(\Sigma_g)]$$

So $n_w(\phi)$ counts the intersections between V_w and the support of ϕ .

We can now introduce the complexes and differentials. Choose $\mathfrak{s} \in \text{spin}^c(Y)$, where Y is a $\mathbb{Q}HS^3$; then $\widehat{CF}(\Sigma_g, \alpha, \beta, z, \mathfrak{s})$ is the free abelian group generated by the elements $x \in \mathbb{T}_\alpha \cap \mathbb{T}_\beta$ with $\mathfrak{s}_z(x) = \mathfrak{s}$, and it is called the *hat Floer complex* of $(\Sigma_g, \alpha, \beta, z, \mathfrak{s})$.

We can endow $\widehat{CF}(\Sigma_g, \alpha, \beta, z, \mathfrak{s})$ with a relative grading $d(x, y) = \mu(\phi) - 2n_z(\phi)$, where $\phi \in \pi_2(x, y)$, and $\mu(\phi)$ is the expected dimension of the moduli space of holomorphic representatives of ϕ , known as the Maslov index. Indeed in the case of $\mathbb{Q}HS^3$ this grading can be lifted to an absolute \mathbb{Q} grading (see [36]).

Now if $x, y \in \mathbb{T}_\alpha \cap \mathbb{T}_\beta$, $\phi \in \pi_2(x, y)$ and $\mu(\phi) = 1$, call¹ $c(\phi)$ the algebraic sum of the signs of points in $\widehat{\mathcal{M}}(\phi)$. If instead $\mu(\phi) \neq 1$ define $c(\phi) = 0$.

The differential is then defined as the map

$$(4) \quad \begin{aligned} \widehat{\partial} : \widehat{CF}(\Sigma_g, \alpha, \beta, z, \mathfrak{s}) &\longrightarrow \widehat{CF}(\Sigma_g, \alpha, \beta, z, \mathfrak{s}) \\ \widehat{\partial}x &= \sum_{\substack{y \in \mathbb{T}_\alpha \cap \mathbb{T}_\beta, \phi \in \pi_2(x, y) \\ \mathfrak{s}_z(y) = \mathfrak{s}, n_z(\phi) = 0}} c(\phi) \cdot y \end{aligned}$$

It is highly non trivial to show that $(\widehat{CF}(\alpha, \beta, z, \mathfrak{s}), \widehat{\partial})$ is a chain complex. But in fact much more is true: the homology of this complex turns out to be independent on the choices made (Theorem 2.1).

¹Again here we are ignoring the perturbations needed to make the theory work properly.

The differential in the hat version is defined in term of holomorphic representatives of disks which do not intersect the submanifold V_z determined by the divisor z . There are also several other version which we describe presently, where we keep track of these intersections.

Denote by $CF^\infty(\alpha, \beta, z, \mathfrak{s})$ the free abelian group generated by the elements $[x, i]$, with $x \in \mathbb{T}_\alpha \cap \mathbb{T}_\beta$ such that $\mathfrak{s}_z(x) = \mathfrak{s}$, and $i \in \mathbb{Z}$. There is a relative grading on such a group, defined as

$$gr([x, i], [y, j]) = gr(x, y) + 2i - 2j$$

We can also endow it with the differential:

$$\begin{aligned} \partial^\infty : CF^\infty(\Sigma_g, \alpha, \beta, z, \mathfrak{s}) &\longrightarrow CF^\infty(\Sigma_g, \alpha, \beta, z, \mathfrak{s}) \\ (5) \quad \partial^\infty[x, i] &= \sum_{y \in \mathbb{T}_\alpha \cap \mathbb{T}_\beta} \sum_{\phi \in \pi_2(x, y)} c(\phi) \cdot [y, i - n_z(\phi)] \end{aligned}$$

Abusing the notation, we denote the resulting homology by $HF^\infty(Y, \mathfrak{s})$; clearly we can get an invariant for 3-manifolds, rather than for couples (Y, \mathfrak{s}) , by taking the direct sum

$$HF^\infty(Y) = \bigoplus_{\mathfrak{s} \in \text{spin}^c(Y)} HF^\infty(Y, \mathfrak{s})$$

over all spin^c structures of Y .

There is a natural endomorphism U of this complex which acts as $U([x, i]) = [x, i - 1]$, and decreases the grading by 2.

It is shown in [41], that if Y is a $\mathbb{Q}HS^3$, then the homology of the complex $(CF^\infty(\alpha, \beta, z, \mathfrak{s}), \partial^\infty)$ is always isomorphic to the module $\mathbb{F}[U, U^{-1}]$, so it does not directly provide a useful invariant. However the extra structure allows the definitions of other derived complexes which will be shown to carry many interesting and unexpected informations on the underlying 3-manifold.

Denote by $CF^-(\Sigma_g, \alpha, \beta, z, \mathfrak{s})$ the subcomplex of $CF^\infty(\Sigma_g, \alpha, \beta, z, \mathfrak{s})$ generated by elements $[x, i]$ with $i \leq 0$, and

$$CF^+(\Sigma_g, \alpha, \beta, z, \mathfrak{s}) = CF^\infty(\Sigma_g, \alpha, \beta, z, \mathfrak{s}) / CF^-(\Sigma_g, \alpha, \beta, z, \mathfrak{s})$$

The endomorphism U can be restricted to the first one, and it induces another endomorphism on the latter, which is going to be denoted in the same way. We also endow these groups with the differential induced by ∂^∞ .

There are some obvious short exact sequences relating these complexes:

$$(6) \quad 0 \rightarrow CF^-(\Sigma_g, \alpha, \beta, z, \mathfrak{s}) \rightarrow CF^\infty(\Sigma_g, \alpha, \beta, z, \mathfrak{s}) \rightarrow CF^+(\Sigma_g, \alpha, \beta, z, \mathfrak{s}) \rightarrow 0$$

and, if $\iota(x) = [x, 0]$:

(7)

$$0 \rightarrow \widehat{CF}(\Sigma_g, \alpha, \beta, z, \mathfrak{s}) \xrightarrow{L} CF^+(\Sigma_g, \alpha, \beta, z, \mathfrak{s}) \xrightarrow{U} CF^+(\Sigma_g, \alpha, \beta, z, \mathfrak{s}) \rightarrow 0$$

The main result of [41] guarantees that these groups are in fact invariants of the underlying spin^c three manifold:

THEOREM 2.1 ([41]). *The groups $H_*(CF^\circ(\alpha, \beta, z, \mathfrak{s}), \partial^\circ) = HF^\circ(Y, \mathfrak{s})$ for $\circ = \pm, \wedge, \infty$ only depend on the couple (Y, \mathfrak{s}) up to isomorphism.*

Since we are going to be dealing only with rational homology spheres, \mathfrak{s} is always going to be torsion, so we can apply the results of [36] and consider the Maslov grading as an absolute \mathbb{Q} -valued degree.

As is customary, \mathcal{T}^- will denote the module $\mathbb{F}[U]$, a so called *tower*. If (Y, \mathfrak{s}) is a spin^c $\mathbb{Q}HS^3$, then²

$$HF^-(Y, \mathfrak{s}) = \mathcal{T}^- \oplus HF_{red}^-(Y, \mathfrak{s})$$

The group $HF_{red}^-(Y, \mathfrak{s})$ is called the *reduced (minus) Heegaard Floer homology*, and in the case at hand is a finitely generated U -torsion module.

The maximum absolute grading of elements in the tower of $HF^-(Y, \mathfrak{s})$ is known as the *correction term* of (Y, \mathfrak{s}) .

DEFINITION 2.2. *A rational homology 3-sphere Y whose Floer homology has minimal rank, is called a L -space. The homology is non trivial in each spin^c structure, so Y is an L -space precisely when*

$$rk_{\mathbb{F}}(\widehat{HF}(Y; \mathbb{F})) = |H_1(Y; \mathbb{Z})|$$

Alternatively Y is an L -space iff all the groups $HF_{red}^-(Y, \mathfrak{s})$ vanish. If a knot $K \subset Y$ has a Dehn surgery yielding an L -space, we will call it a L -space knot.

The hat Heegaard Floer homology of lens spaces can be computed from a minimal Heegaard diagram (as in Figure 1.2).

It is proven in [41] that

$$\widehat{HF}(L(p, q); \mathbb{F}) = \bigoplus_{\mathfrak{s} \in \text{spin}^c(L(p, q))} \mathbb{F}_{d(p, q, \mathfrak{s})}$$

the subscript denotes the grading of the module and $d(p, q, \mathfrak{s})$ is the correction term of $L(p, q)$ in the spin^c structure \mathfrak{s} . For the computation of the correction terms for lens spaces see Definition 2.4.1.

²See [41].

So lens spaces are L -spaces, but the latter class is much wider: it contains all double branched covers of quasi alternating knots (see [42]).

2.2. Knot Floer homology

Soon after its definition it was independently realized in [39] and [49] that a knot $K \subset Y$ induces a filtration on the complex $CF^\circ(Y, \mathfrak{s})$.

The filtered quasi isomorphism class of the resulting complex is an invariant of the triple (Y, K, \mathfrak{s}) .

In order to describe these invariants in the needed form, we must extend the original description, since the first papers on the subject only dealt with nullhomologous knots. The following definitions will be rather based on [46] and [34].

In the various definitions of knot Floer homology, knots are usually encoded in two different ways; in the first approach we just need to place an extra marking point to a pointed Heegaard diagram of Y .

In the second one we increase the number of points and curves. To ease the following definitions, we are going to describe the first, and show how to obtain the latter (which will be used in a simplified form throughout the text) later on.

We can represent a knot inside Y as a *doubly pointed Heegaard diagram* $(\Sigma, \alpha, \beta, z, w)$, where the first part is an Heegaard diagram for Y , and $z, w \in \Sigma \setminus \alpha \cup \beta$ are two points. To produce a knot from this data, connect the two points z and w with a path on $\Sigma \setminus \alpha$ and one on $\Sigma \setminus \beta$. Then push the first path into the handlebody U_α and the second into U_β .

PROPOSITION 2.3 ([39]). *Every knot in a 3-manifold can be represented by a doubly pointed Heegaard diagram.*

As stated in the introduction, the knot invariants we are going to consider originate from a filtration on the complexes $CF^\circ(Y, \mathfrak{s})$, induced by *relative $spin^c$ structures* on the complement of a knot $K \subset Y$.

In analogy with the previous section, we can define a *relative $spin^c$ structure* on Y as a homology class of a non-singular vector field in $Y \setminus \nu(K)$; we are also going to require that the vector field is the outward pointing one on $\partial\nu(K)$.

The set of relative $spin^c$ structures will be denoted by $\underline{spin}^c(Y, K)$, when we consider the complement of a neighborhood of a knot $K \subset Y$. It is proven in [46] that:

$$\underline{spin}^c(Y, K) \cong \text{spin}^c(Y) \times \mathbb{Z}$$

and it is an affine space over $H^2(Y \setminus \nu(K), \partial\nu(K); \mathbb{Z})$.

Choosing an orientation for K gives a canonical nowhere vanishing vector field on the solid torus $\nu(K)$, with boundary conditions matching the ones chosen for the complement of $\nu(K)$.

There is thus a natural map

$$G_{Y,K} : \underline{spin}^c(Y, K) \longrightarrow \text{spin}^c(Y)$$

which is equivariant with respect to the $H^2(Y, \partial Y; \mathbb{Z})$ -action, and realizes an identification

$$\text{spin}^c(Y) \cong \underline{spin}^c(Y, K) / \mathbb{Z} \cdot PD[\mu]$$

where μ is the (oriented) meridian of K . If $\xi \in \underline{spin}^c(Y, K)$, we call $G_{Y,K}(\xi)$ the *underlying spin^c structure* of ξ .

Now define

$$\mathfrak{s}_{w,z} : \mathbb{T}_\alpha \cap \mathbb{T}_\beta \longrightarrow \underline{spin}^c(Y, K)$$

as follows: as in the previous section choose a self-indexing Morse function $f : Y \rightarrow [0, 3]$ adapted to (Σ, α, β) , such that the knot K is realized as the oriented union of two flowlines $\gamma_z - \gamma_w$ which connect maximum and minimum of f , and intersect Σ in z and w respectively.

A generator $x \in \mathbb{T}_\alpha \cap \mathbb{T}_\beta$ induces a g -tuple of flowlines γ_x for ∇f connecting all index 1 to 2 critical points, and passing through points of x . Removing neighborhoods of γ_x, γ_w and γ_z produces³ a relative spin^c structure $\mathfrak{s}_{w,z} \in \underline{spin}^c(Y, K)$ given by the restriction $\nabla f|_{Y \setminus \nu(K)}$.

This construction involves several choices, but it is shown in [46] that the resulting map $\mathfrak{s}_{w,z}$ does not depend upon them. In the same paper it is proven that

$$G_{Y,K}(\mathfrak{s}_{w,z}(x)) = \mathfrak{s}_w(x)$$

and if $\phi \in \pi_2(x, y)$, then

$$\mathfrak{s}_{w,z}(x) - \mathfrak{s}_{w,z}(y) = (n_w(\phi) - n_z(\phi)) \cdot PD[\mu]$$

Choose $\xi \in \underline{spin}^c(Y, K)$, and let $CFK^\infty(Y, K, \xi)$ be the free abelian group generated by triples $[x, i, j] \in \mathbb{T}_\alpha \cap \mathbb{T}_\beta \times \mathbb{Z}^2$ such that $\mathfrak{s}_w(x) = \mathfrak{s}$ and $\mathfrak{s}_{w,z}(x) + (i - j)PD[\mu] = \xi$.

We can endow $CFK^\infty(Y, K, \xi)$ with the differential

$$(8) \quad \partial^\infty x = \sum_{y \in \mathbb{T}_\alpha \cap \mathbb{T}_\beta} \sum_{\phi \in \pi_2(x, y)} c(\phi) \cdot [y, i - n_w(\phi), j - n_z(\phi)]$$

The homology of $(CFK^\infty(Y, K, \xi), \partial^\infty)$ is denoted by $HFK^\infty(Y, K, \xi)$; by itself it is not an interesting⁴ invariant of knots in $\mathbb{Q}HS^3$ s. However

³After a suitable perturbation which makes it everywhere non zero.

⁴It is shown in [39] that in this case $HFK^\infty(Y, K, \xi) \cong \mathbb{F}[U, U^{-1}]$.

there is an easy way to obtain many powerful invariants by considering the natural filtration

$$(9) \quad \begin{aligned} \mathcal{F} : CFK^\infty(Y, K, \xi) &\longrightarrow \mathbb{Z}^2 \\ \mathcal{F}([x, i, j]) &= (i, j) \end{aligned}$$

THEOREM 2.4 ([46]). *The filtered chain homotopy type of the complex $CFK^\infty(Y, K, \xi)$ is an invariant of the oriented knot (Y, K) and $\xi \in \underline{spin}^c(Y, K)$.*

REMARK 2.5. There are more geometric ways to define a filtration on the complex $CFK^\infty(Y, K, \xi)$, by suitably evaluating the first Chern class on the induced relative spin^c structure, seen as an element of $H^2(Y, \nu(K); \mathbb{Q})$ (see [33]). In this setting the target space of the filtration becomes \mathbb{Q} , rather than \mathbb{Z} (cf. with Remark 2.12).

Similarly to what was done in the previous section, we are going to extract the relevant flavors of knot Floer homology from the chain homotopy type of the ∞ flavor; this can be done in two similar ways, according to the conventions of [46] or [33].

In the first case we are going to obtain an integer-valued degree from this filtration; in the latter this degree, known as the Alexander degree, will be \mathbb{Q} -valued.

We will exploit this difference in the following chapters, and use the second convention (which is used in [4]) when defining the combinatorial version of HF° .

Given $\mathfrak{s} \in \text{spin}^c(Y)$ consider the set $G_{(Y, K)}^{-1}(\mathfrak{s})$ of relative structures which have the same underlying spin^c structure. We can endow this set with the well-ordering $\xi_1 \leq \xi_2$ if $\xi_1 = \xi_2 + j \cdot PD[\mu]$ for some $j \geq 0$.

We can pull back this ordering to a well-ordering of the complex using the function $\underline{\mathfrak{s}}_{w, z}$.

It is then shown in [46, Sec. 3] that this ordering induces a \mathbb{Z} filtration on $CF^\circ(Y, \mathfrak{s})$. Note that the infinity and minus versions inherit an extra \mathbb{Z} -filtration induced by powers of the U variable.

Now, for the second convention, define the map

$$\mathfrak{H} : \underline{spin}^c(Y, K) \longrightarrow H^2(Y, K; \mathbb{Q})$$

as $\mathfrak{H}(\mathfrak{s}) = \frac{c_1(\mathfrak{s}) - PD[\mu]}{2}$, and if $x \in \mathbb{T}_\alpha \cap \mathbb{T}_\beta$ define $\mathfrak{h}(x) = \mathfrak{H}(\underline{\mathfrak{s}}_{w, z}(x))$.

As shown in [33, Lemma 4.2] this defines a \mathbb{Q} -valued filtration on $CF^\circ(Y, \mathfrak{s})$. In both cases we call the resulting filtration the *Alexander filtration* of $CF^\circ(Y, \mathfrak{s})$ induced by the knot K . If we consider the associated graded object instead we call the induced grading *Alexander degree*.

We remark here that the same result can be obtained (cf. [4]) considering⁵ multi-pointed Heegaard diagrams and evaluations of the first Chern class of *rational Seifert surfaces* (cf. Section 5.1).

There are two natural subcomplexes we can extrapolate from $CFK^\infty(Y, K, \xi)$: the first is the *minus knot Floer complex* $CFK^-(Y, K, \xi)$, given by the elements in $CFK^\infty(Y, K, \xi)$ whose filtration level (i, j) satisfies $i \leq 0$.

The second is the *hat knot Floer complex* $\widehat{CFK}(Y, K, \xi)$, and it corresponds to elements with $i = 0$, which belong to the kernel of the U -action. Their induced filtrations can be thought of as filtrations on $CF^-(Y, \mathfrak{s})$ and $\widehat{CF}(Y, \mathfrak{s})$ respectively, where $\mathfrak{s} \in \text{spin}^c(Y)$ extends ξ .

There is thus a spectral sequence starting from $CFK^\circ(Y, K, \xi)$ and converging to $HF^\circ(Y, \mathfrak{s})$, obtained by forgetting about the extra marking point w . In particular

$$rk\left(\widehat{HFK}(Y, K, \mathfrak{s})\right) \geq rk\left(\widehat{HF}(Y, \mathfrak{s})\right)$$

When dealing with knots in the three sphere we will often abbreviate $HFK^\circ(S^3, K)$ with $HFK^\circ(K)$.

We can split the hat homology into the components determined by the bigrading:

$$\widehat{HFK}(K) = \bigoplus_{m, a \in \mathbb{Z}^2} \widehat{HFK}_m(K, a)$$

where $\widehat{HFK}_m(K, a)$ is the part in Maslov degree m and Alexander degree a .

We make here a notational remark: in order to avoid confusion, when dealing with the general case of a tri-graded homology or complex, the subscripts m, a, \mathfrak{s} will be used to denote the Maslov, Alexander and spin^c degrees respectively.

Now, given a finitely generated module endowed with a \mathbb{Z}^2 grading, $M = \bigoplus_{i, j \in \mathbb{Z}} M_{i, j}$ we can take its decategorification, which is just a weighted Euler characteristic:

$$(10) \quad \chi_t(M) = \sum_{i, j \in \mathbb{Z}} (-1)^i rk(M_{i, j}) \cdot t^j \in \mathbb{Z}[t^{\pm 1}]$$

THEOREM 2.6 ([39]). *If (S^3, K) is a knot, then the decategorification of the hat knot Floer homology coincides with the Alexander*

⁵Multi-pointed diagrams will be defined in the end of this Section, and rational surfaces in Section 5.1.

polynomial of K :

$$\chi_t(\widehat{HF\!K}(K)) = \sum_{m,a \in \mathbb{Z}^2} (-1)^m r_{k_{\mathbb{F}}} \left(\widehat{HF\!K}_m(K, a) \right) \cdot t^a = \Delta_K(t)$$

So $\widehat{HF\!K}$ contains at least the same amount of information as $\Delta(t)$; it is however easy to exhibit knots with the same Alexander polynomial whose homologies are distinct, so $\widehat{HF\!K}$ is a more refined invariant.

Furthermore, the Alexander polynomial of a split link vanishes, while $\widehat{HF\!K}$ exhibits a more subtle behavior (see Chapter 4).

The skein relation (Equation (2)) satisfied by $\Delta(t)$ can be lifted to its categorification; here it takes the form⁶ of a long exact sequence, usually called *skein exact triangle*.

THEOREM 2.7 ([39]). *Consider three links L, L_0 and L_1 in Y differing as in Figure 1.5. Then if the two strands in the crossing belong to the same component the following sequence is exact:*

$$\begin{aligned} &\rightarrow \widehat{HF\!K}(Y, L_-) \rightarrow \widehat{HF\!K}(Y, L_0) \rightarrow \widehat{HF\!K}(Y, L_+) \rightarrow \widehat{HF\!K}(Y, L_-) \rightarrow \\ &\textit{otherwise} \\ &\rightarrow \widehat{HF\!K}(Y, L_-) \rightarrow \widehat{HF\!K}(Y, L_0) \otimes Z \rightarrow \widehat{HF\!K}(Y, L_+) \rightarrow \widehat{HF\!K}(Y, L_-) \rightarrow \end{aligned}$$

is exact, with $Z = \mathbb{F}_{[0,1]} \oplus \mathbb{F}_{[-1,0]} \oplus \mathbb{F}_{[-1,0]} \oplus \mathbb{F}_{[-2,-1]}$.

Moreover knot Floer homology is known (see *e.g.* [39]) to satisfy a formula⁷ for the connected sum of two knots in rational homology 3-spheres; if $(Y, K) = (Y_0, K_0) \# (Y_1, K_1)$, then

$$(11) \quad HF\!K^\circ(Y, K, \mathfrak{s}) \cong \bigoplus_{\mathfrak{s}_0 \# \mathfrak{s}_1 = \mathfrak{s}} HF\!K^\circ(Y_0, K_0, \mathfrak{s}_0) \otimes HF\!K^\circ(Y_1, K_1, \mathfrak{s}_1)$$

where the tensor product is taken over the appropriate ring.

In Section 2.4.3 we will prove that $\widehat{HF\!K}$ satisfies a symmetry property (Proposition 2.27) under orientation reversal of the knot (see also [50, Sec. 3.8] for an alternative viewpoint).

There is another result regarding symmetries of the knot Floer homology of rationally nullhomologous knots in $\mathbb{Q}HS^3$'s, due to Ni and Wu [34], which is going to be useful in Section 5.2:

⁶We postpone the definition of the homology for links to Chapter 4.

⁷We do not specify here the various conventions involved for spin^c structures, since in what follows we will only deal with $Y = S^3, L(p, q)$.

PROPOSITION 2.8 ([34]). *If K is a nullhomologous knot in a rational homology 3-sphere Y , there is an isomorphism:*

$$\widehat{HFK}(Y, K, \mathfrak{s}) \cong \widehat{HFK}(Y, K, J\mathfrak{s} + PD[K])$$

where $J : \text{spin}^c(Y) \rightarrow \text{spin}^c(Y)$ is the conjugation map described in Section 2.1.

There are several different ways to generalize knot Floer homology to links; in [39, Sect. 2.1] it is shown that a nullhomologous m -component link $L \subset Y$ uniquely corresponds to a knot inside the manifold $Y \#^{m-1} S^1 \times S^2$. The definition of HFK° for L was given as the homology of the corresponding knot in this new manifold.

As mentioned in the beginning of the section, there is another procedure to encode knots and links in 3-manifolds in a way which is compatible with a Heegaard decomposition. It was first introduced in [44] to encode links more easily.

A *multi-pointed Heegaard diagram* for a link (Y, L) is a fivetuple $(\Sigma_g, \alpha, \beta, \underline{w}, \underline{z})$ where this time α and β are two sets of $g + n - 1$ simple closed curves, each spanning a g -dimensional subspace of $H_1(\Sigma_g; \mathbb{Z})$.

Accordingly, \underline{w} and \underline{z} are two sets of n points, which record the signed intersections of the link with Σ_g . In other words the link is made up of trajectories of the Morse flow, connecting maxima to minima points.

At a Morse-theoretic level, this just corresponds to changing the Morse function so that it has n maxima and minima, and recording on the Heegaard surface the flowlines between them.

The complex $CFK^-(\Sigma_g, \alpha, \beta, \underline{w}, \underline{z})$ is then just the freely generated $\mathbb{F}[U_1, \dots, U_n]$ -module over $\mathbb{T}_\alpha \cap \mathbb{T}_\beta$, with differential:

$$(12) \quad \partial^- x = \sum_{y \in \mathbb{T}_\alpha \cap \mathbb{T}_\beta} \sum_{\phi \in \pi_2(x, y)} c(\phi) \cdot \left(\prod_{i=1}^n U_i^{n_{w_1}(\phi)} \right) y$$

The homology of this complex, despite having $\mathbb{F}[U_1, \dots, U_n]$ as ground ring, is isomorphic to the previously defined one (at least for knots). This is due to the fact that the actions of two different U -variables are chain homotopic, so the homology itself is chain homotopic to an $\mathbb{F}[U]$ -module (compare also with Sections 2.4.3 and 4.2).

We will describe in detail two definitions of link Floer homology in the combinatorial context in Chapter 4.

2.3. From holomorphic to combinatorial

From the definitions of the previous section it should be quite clear that, with the exception of some specific family of knots, the computations of $HF\mathcal{K}^\circ(K)$ for a generic $K \subset S^3$ are hard.

The main issue preventing a systematic calculation of these groups resides in the differential: there is no algorithm to sort out the count of points in the quotient space $\widehat{\mathcal{M}}$ for the holomorphic disks involved.

Nonetheless, in 2006 S. Sarkar and J. Wang [53] showed that if a Heegaard diagram for Y is of a particular form, this count could be performed algorithmically.

More formally, they introduced the notion of a *nice* Heegaard diagram for a 3-manifold Y . This is just an ordinary multi-pointed Heegaard diagram for Y , such that all regions in the complement of the attaching curves either contain a basepoint w_i or are bigons and squares. They proved that on these regions there is only one holomorphic representative (up to \mathbb{R} shifts), so $\#\widehat{\mathcal{M}}(\phi) = 1$.

In the same paper they gave an algorithm that, starting from an arbitrary Heegaard diagram of a 3-manifold, produced an equivalent nice Heegaard diagram, thus proving that each 3-manifold admits one.

This key result opened the possibility for a combinatorial reformulation of Knot Floer homology. Indeed in [30] Manolescu, Ozsváth and Sarkar managed to give a description of a combinatorial homology theory, proving it was in fact isomorphic to its holomorphic counterpart.

They considered a genus 1 multi-pointed Heegaard diagram for the three sphere (as in Figure 2.1). As shown, in this case all the complementary regions of the attaching curves are squares, so this is in fact a nice Heegaard diagram for S^3 .

As done in Section 1.2, we can encode a knot $K \subset S^3$ by marking the intersection between the splitting surface and K . As is customary we do this by placing an \odot marking for ascending flowlines and an \times marking in the other case, which take the place of the z_i and w_i base points.

There are exactly n maxima and n minima for the Morse function determining this splitting, so all the annuli made on the torus by two adjacent α or β curves must contain exactly one marking of each kind. Now, fix a cyclic labelling for the α and β curves, and cut the torus along α_1 and β_1 .

This produces a grid diagram for K as in Figure 2.2. In this setting the points of $\mathbb{T}_\alpha \cap \mathbb{T}_\beta$ correspond to n -tuples of intersection points between α and β curves, such that each curve contains exactly one. In

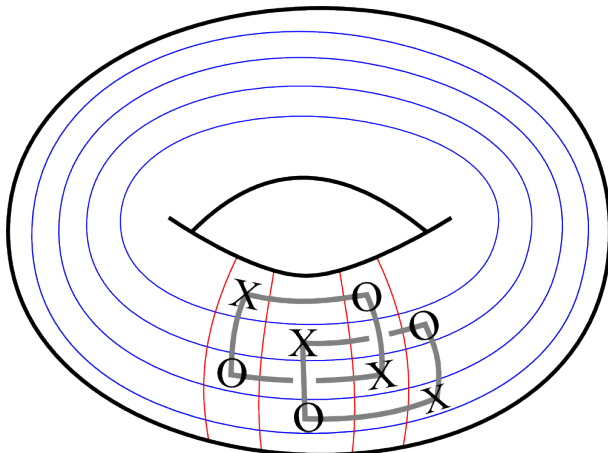


FIGURE 2.1. A grid diagram on the torus representing the Hopf link in S^3 .

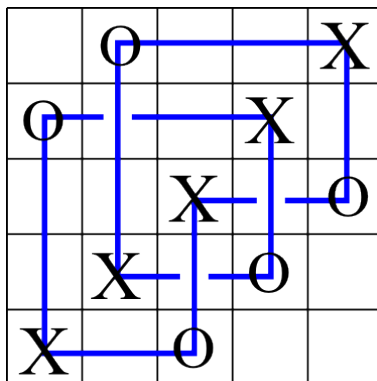


FIGURE 2.2. A grid diagram for the trefoil in S^3 .

turn the set of such n -tuples can be put in correspondence with the symmetric group on n elements.

In the same paper they also gave a combinatorial formula for deriving the Maslov and Alexander degrees of a generator in the complex.

The differential, which was the main source of the computational issues, takes the milder form of embedded rectangles in the grid.

The boundary conditions for maps in $\pi_2(x, y)$ implies that such rectangles will have sides which are alternatively embedded on the vertical and horizontal arcs composing the grid. These rectangles might contain markings and/or other components of the generators; the different flavors of the homology will depend upon a choice of which of these are admissible. The resulting homology is referred to as *grid homology*.

In the next section we are going to define rigorously this combinatorial approach to knot Floer homology in the more general case of links in lens spaces. As explained in the first Chapter, the S^3 case can be recovered by choosing $p, q = 1, 0$.

2.4. Grid homology in lens spaces

In the following we are going to define several different *flavors* of the grid homology for links in lens spaces, following [4], and paralleling the definitions of Section 2.2.

All these versions can be defined by slight variations in the complex, the ground ring or the differential we are going to introduce below.

For clarity we are going to restrict ourselves to $\mathbb{F} = \mathbb{Z}_2$ coefficients until Chapter 3, and to knots up to Chapter 4.

2.4.1. The complex.

DEFINITION 2.9. *Given a grid G of dimension n representing a knot $(L(p, q), K)$, the generating set for G is the set $S(G)$ comprising all bijections between α and β curves. This corresponds to choosing n points in $\alpha \cap \beta$ such that there is exactly one on each α/β curve.*

There is a bijection

$$S(G) \longleftrightarrow \mathfrak{S}_n \times (\mathbb{Z}_p)^n$$

which can be described as follows: since we fixed a cyclic labeling of the α and β curves it makes sense to speak of the m -th intersection between two curves, with $0 \leq m \leq p-1$; so if the l -th component of a generator lies on the m -th intersection of α_l and β_j then the associated permutation $\sigma \in \mathfrak{S}_n$ will be such that $\sigma(l) = j$ and the l -th component of $(\mathbb{Z}_p)^n$ will be m . If $x \in S(G)$, we can thus write $x = (\sigma_x, (x_1^p, \dots, x_n^p))$; we will refer to σ_x as the permutation component of the generator, and to (x_1^p, \dots, x_n^p) as its p -coordinates.

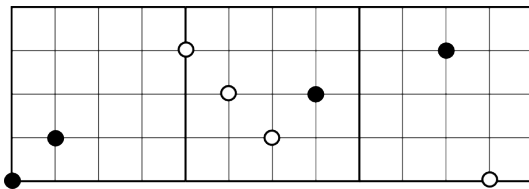


FIGURE 2.3. Under the bijection described before the white generator corresponds to $((14)(23), (2, 1, 1, 1))$, and the black to $((34), (0, 0, 1, 2)) \in \mathfrak{S}_4 \times (\mathbb{Z}_3)^4$.

$S(G)$ can be endowed with a $(\mathbb{Q}, \mathbb{Q}, \mathbb{Z}_p)$ -valued grading. The first two degrees are known as *Maslov* and *Alexander* degrees. The last one is the spin^c degree; since it is preserved by the differential (Proposition 2.16), it will provide a splitting of the complex in p direct summands. All these degrees are going to be defined in a purely combinatorial way. To define the first two degrees we need to borrow some terminology from [29] and [4]:

DEFINITION 2.10. *Let A and B denote two finite sets of points in \mathbb{R}^2 ; call $\mathcal{I}(A, B)$ the number of pairs*

$$((a_1, a_2), (b_1, b_2)) \subset A \times B$$

such that $a_i < b_i$ for $i = 1, 2$.

Denote by $X(p, n)$ (respectively $Y(p, n)$) the set of n -tuples (respectively pn -tuples) of points contained in the $n \times pn$ (respectively $pn \times pn$) rectangle in \mathbb{R}^2 whose bottom vertices are $(0, 0)$ and $(pn, 0)$; next define

$$C_{p,q} : X(p, n) \longrightarrow Y(p, n)$$

as the function which sends an n -tuple $\{(c_i, b_i)\}_{i=1, \dots, n}$ to the pn -tuple

$$\{(c_i + nqk \pmod{np}, b_i + nk)\}_{\substack{i=1, \dots, n \\ k=0, \dots, p-1}}$$

As in [4], to avoid notational overloads, we are going to write \tilde{x} instead of $C_{p,q}(x)$.

Note that the distance between any two markings on the same column of the lifted grid $C_{p,q}(G)$ is the homology class of the knot represented by G , in accord with Remark 1.10.

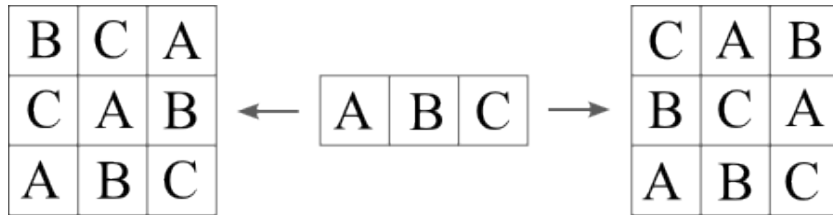


FIGURE 2.4. A representation of the action of $C_{p,q}$ for $(p, q) = (3, 1)$ and $(3, 2)$ (on the left and right respectively).

We can then define the Maslov degree:

$$(13) \quad M(x) = \frac{1}{p} \left[\mathcal{I}(\tilde{x}, \tilde{x}) - \mathcal{I}(\tilde{x}, \tilde{\mathcal{O}}) - \mathcal{I}(\tilde{\mathcal{O}}, \tilde{x}) + \mathcal{I}(\tilde{\mathcal{O}}, \tilde{\mathcal{O}}) \right] + d(p, q, q - 1) + 1$$

$d(p, q, q - 1)$ is a rational number known as the *correction term* of $L(p, q)$ associated to the $(q - 1)$ -th spin^c structure. Following [36], it can be computed recursively as follows⁸:

- $d(1, 0, 0) = 0$
- $d(p, q, i) = \left(\frac{pq - (2i + 1 - p - q)^2}{4pq} \right) + d(q, r, j)$ where r and j denote the reduction of p and i ($\text{mod } q$).

Similarly the Alexander grading can be defined as:

$$(14) \quad A(x) = \frac{1}{2p} \left[\mathcal{I}(\tilde{\mathbb{O}}, \tilde{\mathbb{O}}) - \mathcal{I}(\tilde{\mathbb{X}}, \tilde{\mathbb{X}}) + 2\mathcal{I}(\tilde{\mathbb{X}}, \tilde{x}) - 2\mathcal{I}(\tilde{\mathbb{O}}, \tilde{x}) \right] + \frac{1 - n}{2}$$

REMARK 2.11. By slightly modifying the differential, A can be demoted to a filtration on the complex, rather than a degree. The complexes we are going to consider should be thought of as the graded objects associated to this filtration.

Note that Equation (14) is not the standard formula used to define A . Here we are using the fact (see [14]) that in a grid of dimension n for a knot in S^3

$$\mathcal{I}(x, J) - \mathcal{I}(J, x) = n$$

with $J = \mathbb{O}$ or \mathbb{X} . Now call $(a_1^{\mathbb{O}}, \dots, a_n^{\mathbb{O}})$ the p -coordinates of the generator whose components are in the lower left vertex of the squares which contain an \mathbb{O} marking. The spin^c degree of $x = (\sigma_x, (a_1, \dots, a_n)) \in S(G)$ is defined⁹ as:

$$S : \mathfrak{S}_n \times (\mathbb{Z}_p)^n \longrightarrow \mathbb{Z}_p$$

$$(15) \quad S(x) = q - 1 + \sum_{i=1}^n (a_i - a_i^{\mathbb{O}}) \pmod{p}$$

The Alexander grading depends on the placement of all the markings, whilst M and S only on the position of the \mathbb{O} markings.

REMARK 2.12. A proof of the equality between these combinatorial definitions and the ones given in Section 2.2 can be found in [4].

There are several different conventions hidden in the various papers throughout the history of HFK . In particular there seems to be (at least) two ways to interpret the target space of the degree for a rationally nullhomologous knot in a rational homology sphere. In the usual convention [50], [46] the Alexander filtration takes values in \mathbb{Z} , while

⁸A user-friendly online calculator for these correction terms can be found at http://poisson.dm.unipi.it/~celoria/correction_tems.html

⁹We are implicitly using a fixed identification between $\text{spin}^c(L(p, q))$ and \mathbb{Z}_p (cf. [36, Sec. 4.1]).

in [4], [34] A takes values in a copy of \mathbb{Z} shifted by a rational number (which depends on the homology class of the knot and the spin^c degree).

The combinatorial definition of this degree is easily obtainable from Equation (14); if we denote $A_{\mathbb{Z}}$ the integer-valued Alexander degree we have:

$$A_{\mathbb{Z}}(x) = p \cdot A(x)$$

Let $R = \mathbb{F}[V_1, \dots, V_n]$ denote the ring of n -variables polynomials with \mathbb{F} coefficients, and $\widehat{R} = R / \{V_1 = 0\}$. These V variables¹⁰ are graded endomorphisms of the complex. Their function is to keep track of the \mathbb{O} markings in the differential. We can now define at least the underlying module structure of the complexes we are going to use in the following:

DEFINITION 2.13. *The minus complex $GC^-(G)$ is the free R module generated over $S(G)$. The hat complex $\widehat{GC}(G)$ is the free \widehat{R} -module generated over $S(G)$. Extend the gradings to the whole module by setting the behavior of the action for the variables in the ground ring:*

$$\begin{aligned} A(V \cdot x) &= A(x) - 1 \\ M(V \cdot x) &= M(x) - 2 \\ S(V \cdot x) &= S(x) \end{aligned}$$

where V is any of the V_i s.

EXAMPLE 2.14. In this example we are going to exhibit the generating set of the grid G on the left of Figure 2.5, in the 0-th spin^c structure, which we are going to denote by $S(G, 0)$. $S(G, 0)$ is composed by 4 elements:

$$a = \mathbb{F}_{[-\frac{1}{4}, -\frac{1}{4}]}, b = \mathbb{F}_{[-\frac{1}{4}, -\frac{1}{4}]}, c = \mathbb{F}_{[\frac{3}{4}, -\frac{1}{4}]}, d = \mathbb{F}_{[-\frac{5}{4}, -\frac{5}{4}]}$$

The notation $\mathbb{F}_{[a,b]}$ denotes a generator having (a, b) bidegree.

2.4.2. The differential. As already mentioned in the introduction, grid homology hinges upon the result by Sarkar and Wang [53]; in their terminology, (twisted) grid diagrams are *nice* (multi-pointed, genus 1) Heegaard diagram for $L(p, q)$, so the differential of CFK° can be computed combinatorially. In this context the holomorphic disks of Knot Floer homology become embedded rectangles on the grid.

¹⁰We adopt here the convention of [47], in order to stress the difference between the endomorphisms on the complex (the V_i s) and the induced map on homology, which will be denoted by U .

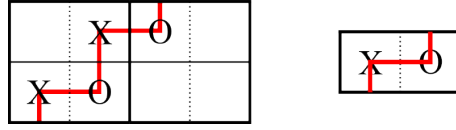


FIGURE 2.5. A grid for the knot considered, and the same grid after a destabilization.

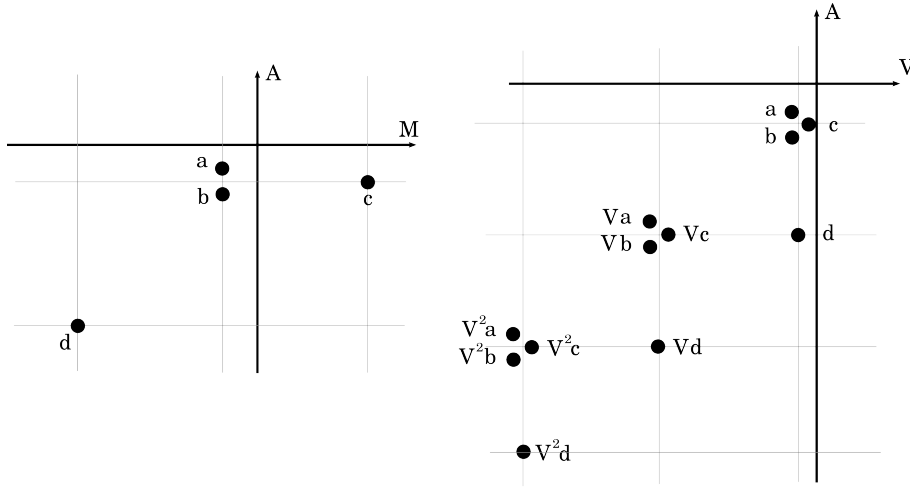


FIGURE 2.6. (left) The generating set $S(G, 0)$ (with the bidegree (M, A) on the axes). (right) The complex $\widehat{GC}(G, 0) = GC^-(G, 0)$ with axes labeled by powers of the V variables and Alexander degree. The dots represent generators over \mathbb{F} .

Consider two generators x and $y \in S(G)$ having the same spin^c degree. If the permutations associated to x and y differ by a transposition, then the two components where the generators differ are the vertices of four immersed rectangles r_1, \dots, r_4 in the grid; the sides of the r_i are alternately arcs on the α and β curves. We can fix an orientation for such a rectangle r , by prescribing that r goes from x to y if its lower left and upper right corners are on x components. This cuts the number of rectangles connecting two generators that differ by a transposition to 2.

DEFINITION 2.15. *Given a grid G , and x, y of $S(G)$, call $\text{Rect}(x, y)$ the set of embedded oriented rectangles connecting x to y ; we will denote*

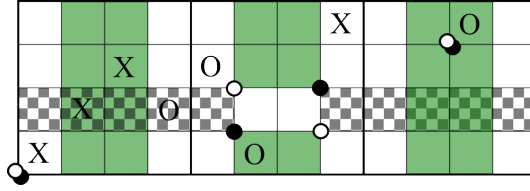


FIGURE 2.7. Two oriented rectangles connecting x (white) to y (black). Only the horizontal one (colored with a checkerboard pattern) is empty.

by

$$Rect(G) = \bigcup_{x,y \in S(G)} Rect(x,y)$$

the set of all oriented rectangles between generators in G . Similarly $Rect^\circ(G)$ is going to be the set of empty rectangles, that is the rectangles $r \in Rect(x,y)$ for which $Int(r) \cap x = \emptyset$. Note that by assumption if $r \in Rect(x,y)$ is empty, then it does not contain any point of y either.

If $x, y \in S(G)$, then $|Rect(x,y)| \in \{0, 2\}$, and it can be non zero only for generators in the same $spin^c$ degree which differ by a single transposition. On the other hand with the same hypothesis on the generators, $|Rect^\circ(x,y)| \in \{0, 1, 2\}$. If $r_1 \in Rect(x,y)$ and $r_2 \in Rect(y,z)$ we can consider their concatenation $r_1 * r_2$, which we call a *polygon* connecting x to z through y .

We are going to denote by $Poly(x,z)$ the set of polygons connecting x to z , and by $Poly^\circ(x,z)$ the empty ones. If P is an empty rectangle or polygon, denote by $O_i(P)$ the number of times that the i -th \mathbb{O} marking appears in P . In a grid diagram for knots in S^3 , $O_i(P) \in \{0, 1\}$, but if P is an empty polygon in a twisted grid, then $O_i(P) \in \{0, 1, 2\}$ (see Figure 2.11). The differential is just going to be a count of empty rectangles, satisfying some additional constraints according to the flavor chosen.

For the two flavors of grid homology considered here¹¹ we keep track of the \mathbb{O} markings contained in the rectangles, by multiplying with the corresponding variable V_i :

$$(16) \quad \partial(x) = \sum_{y \in S(G)} \sum_{\substack{r \in Rect^\circ(x,y) \\ r \cap \mathbb{X} = \emptyset}} \left(\prod_{i=1}^n V_i^{O_i(r)} \right) y$$

PROPOSITION 2.16. *Given a grid diagram G of parameters (n, p, q) , the modules $GC^-(G)$ and $\widehat{GC}(G)$ endowed with the endomorphism ∂*

¹¹Keep in mind that for \widehat{GC} we set $V_1 = 0$.

are chain complexes, that is $\partial^2 = 0$ in both cases. Moreover ∂ acts on the trigrading as follows:

- (1) $S(\partial(x)) = S(x)$
- (2) $M(\partial(x)) = M(x) - 1$
- (3) $A(\partial(x)) = A(x)$

REMARK 2.17. This Proposition is implicit in [4], and it can be seen as a direct consequence of Theorem 1.1 therein; however some of the considerations in our proof will be useful in the following section. Moreover this proof will rely only on combinatorial considerations, showing that the result can be obtained without any reference to the holomorphic theory of [39] and [49].

PROOF. We begin by examining the behavior of the degrees under the differential; condition (1) is easy to prove: by Equation (15) the only relevant part of a generator x for the computation of $S(x)$ is given by its p -coordinates. If y appears in the differential of x , all their components except two coincide, but the distance between the different components is the same, since they enclose the upper/lower edges of a rectangle, so $S(x) = S(y)$.

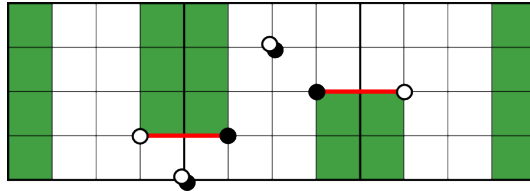


FIGURE 2.8. The non equal p -coordinates of the generators compensate each other.

If x and y are generators in G connected by an empty rectangle r , then their lifts \tilde{x} and \tilde{y} will differ in $2p$ positions, according to the pattern suggested in Figure 2.4. This implies that the corresponding

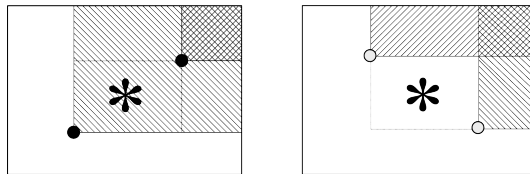


FIGURE 2.9. The difference between the functions $\mathcal{I}(x, *)$ and $\mathcal{I}(y, *)$ for two generators whose permutations differ by a transposition.

\mathcal{I} function will change accordingly:

$$\begin{aligned}\mathcal{I}(\tilde{x}, \tilde{x}) &= \mathcal{I}(\tilde{y}, \tilde{y}) + p \\ \mathcal{I}(\tilde{x}, \tilde{\mathbb{O}}) &= \mathcal{I}(\tilde{y}, \tilde{\mathbb{O}}) + p \sum_{i=1}^n O_i(r) \\ \mathcal{I}(\tilde{\mathbb{O}}, \tilde{x}) &= \mathcal{I}(\tilde{\mathbb{O}}, \tilde{y}) + p \sum_{i=1}^n O_i(r)\end{aligned}$$

And the same result holds with \mathbb{X} markings instead of \mathbb{O} 's. Then from Equation (16) we get for (2) and (3) respectively:

$$\begin{aligned}M(\partial(x)) &= \sum_{y \in S(G)} \sum_{\substack{r \in \text{Rect}^\circ(x,y) \\ r \cap \mathbb{X} = \emptyset}} \left(\sum_{i=1}^n -2O_i(r) \right) M(y) \\ A(\partial(x)) &= \sum_{y \in S(G)} \sum_{\substack{r \in \text{Rect}^\circ(x,y) \\ r \cap \mathbb{X} = \emptyset}} \left(\sum_{i=1}^n -O_i(r) \right) A(y)\end{aligned}$$

A substitution using equations (13) and (14) defining the Maslov and Alexander degrees yields (2) and (3).

We are left to show that $\partial^2 = 0$; we thus need to study the possible decompositions in rectangles of polygons connecting two generators. We will prove the result for the minus flavored complex, since the analogous result for the hat version follows immediately.

From Equation (16) we can compute:

$$(17) \quad \partial^2(x) = \sum_{z \in S(G)} \sum_{\substack{\psi \in \text{Poly}^\circ(x,z) \\ \psi \cap \mathbb{X} = \emptyset}} N(\psi) \left(\prod_{i=1}^n V_i^{O_i(\psi)} \right) z$$

where ψ is a polygon connecting x to z , and $N(\psi)$ is the number of possible ways of writing ψ as the composition of two empty rectangles $r_1 * r_2$, with $r_1 \in \text{Rect}^\circ(x, y)$ and $r_2 \in \text{Rect}^\circ(y, z)$ for some $y \in S(G)$. Note that a polygon P connecting two generators is empty if and only if so are the rectangles P is made of.

In order to complete the proof we need to show that $N(\psi) \equiv 0 \pmod{2}$, *i.e.* there is an even number of ways¹² (in fact 2) to decompose into rectangles a fixed ψ that appears in the squared differential ∂^2 . We can also take advantage of the proof in [47, Lemma 4.4.6] to reduce the number of cases to examine; as a matter of fact, if a polygon

¹²This is not true for the *filtered* versions of these complexes. Nonetheless the contributions from polygons that can not be split in two different ways cancel each other out nicely in that case too.

ψ does not cross one of the α curves, we can cut the torus open along it, and think of the polygon as living in a portion of an $np \times np$ grid for S^3 .

Thus we only need to worry about polygons that intersect all the α circles. There are four possibilities to be considered a priori, according to the quantity $M = |x \setminus (x \cap z)| \in \{0, \dots, 4\}$, as schematically shown in Figure 2.10.

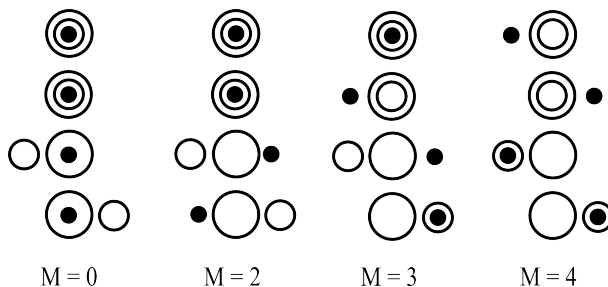


FIGURE 2.10. A representation of the possibilities for M (in a grid of dimension 4). The circles correspond (from big to small) to the components of generators x , y and z . Two circles are concentric if the corresponding generators coincide.

If $M = 0$, that is $x = z$, the only possible polygons are *thin* rectangles, called α and β degenerations. These are strips of respectively height or width 1 (otherwise they would not be empty). We are not concerned with these strips, since each of them contains exactly one \mathbb{X} marking, hence they do not contribute to the differential. As an aside we note here that there is only one way to decompose such a strip into two rectangles (one starting from x , and one arriving to it).

The cases with $M = 1$ can be dismissed too, since rectangles can only connect generators which differ in exactly two points¹³. If $M = 4$, that is the corners of the two rectangles are all distinct, we can apply the same approach of [47]; there are two ways of counting them, as shown in Figure 2.11.

Basically the two decompositions correspond to taking the two rectangles in either order. We remark that one rectangle might wrap around the other, but the number of decompositions does not depend on this wrapping.

¹³And a product of two nontrivial and different transpositions is never a transposition.

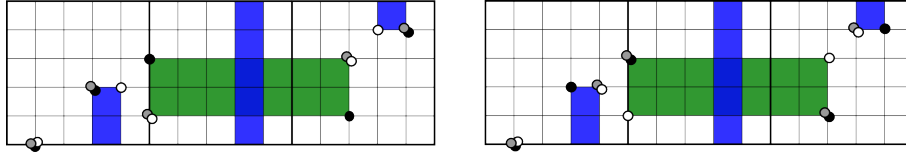


FIGURE 2.11. When $M = 4$ we can consider the two rectangles (from white to black) in either order, by choosing a suitable intermediate generator y (gray).

The case $M = 2$ needs a bit more care since it has no S^3 counterpart (see [47, Ch. 4]). In this case the two rectangles must share part of 2 edges. There are two possibilities:

- (1) the rectangle starting from x does not cross all the α curves. Up to vertical/horizontal translations it can be placed in such a way that it does not intersect the boundary of the planar grid.
- (2) the rectangle starting from x intersects all the α curves at least once.

In both cases, the second rectangle joining the intermediate generator (y or w in the notation above) to z must end and start on the same α curves of the first rectangle; the configuration in both cases are shown Figure 2.12, together with their decompositions.

Lastly, if $M = 3$ we can again distinguish two possibilities as in the previous case; the combinatorially inequivalent configurations are shown in Figures 2.13 and 3.4, again with their two decompositions. \square

EXAMPLE 2.18. We continue here the computations of example 2.14: we can now complete the picture by adding the differentials and computing the various homologies. We have:

$$\begin{aligned} \partial(a) &= \partial(b) = 0 \\ \partial(c) &= a + b \\ \partial(d) &= V_1a + V_2b \end{aligned}$$

It is then an easy task to compute the grid homologies in the two flavors:

$$\widehat{GH}(G, 0) = \mathbb{F}\langle a \rangle \cong \mathbb{F}_{[-\frac{1}{4}, -\frac{1}{4}]}$$

$$GH^-(G, 0) = \mathbb{F}[V_1]\langle a \rangle \cong \mathbb{F}[U]_{[-\frac{1}{4}, -\frac{1}{4}]}$$

Compare these computations with Remark 2.25.

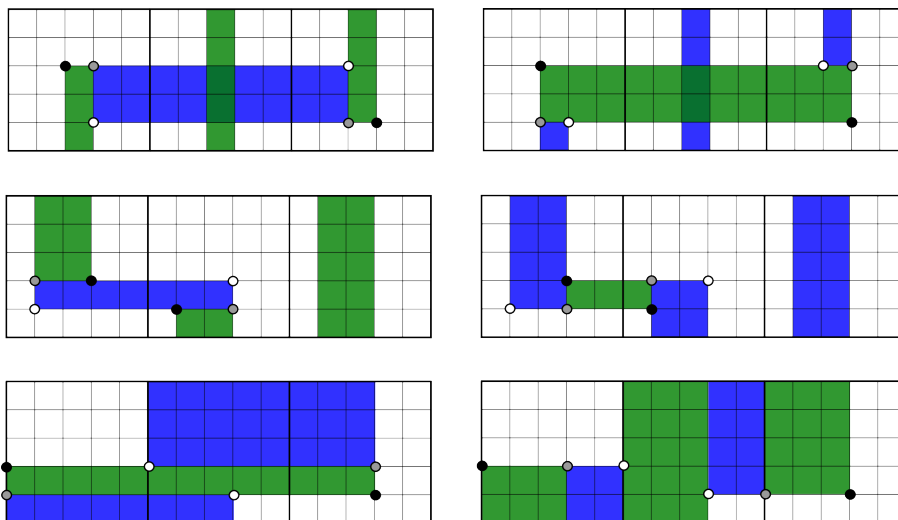


FIGURE 2.12. Relevant combinatorial possibilities for $M = 2$ on a grid for $L(3, 1)$. On each row the two possible decompositions are shown. Again we adopt the convention $x, y, z = \text{white/gray/black dots}$, showing only the relevant components.

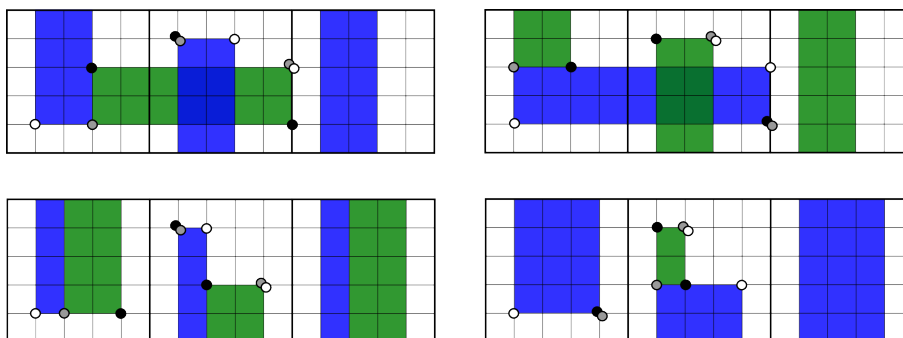


FIGURE 2.13. Some configurations for the $M = 3$ case. The complete combinatorial classification up to wrapping is presented in Figure 3.4.

2.4.3. The homologies. From the definitions given up to now it might seem strange that the homology of such a complex could be a knot invariant, since even the ground ring depends on the dimension of a grid representing it. Theorem 2.20 below ensures however that GH^- and \widehat{GH} are quasi-isomorphic to a finitely generated $\mathbb{F}[U]$ and \mathbb{F} modules respectively. The algebraic reason behind this is the content of the following Proposition:

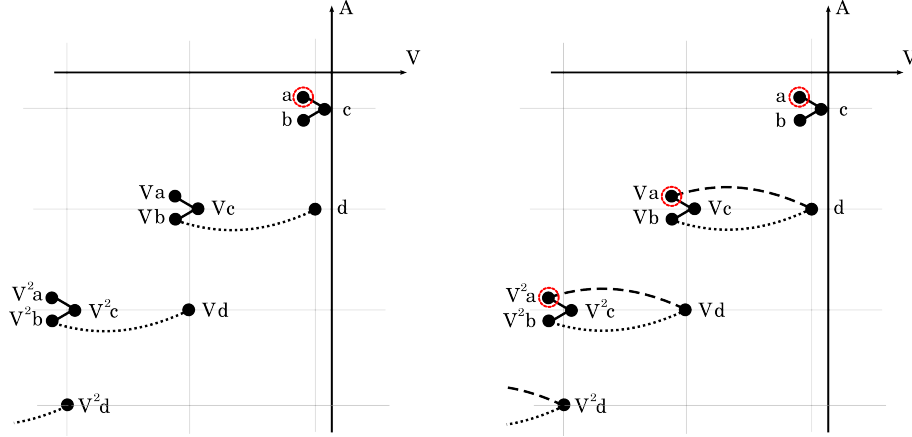


FIGURE 2.14. On the left the complex $\widehat{GC}(L(2, 1), G, 0)$ and on the right the complex $GC^-(L(2, 1), G, 0)$; the dotted line corresponds to multiplication by V_2 , and the hatched one to multiplication by V_1 . Non trivial elements in homology are circled.

PROPOSITION 2.19. *Let G be a grid of parameters (n, p, q) for a knot K . Then the action of multiplication by V_i on the complex $GC^-(G)$ is quasi isomorphic to multiplication by V_j .*

PROOF. See [47, Lemma 4.6.9]; the same homotopies \mathcal{H}_i used there work for knots in lens spaces as well. \square

THEOREM 2.20 ([4]). *The homologies*

$$GH^-(L(p, q), K) = H_*(GC^-(G), \partial)$$

and

$$\widehat{GH}(L(p, q), K) = H_*(\widehat{GC}(G), \partial)$$

regarded as $(\mathbb{Q}, \mathbb{Q}, \mathbb{Z}_p)$ -graded modules over the appropriate ring are invariants of the knot $(L(p, q), K)$. Moreover $(GC^-(G), \partial)$ is quasi isomorphic to a finitely generated $\mathbb{F}[U]$ module, where U acts as any of the V_i , and (\widehat{GC}, ∂) is quasi isomorphic to a finitely generated \mathbb{F} module.

PROOF. Rather than adapting the analogous of the combinatorial proof in [47] to $L(p, q)$, we appeal to the main result of [4]. \square

Due to this Theorem we will sometimes make the notational abuse of writing $\widehat{GH}(L(p, q), K)$ instead of $\widehat{GH}(G)$, G being a grid of parameters (n, p, q) representing K .

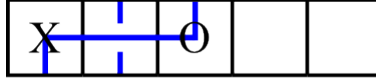


FIGURE 2.15. A grid of dimension 1 for the simple knot $T_2^{5,1}$.

REMARK 2.21. Since the differential preserves the decomposition of the complex in spin^c structures (Proposition 2.16), we can write

$$GH^-(L(p, q), K) = \bigoplus_{\substack{\mathfrak{s} \in \mathbb{Z}_p \\ m, a \in \mathbb{Q}}} GH_m^-(L(p, q), K, a, \mathfrak{s})$$

$$\widehat{GH}(L(p, q), K) = \bigoplus_{\substack{\mathfrak{s} \in \mathbb{Z}_p \\ m, a \in \mathbb{Q}}} \widehat{GH}_m(L(p, q), K, a, \mathfrak{s})$$

and the endomorphism U induced in homology by any of the V_i acts as

$$U : GH_m^-(L(p, q), K, a, \mathfrak{s}) \longrightarrow GH_{m-2}^-(L(p, q), K, a-1, \mathfrak{s})$$

We can finally state the main result of [4]:

THEOREM 2.22 ([4]). *Let G be a grid for a knot $K \subset L(p, q)$. There is a graded isomorphism of $\mathbb{F}[U]$ and \mathbb{F} , respectively, trigraded modules:*

$$HFK^-(L(p, q), K) \cong GH^-(G)$$

$$\widehat{HFK}(L(p, q), K) \cong \widehat{GH}(G)$$

EXAMPLE 2.23. We sketch the computation of the knot Floer homology groups $\widehat{HFK}(L(5, 1), T_2^{5,1})$ (Figure 2.15) contained in Rasmussen's paper [50, Sec. 3.7] for the dual of -5 surgery on the trefoil, and compare it with the same computation made with the definitions of [4]. Rasmussen's computation yields 5 generators (one in each spin^c degree) x_0, \dots, x_4 with Alexander degrees -3, -1, 1, 3 and 0; we get again five generators y_0, \dots, y_4 with tridegree

$$\left(d(5, 1, \mathfrak{s}), \frac{A_{\mathbb{Z}}(x_{\mathfrak{s}})}{5}, \mathfrak{s} \right) \in (\mathbb{Q}, \mathbb{Q}, \mathbb{Z}_p)$$

REMARK 2.24. In each connected 3-manifold Y the isotopy class of the homologically trivial unknot \bigcirc is unique (since it bounds an embedded disk and manifolds are homogeneous); thus we can think of a *local* knot K , *i.e.* a knot contained in a 3-ball inside Y as the connected sum

$$(Y, K) = (Y, \bigcirc) \# (S^3, K')$$

for some knot K' in S^3 . It is a straightforward computation to shown that the grid homology of the unknot $\bigcirc \subset L(p, q)$ is:

$$\begin{aligned} GH^-(L(p, q), \bigcirc) &= \bigoplus_{\mathfrak{s} \in \text{spin}^c(L(p, q))} \mathbb{F}[U]_{[d(p, q, \mathfrak{s}), 0]} \\ \widehat{GH}(L(p, q), \bigcirc) &= \bigoplus_{\mathfrak{s} \in \text{spin}^c(L(p, q))} \mathbb{F}_{[d(p, q, \mathfrak{s}), 0]} \end{aligned}$$

So by Equation (11)

$$(18) \quad GH^-(L(p, q), K) = \bigoplus_{\mathfrak{s} \in \text{spin}^c(L(p, q))} GH^-(S^3, K')_{[d(p, q, \mathfrak{s}), *]}$$

In other words the grid homology of a local knot is completely determined by the homology of the same knot viewed as living in S^3 (and in particular its Alexander degrees are integers).

REMARK 2.25. Recall the definition of *simple knots* from Section 1.2. If G is a dimension 1 grid representing $T_m^{p, q}$, then $|S(G)| = p$, and there is exactly one generator in each spin^c degree. There cannot be any differentials (since ∂ preserves the spin^c degree), so the homologies of $T_m^{p, q}$ are:

$$\begin{aligned} GH^-(T_m^{p, q}) &\cong \bigoplus_{\mathfrak{s} \in \text{spin}^c(L(p, q))} R_{[d(p, q, \mathfrak{s}), A(x_{\mathfrak{s}})]} \\ \widehat{GH}(T_m^{p, q}) &\cong \bigoplus_{\mathfrak{s} \in \text{spin}^c(L(p, q))} \mathbb{F}_{[d(p, q, \mathfrak{s}), A(x_{\mathfrak{s}})]} \end{aligned}$$

where $A(x_{\mathfrak{s}})$ is the Alexander degree of the unique generators in degree \mathfrak{s} . A recursive formula for $A(x_{\mathfrak{s}})$ can be found in [50, Sect. 6], while we carry out some explicit computations in Section 5.1.

As in [4] we say that these knots are *Floer simple* (or *U-knot* in the terminology of [36]), meaning that the rank of the grid homology (over the appropriate ground ring) is exactly one in each spin^c degree.

We introduce yet another version of the complex, which is almost a knot invariant. We will need it shortly after to prove a symmetry property of \widehat{GH} . More importantly, it will be used in the computations of Chapter 6, since the differential is easier to describe and compute.

Consider a grid G of dimension n representing a knot $(L(p, q), K)$; the *tilde complex* $\widetilde{GC}(G)$ is simply the free \mathbb{F} module generated over $S(G)$, with differential counting only those empty rectangles that do not contain any marking either:

$$(19) \quad \widetilde{\partial}(x) = \sum_{y \in S(G)} \sum_{\substack{r \in \text{Rect}^\circ(x, y) \\ (\mathbb{X} \cup \bigcirc) \cap r = \emptyset}} y$$

The tilde-flavored version is not an invariant of the knot represented by the grid. This can be easily seen by computing $\widetilde{GH}(G)$ in any spin^c degree, for the grids of Example 2.14.

However, the hat version can be recovered from it as shown in the next Proposition:

PROPOSITION 2.26 ([47]). *Given a grid G of dimension n representing the knot $K \subset L(p, q)$, there is a trigraded isomorphism*

$$\widehat{GH}(G) = H_* \left(\widetilde{GC}(G), \widetilde{\partial} \right) \cong \widehat{GH}(L(p, q), K) \otimes W^{\otimes(n-1)}$$

where $W = \mathbb{F}_{[0,0]} \oplus \mathbb{F}_{[-1,-1]}$.

We turn now to the behaviour of \widehat{GH} under orientation reversal of the knot:

PROPOSITION 2.27. *If G is a grid of dimension n representing a knot $(L(p, q), K)$ with homology class $m = [K]$, denote by $-G$ the grid with the \mathbb{X} and \mathbb{O} markings exchanged, representing $(L(p, q), -K)$. Then*

$$\widehat{GH}(G, a, \mathfrak{s}) \cong \widehat{GH}(-G, -a, \mathfrak{s} + qm).$$

PROOF. The proof works better with the *tilde* grid homology. As in Lemma 1.11, we identify the generators in the two grids G and $-G$ representing $(L(p, q), K)$ and $(L(p, q), -K)$ respectively. The generators on the two grids have different tridegrees; in particular the (anti-)symmetry of Definition (14) under a swap of the markings, tells us immediately that $A(x) = -A(x')$, where x and x' are the same generator seen in G and $-G$ respectively.

Note that the rectangles which are admissible for $\widetilde{\partial}$ are precisely the same in both cases, so $\widetilde{\partial}x = \widetilde{\partial}x'$. This also means that we do not need to worry about the Maslov gradings, since by Proposition 2.16 two generators connected by a rectangle have Maslov degrees differing by 1.

The Proposition then follows from Lemma 1.11, observing that

$$S(x) - S(x') \equiv \sum_{i=1}^n a_i^{\mathbb{X}} - a_i^{\mathbb{O}} \equiv -mq \pmod{p}$$

□

CHAPTER 3

Sign refined theory

The complexes we have used until now were specifically defined to work with \mathbb{F} as base ring; in particular the proof of Proposition 2.16 relied on the parity of polygon decompositions to ensure that GC^- is in fact a chain complex.

This chapter is devoted to a combinatorial extension of the previous construction with \mathbb{Z} coefficients. This was done in the combinatorial setting for S^3 in [30] (see also [35]).

We will adopt the group theoretic approach first developed in [17] to define a sign function on rectangles, whose properties are precisely tuned to have $\partial^2 = 0$.

One might ask how the theory changes under such a change of coefficients; at the time of writing there is no example of a knot in S^3 whose knot Floer homology with \mathbb{Z} coefficients exhibits torsion (see Problem 17.2.9 of [47]). Even in the lens space case the computations displayed in Section 6 seem to show an analogous situation.

We will find it convenient to define signs on $Rect(G)$, rather than directly on $Rect^\circ(G)$. Moreover the signs will not depend on the choice of a knot, but just on the parameters of the grid.

DEFINITION 3.1. *Given a grid diagram G , a sign assignment on G is a function*

$$\mathcal{S} : Rect(G) \longrightarrow \{\pm 1\}$$

such that the following conditions hold:

- (1) *If $r_1 * r_2 = r_3 * r_4$ then $\mathcal{S}(r_1)\mathcal{S}(r_2) = -\mathcal{S}(r_3)\mathcal{S}(r_4)$*
- (2) *If $r_1 * r_2$ is a horizontal annulus (α -strip), then $\mathcal{S}(r_1)\mathcal{S}(r_2) = 1$*
- (3) *If $r_1 * r_2$ is a vertical annulus (β -strip), then $\mathcal{S}(r_1)\mathcal{S}(r_2) = -1$*

Such a sign \mathcal{S} can be used to promote $\widehat{GC}(G)$ and $GC^-(G)$ from $\mathbb{F}[V_1, \dots, V_n]$ to $\mathbb{Z}[V_1, \dots, V_n]$ complexes. We will prove in Theorem 3.8 that sign assignments actually exist on twisted grid diagrams, and deal with problems relating their uniqueness later on.

To see why the properties given in the previous definition are indeed the right ones, fix a sign assignment \mathcal{S} for G , and define

$$\partial_{\mathcal{S}}^-(x) = \sum_{y \in S(G)} \sum_{\substack{r \in \text{Rect}^\circ(x,y) \\ r \cap \mathbb{X} = \emptyset}} \mathcal{S}(r) \left(\prod_{i=1}^n V_i^{O_i(r)} \right) y$$

Now we can examine the coefficient of a generator $z \neq x$ in $\partial_{\mathcal{S}}^-(x)$; each polygon connecting x to z can be decomposed in two ways (as seen in Proposition 2.16). The pairs corresponding to inequivalent decompositions of the same polygon cancel out due to condition (1).

If instead $x = z$ there are exactly $2n$ possible ways of connecting a generator to itself through empty polygons, which are α and β degenerations; as noted before all of these strips contain one \mathbb{X} marking, so they do not contribute to the differential. Conditions 2 and 3 on \mathcal{S} are necessary when dealing with the filtered case (which we do not consider presently).

The proof of the following result will occupy the rest of the chapter:

THEOREM 3.2. *Sign assignments exist on twisted grid diagrams. Moreover the homology*

$$GH^-(L(p, q), K; \mathbb{Z}) = H_*(GC^-(G), \partial_{\mathcal{S}}^-)$$

does not depend on the choice of the sign assignment.

In order to prove existence, we are going to adopt the approach used in [47], which relies on the paper [17] of Gallais regarding the Spin extension of the permutation groups, introduced in the next definition.

DEFINITION 3.3. *The Spin central extension of the symmetric group \mathfrak{S}_n is the group $\tilde{\mathfrak{S}}_n$ generated by the elements*

$$\langle z, \tilde{\tau}_{i,j} \mid 1 \leq i \neq j \leq n \rangle$$

subject to the following relations:

- $z^2 = 1$ and $z\tilde{\tau}_{i,j} = \tilde{\tau}_{i,j}z$ for $1 \leq i \neq j \leq n$
- $\tilde{\tau}_{i,j}^2 = z$ and $\tilde{\tau}_{i,j} = z\tilde{\tau}_{j,i}$
- $\tilde{\tau}_{i,j}\tilde{\tau}_{k,l} = z\tilde{\tau}_{k,l}\tilde{\tau}_{i,j}$ for distinct $1 \leq i, j, k, l \leq n$
- $\tilde{\tau}_{i,j}\tilde{\tau}_{j,k}\tilde{\tau}_{i,j} = \tilde{\tau}_{j,k}\tilde{\tau}_{i,j}\tilde{\tau}_{j,k} = \tilde{\tau}_{i,k}$ for distinct $1 \leq i, j, k \leq n$

REMARK 3.4. The name Spin central extension is justified by the fact that this group can be derived as a $\mathbb{Z}/2\mathbb{Z}$ extension of \mathfrak{S}_n induced by the short exact sequence

$$(20) \quad 1 \longrightarrow \mathbb{Z}/2\mathbb{Z} \longrightarrow \tilde{\mathfrak{S}}_n \xrightarrow{\pi} \mathfrak{S}_n \longrightarrow 1$$

π is the surjective homomorphism defined by $\pi(z) = 1$ and $\pi(\tilde{\tau}_{i,j}) = \tau_{i,j}$.

DEFINITION 3.5. A section for $\tilde{\mathfrak{S}}_n$ is a map

$$\rho : \mathfrak{S}_n \longrightarrow \tilde{\mathfrak{S}}_n$$

such that $\pi \circ \rho = Id_{\mathfrak{S}_n}$. Denote the set of sections by Sec_n . We will make a slight notational abuse, and also call sections the maps

$$\rho : \mathfrak{S}_n \times (\mathbb{Z}_p)^n \longrightarrow \tilde{\mathfrak{S}}_n \times (\mathbb{Z}_p)^n$$

obtained by taking the product of a section with the identity map on $(\mathbb{Z}_p)^n$.

We are going to define a map

$$(21) \quad \varphi : Rect(G) \longrightarrow \tilde{\mathfrak{S}}_n \times (\mathbb{Z}_p)^n$$

that associates to a rectangle $r \in Rect(x, y)$ an element in $\tilde{\mathfrak{S}}_n \times (\mathbb{Z}_p)^n$, enabling us to “compare” the generators containing the vertices of r . If the elements of x and y in the bottom edge of r belong respectively to β_i and β_j , the first component of $\varphi(r)$ is given by the generalized transposition $\tilde{\tau}_{i,j}$. The second component of φ is given by the difference between the p -coordinates of x and y . The two generators differ only in two components, so necessarily

$$(a_1^x - a_1^y, \dots, a_n^x - a_n^y) = (0, \dots, 0, \pm k, 0, \dots, 0, \mp k, 0, \dots, 0)$$

for some $k \in \{0, \dots, p - 1\}$.

REMARK 3.6. To simplify the proof of the theorem, we observe here that the generalized permutation part of the map φ does not depend on the possible “wrapping” of a rectangle on the grid, while the $(\mathbb{Z}_p)^n$ part does.

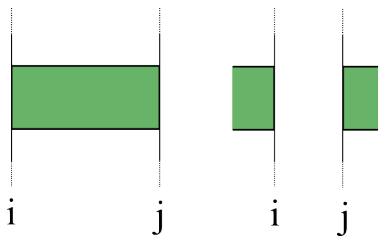


FIGURE 3.1. The generalized transpositions associated to these two rectangles are $\tilde{\tau}_{ij}$ and $\tilde{\tau}_{ji} = z \cdot \tilde{\tau}_{ij}$.

EXAMPLE 3.7. Consider the rectangles R in the left part of Figure 2.11; the value $\varphi(R)$ associated is $(\tilde{\tau}_{1,3}, (0, -1, 0, 1, 0))$ for the horizontal one and $(\tilde{\tau}_{4,5}, (0, 0, 0, 0))$ for the vertical.

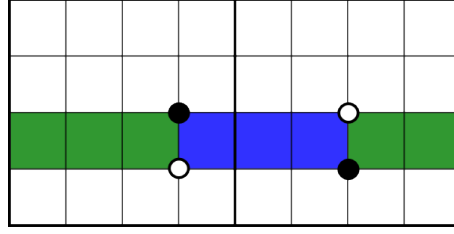


FIGURE 3.2. An α -strip of height 1. Only the relevant parts of the generators are shown.

Given a section ρ we can build a sign assignment as follows¹:

$$(22) \quad \mathcal{S}_\rho(r) = \begin{cases} 1 & \text{if } \rho(x)\varphi(r) = \rho(y) \\ -1 & \text{if } \rho(x)\varphi(r) = z \cdot \rho(y) \end{cases}$$

for $r \in \text{Rect}(x, y)$.

THEOREM 3.8. *For a given section ρ , the function \mathcal{S}_ρ defined above is a sign assignment.*

PROOF. First we deal with α -strips; write²

$$\begin{aligned} \varphi(R_1) &= (\tilde{\tau}_{i,j}, (\dots, k, \dots, -k, \dots)) \\ \varphi(R_2) &= (\tilde{\tau}_{j,i}, (\dots, -k, \dots, k, \dots)) \end{aligned}$$

With $R_1 \in \text{Rect}^\circ(x, y)$, $R_2 \in \text{Rect}^\circ(y, x)$. So if

$$\rho(x)\varphi(R_1) = \rho(y)$$

then, recalling that $\tilde{\tau}_{j,i}\tilde{\tau}_{i,j} = 1$,

$$\rho(x) = \rho(x)\varphi(R_1)\varphi(R_2) = \rho(y)\varphi(R_2)$$

which implies $\mathcal{S}(R_1) = \mathcal{S}(R_2) = 1$.

If instead we had

$$\rho(x)\varphi(R_1) = z \cdot \rho(y) \quad \Rightarrow \quad \mathcal{S}(R_1) = -1$$

then

$$z \cdot \rho(x) = \rho(y)\varphi(R_2) \quad \Rightarrow \quad \mathcal{S}(R_2) = -1$$

In both cases $\mathcal{S}(R_1)\mathcal{S}(R_2) = 1$.

¹The operation on $\tilde{\mathfrak{S}}_n \times (\mathbb{Z}_p)^n$ considered consists in the product of generalized permutations on the first factor, and addition on the p -coordinates. Multiplication by an element of $\tilde{\mathfrak{S}}_n$ only affects the first component.

²The dots correspond to 0 components.

Next we examine the behavior of signs for β -strips. As in the previous case there is only one possible generator y that induces a decomposition of an annulus starting from x . The permutation components of the images under φ of the two rectangles $R_1 \in \text{Rect}(x, y)$ and $R_2 \in \text{Rect}(y, x)$ are both $\tilde{\tau}_{i,j}$. So if

$$\rho(x)\varphi(R_1) = \rho(y)$$

$$\rho(x)z = \rho(x)\varphi(R_1)\varphi(R_2) = \rho(y)\varphi(R_2)$$

which implies $\mathcal{S}(R_1)\mathcal{S}(R_2) = -1$.

The centrality of z tells us that the case with $\mathcal{S}(R_1) = -1$ gives the same result.

Now, given a general polygon $P = r * r'$ connecting two different generators x to t , it is easy to check that Definition 3.3 implies that

$$\rho(x) = z^{\frac{1-\mathcal{S}(r)\mathcal{S}(r')}{2}} \varphi(r)\varphi(r')\rho(t).$$

According to the proof of Proposition 2.16, each polygon which is not a degeneration can be written as the concatenation of two distinct pairs of rectangles; so we just need to check for all possible polygons

$$P = r(x, y) * r(y, t) = r(x, w) * r(w, t)$$

that the following identity, which ensures the two polygons have opposite signs, is verified:

$$(23) \quad \varphi(r(x, y))\varphi(r(y, t)) = z \cdot \varphi(r(x, w))\varphi(r(w, t))$$

where $y \neq w$ are two auxiliary generators which differ by only one transposition from x and t . All we need to do is verify Equation (23) in the cases $M = 2, 3, 4$ from the proof³ of Proposition 2.16.

It is easy to check that the generalized permutations associated to polygons corresponding to the $M = 3$ case are the same of [47, Ch. 15] in the S^3 case; in particular this is true even when the rectangles wrap around the grid, since the generalized permutation part does not depend on the p -coordinates of the generators. $M = 4$ is immediate: as shown in Figure 3.3 the permutations associated to the two decompositions are such that Equation (23) becomes the third relation defining $\tilde{\mathfrak{S}}_n$.

Lastly we deal with $M = 2$; the generalized transpositions associated to $r(x, y)$ and $r(y, z)$ are $\tilde{\tau}_{ij}$ and $\tilde{\tau}_{ji}$ for one decomposition, and $\tilde{\tau}_{ij}, \tilde{\tau}_{ij}$ for the other.

So in particular this implies that if $\mathcal{S}(r(x, y))\mathcal{S}(r(y, z)) = -1$ then $\mathcal{S}(r(x, w))\mathcal{S}(r(w, z)) = 1$ and viceversa, and Equation (23) is always satisfied.

³We already considered $M = 0$, and $M = 1$ was discarded.

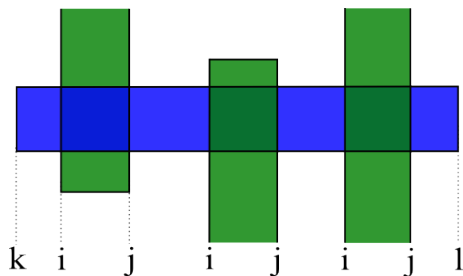


FIGURE 3.3. The generalized permutations associated to the two rectangles are $\tilde{\tau}_{ij}$ and $\tilde{\tau}_{kl}$.

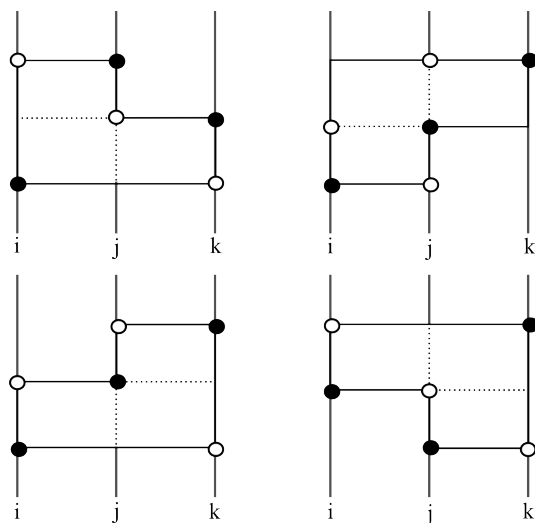


FIGURE 3.4. The four relevant combinatorial possibilities for the $M = 3$ case in the S^3 setting. Remember that the possible wrapping of one rectangle over the other does not change the relations in $\tilde{\mathfrak{S}}_n$.

□

REMARK 3.9. It is worth noting that the trivial choice for signs (treating each rectangle just as a generalized permutation, like for the S^3 setting) can't distinguish a β degeneration from other polygons which admit two distinct decompositions into rectangles, as shown in Figure 3.5.

REMARK 3.10. The techniques used in [47, Ch.15] can be applied *verbatim* for sign assignments in lens spaces, proving that each sign assignment is induced by exactly two sections.

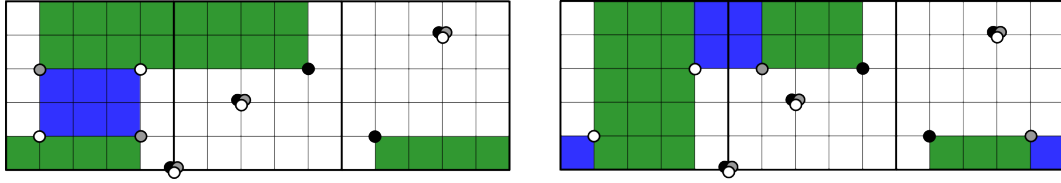


FIGURE 3.5. The white and black generators have the same permutation component, but the polygon connecting them admits two distinct decompositions. In particular it can not be an α/β -strip.

Now, for the uniqueness denote by $\mathcal{G}auge(G)$ the group of maps

$$v : S(G) \longrightarrow \mathbb{Z}/2\mathbb{Z}.$$

$\mathcal{G}auge(G)$ acts on sections as follows:

$$(24) \quad \rho^v(x) = \begin{cases} \rho(x) & \text{if } v(x) = 1 \\ z \cdot \rho(x) & \text{if } v(x) = -1 \end{cases}$$

This action is free and transitive; $\mathcal{G}auge(G)$ also acts on the set of sign assignments: if \mathcal{S} is a sign on a grid G and $v \in \mathcal{G}auge(G)$, define $\mathcal{S}^v(r) = v(x)\mathcal{S}(r)v(y)$ for $r \in Rect(x, y)$.

As in the S^3 case it is easy to show that there is only one sign assignment on a grid, up to this action of $\mathcal{G}auge(G)$.

The uniqueness now follows by noting that if \mathcal{S}_1 and \mathcal{S}_2 are two sign assignments on a grid G , then $\mathcal{S}_2 = \mathcal{S}_1^v$ for some $v \in \mathcal{G}auge(G)$, and the map

$$f : (GC^-(G), \partial_{\mathcal{S}_1}) \longrightarrow (GC^-(G), \partial_{\mathcal{S}_2})$$

given by $f(x) = v(x)x$ is an isomorphism (of trigraded R modules).

This concludes the proof of Theorem 3.2.

3.0.1. A small example. Knot theory (and hence grid homology) in lens spaces is much more complicated than its 3-sphere counterpart: besides the fact that knots need not to be homologically trivial, they can also be nontrivial for grids with small parameters. Define

$$f(p) = \min\{\text{dimension of a grid representing a non-simple knot in } L(p, q)\}$$

Then $f(1) = 5$, $f(2) = 3$ and $f(p > 2) = 2$. What follows is an explicit computation of the grid homologies for the smallest (in the sense above) non-trivial knot in $L(3, 1)$.

EXAMPLE 3.11. We sketch here the computation for the various flavors for the sign refined grid homology in the case of the knot in

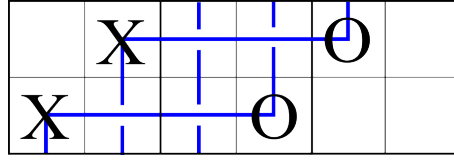


FIGURE 3.6. The knot in $L(3, 1)$ described by $\mathbb{X}, \mathbb{O} = [0, 1], [3, 4]$.

Figure 3.6. The generating set $S(G, \mathfrak{s})$ in each spin^c degree has 6 elements, which we will denote x_s^0, \dots, x_s^5 for⁴ $\mathfrak{s} = 0, 1$. After choosing a sign assignment, we can list the generators, with their bidegree and differential:

generator	(M, A)	differential
<hr/>		
spin^c degree = 0		
x_0^0	$\left(\frac{3}{2}, 1\right)$	$\partial(x_0^0) = 0$
x_0^1	$\left(\frac{1}{2}, 0\right)$	$\partial(x_0^1) = (V_1 - V_2)x_0^0$
x_0^2	$\left(\frac{1}{2}, 0\right)$	$\partial(x_0^2) = (V_2 - V_1)x_0^0$
x_0^3	$\left(-\frac{1}{2}, -1\right)$	$\partial(x_0^3) = V_2(x_0^1 + x_0^2)$
x_0^4	$\left(-\frac{1}{2}, -1\right)$	$\partial(x_0^4) = V_1(x_0^1 + x_0^2)$
x_0^5	$\left(-\frac{3}{2}, -2\right)$	$\partial(x_0^5) = -V_1x_0^3 + V_2x_0^4$
<hr/>		
spin^c degree = 1		
x_1^0	$\left(\frac{7}{6}, 0\right)$	$\partial(x_1^0) = -x_1^1 + x_1^2$
x_1^1	$\left(\frac{1}{6}, 0\right)$	$\partial(x_1^1) = 0$
x_1^2	$\left(\frac{1}{6}, 0\right)$	$\partial(x_1^2) = 0$
x_1^3	$\left(\frac{1}{6}, -1\right)$	$\partial(x_1^3) = x_1^4 - x_1^5$
x_1^4	$\left(-\frac{5}{6}, -1\right)$	$\partial(x_1^4) = V_2x_1^1 - V_1x_1^2$
x_1^5	$\left(-\frac{5}{6}, -1\right)$	$\partial(x_1^5) = V_2x_1^1 - V_1x_1^2$

Since $\widetilde{GC}(G, 0)$ has no nontrivial differentials (as can be seen by imposing $V = 0$ in the list above), the homology coincides with the complex. In spin^c degree 1 instead the tilde homology is generated by x_1^1 and x_1^4 , so $\widetilde{GH}(G, 1) \cong \mathbb{Z}_{[\frac{1}{6}, 0]} \oplus \mathbb{Z}_{[-\frac{5}{6}, -1]}$.

The computation of the minus flavor is just slightly more involved; $GH^-(L(3, 1), K, 0)$ is composed by a copy of $\mathbb{Z}[U]$ generated by x_0^0 , plus two U -torsion components, generated by $x_0^1 + x_0^2$ and $x_0^3 + x_0^4$.

⁴The homologies in spin^c degrees 1 and 2 have a similar behavior, so we omit the latter.

Altogether

$$GH^-(L(3,1), K, 0) = \mathbb{Z}[U]_{[\frac{3}{2},1]} \oplus \mathbb{Z}_{[\frac{1}{2},0]} \oplus \mathbb{Z}_{[-\frac{1}{2},-1]}$$

In the last case we get

$$GH^-(L(3,1), K, 1) = \mathbb{Z}[U]_{[\frac{1}{6},0]}$$

generated over $\mathbb{Z}[U]$ by x_1^1 .

The hat homology can be obtained either by factoring out the tensor product with $\mathbb{Z}_{[0,0]} \oplus \mathbb{Z}_{[-1,-1]}$ from the tilde flavor, or deleting all dotted differentials in the minus complex of Figure 3.7, then computing the homology:

$$(25) \quad \widehat{GH}(L(3,1), K, \mathfrak{s}) = \begin{cases} \mathbb{Z}_{[\frac{3}{2},1]} \oplus \mathbb{Z}_{[\frac{1}{2},0]} \oplus \mathbb{Z}_{[-\frac{1}{2},-1]} & \text{if } \mathfrak{s} = 0 \\ \mathbb{Z}_{[\frac{1}{6},0]} & \text{if } \mathfrak{s} = 1 \end{cases}$$

REMARK 3.12. This particular knot is interesting for several reasons; for example it can be proved that despite being nullhomologous it is not even concordant to a local knot (see Chapter 4, and example 4.13).

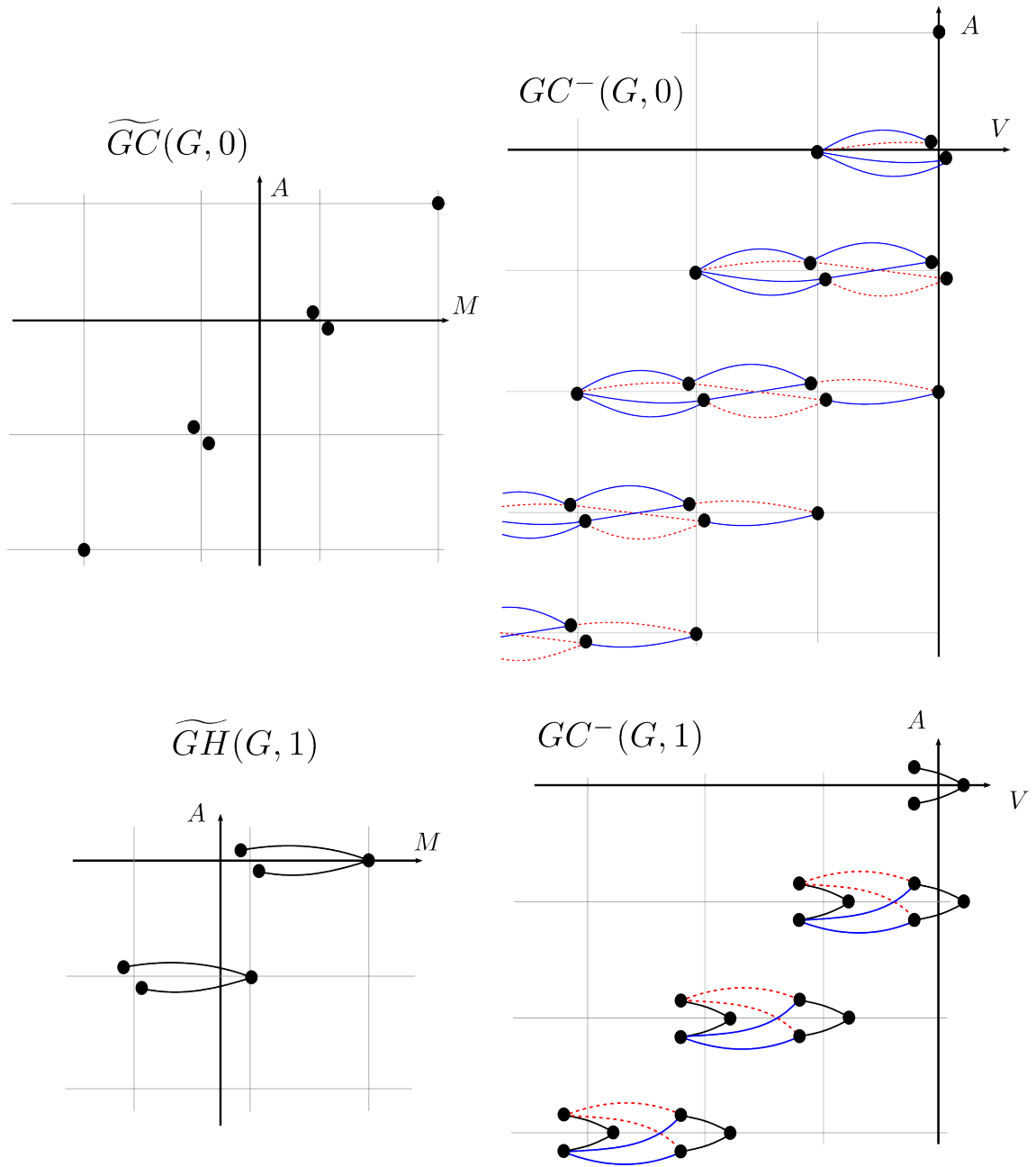


FIGURE 3.7. The complexes $\widetilde{GC}(G, \mathfrak{s})$ (on the left) and $GC^-(G, \mathfrak{s})$ (on the right) for $\mathfrak{s} = 0, 1$. Dotted red lines denote multiplication by V_1 and blue lines by V_2 .

CHAPTER 4

4-dimensional aspects

In this chapter we analyze some aspects of the fruitful interaction between 4-dimensional knot theoretic constructions and Knot Floer homology. In particular we adapt a Floer theoretic bound for cobordisms of knots in the three sphere to knots in lens spaces, and investigate the structure of concordances of knots in lens spaces.

4.1. Definitions

In a lens space there are at least two different ways to generalize the notion of slice genus to rationally nullhomologous knots. We introduce the first one here, and postpone the second one to the end of this chapter.

DEFINITION 4.1.

$$\tilde{g}(K) = \min\{g(\Sigma) \mid \Sigma \text{ is a smooth cobordism between } K \text{ and } T_{[K]}^{p,q}\}$$

so $\Sigma \subset L(p, q) \times [0, 1]$, in such a way that $\Sigma \cap L(p, q) \times \{0\} = K$ and $\Sigma \cap L(p, q) \times \{1\} = T_{[K]}^{p,q}$. This definition relies on [10, Prop. 4.6] (see also Proposition 5.16).

It is possible to define a notion of *concordance* between knots in lens spaces which closely resembles the usual one, but with a few caveats:

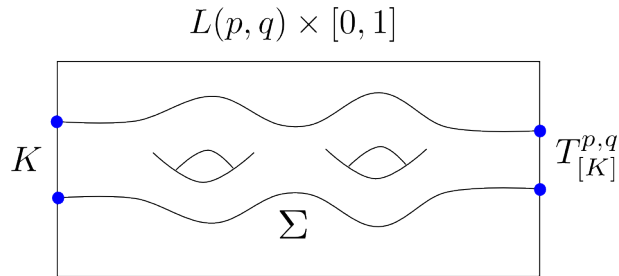


FIGURE 4.1. A cobordism to a trivial knot for $\tilde{g}(K)$.

- The connected sum of two lens spaces is not a lens space if either one is non trivial, so there is no general notion of connected sum of knots. This implies that the set of concordance classes is not a group in a natural way.
- We can still however take the connected sum of a knot $(L(p, q), K)$ with a classical knot (S^3, K') ; this will give us an action on lens space concordances by the usual concordance group.
- Since concordances preserve the homology class, the set of concordances will split according to homology classes.

DEFINITION 4.2. A concordance between two knots $K_0, K_1 \subset L(p, q)$ is a smoothly embedded annulus

$$A = S^1 \times I \hookrightarrow L(p, q) \times I$$

such that $A \cap L(p, q) \times \{i\} = K_i$ for $i = 0, 1$.

In other words a concordance is just a cobordism of genus 0, as usual. We are going to denote by $\mathcal{C}^{p,q}$ the set of knots in $L(p, q)$ up to concordance; that is we regard two knots as equal, and write $[K_0] \sim [K_1]$, if they are connected by a concordance.

As pointed out above, there is a natural splitting of $\mathcal{C}^{p,q}$:

$$\mathcal{C}^{p,q} = \bigoplus_{m \in H_1(L(p,q); \mathbb{Z})} \mathcal{C}_m^{p,q}$$

REMARK 4.3. Denote by $\mathcal{K}(S^3)$ the set of isotopy classes of knots in S^3 ; there is a natural action of $\mathcal{K}(S^3) \curvearrowright \mathcal{C}^{p,q}$ which respects the splitting in to homology components. It is defined simply as

$$(S^3, K) \cdot [(L(p, q), K')] = [(L(p, q), K \# K')]$$

We can show that this action is in fact well defined and factors through the concordance group \mathcal{C} :

PROPOSITION 4.4. If $K_0 \sim K_1$ in \mathcal{C} , then

$$(S^3, K_0) \cdot [(L(p, q), K)] \sim (S^3, K_1) \cdot [(L(p, q), K)]$$

PROOF. Denote by $A \subset S^3 \times [0, 1]$ an annulus realizing the concordance between K_0 and K_1 . Then, as in [28, Thm 3.3.2] we can suppose that A locally coincides with the product $a \times [0, 1]$ for a small arc $a \subset K_0$. Remove from $S^3 \times [0, 1]$ the product $D \times [0, 1]$, where D is a 3-disk intersecting K_0 only in a ; the complement is homeomorphic to $\mathbb{D}^3 \times [0, 1]$.

Take the trivial concordance $K \times [0, 1] \subset Y \times [0, 1]$ and remove a product $D' \times [0, 1]$, where D' is a 3-disk intersecting K in an unknotted arc. Then we just need to glue $S^3 \setminus D \times [0, 1]$ to $Y \setminus D' \times [0, 1]$, in

such a way that the two concordances are glued along their vertical boundaries¹, making the edges of the annuli coincide: the resulting annulus is a concordance from $K_0\#K$ to $K_1\#K$ in $Y \times [0, 1]$. \square

So we have in fact an action of \mathcal{C} on each $\mathcal{C}_m^{p,q}$. We will show that there are knots in any lens space which are not concordant to a connected sum of a simple knot with a knot in S^3 . We can however introduce yet another notion of concordance on knots in $L(p, q)$, by taking the \mathcal{C} -action in to account:

DEFINITION 4.5. *Two knots K_0 and K_1 in $L(p, q)$ are almost concordant, written $K_0 \sim K_1$, if there exist two knots $K'_0, K'_1 \subset S^3$ such that*

$$K_0\#K'_0 \sim K_1\#K'_1$$

Clearly two concordant knots are also almost concordant (just choose $K'_0 = K'_1 = \bigcirc$), but the converse does not hold. Towards the end of this chapter we will outline a way to obstruct the existence of almost-concordances, after introducing a new invariant τ_{sh} capable of distinguishing them.

In a similar way we can consider knots which are not in the image of the previously defined action:

DEFINITION 4.6. *Call a knot $(L(p, q), K)$ genuine if it is not a connected sum with a knot in S^3 , so there is no embedded 3-ball B that intersects K non trivially and whose boundary² intersects K exactly twice. By triviality of the intersection with B we mean that the pair $(B, K \cap B)$ is isotopic (relatively to the boundary) to the couple $(\mathbb{D}^2 \times \mathbb{D}^1, \{0\} \times \mathbb{D}^1)$.*

It was first proven by Kirby and Lickorish that every knot in S^3 is concordant to a prime knot. Using the same argument of Livingston [27], we can obtain an analogous result:

THEOREM 4.7. *Every knot $K \subset L(p, q)$ is concordant to a genuine knot.*

PROOF. Consider the knot $P \subset S^1 \times \mathbb{D}^2$ shown in Figure 4.2.

Given any knot $(L(p, q), K)$, we can remove a tubular neighborhood $\nu(K)$ and glue in the solid torus containing the pattern, obtaining a new knot $(L(p, q), K_P)$. The concordance suggested in Figure 4.2 induces a concordance from K_P to K . Now we just need to check that

¹By vertical we mean the part created by removing the intersection with the disks D or D' times $[0, 1]$.

²The boundary of a ball as such is usually called a *Conway sphere*.

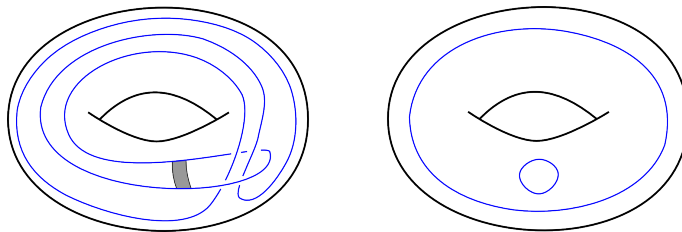


FIGURE 4.2. The pattern for the satellite construction. Attaching the grey band, and capping the null-homologous component, yields a genus-0 cobordism in $S^1 \times \mathbb{D}^2 \times [0, 1]$ between P and the core of the solid torus with a trivial component (on the right). Capping the component bounding a disk gives the required concordance.

K_P is in fact genuine; we start by noting that the pattern inside the solid torus is prime³, *i.e.* it can not be split into non trivial knots by a Conway sphere. Then we just need to argue by contradiction that any sphere S giving a decomposition of K_P can be isotoped away from the torus given by the boundary of the neighborhood for the original knot K . So $S \subset \nu(K)$, and we can conclude by the primeness of P . This can be done exactly as in [27, Thm. 4.2]. We sketch the construction here, since it will be useful in answering Question 4.32. If S is the embedded sphere giving a decomposition in two summands of K_P , call R the annulus obtained by deleting from S a small neighborhood of the two points $K_P \cap S$. The intersection between R and $\partial\nu(K)$ is composed of nullhomologous circles (in R), and circles which are parallel to ∂R . The first kind can be eliminated by isotopies, starting from the innermost ones. We want to show that there can not be any intersection component which is parallel to ∂R ; if such intersections existed, by considering one closest to ∂R we could find a disk bounding a meridian of $\partial\nu(K)$ having intersection 1 with P . But this is absurd, since the minimal number of intersections between P and a disk cobounding a meridian $p \times S^1$ in the solid torus is 3. \square

REMARK 4.8. If a knot $(L(p, q), K)$ is such that

$$rk\left(\widehat{GH}(L(p, q), K, \mathfrak{s})\right) = 1 \quad \text{and} \quad rk\left(\widehat{GH}(L(p, q), K, \mathfrak{s}')\right) \neq 1$$

for some $\mathfrak{s}' \neq \mathfrak{s}$, then it is genuine by Equation (11), coupled with the unknot recognition of \widehat{HFK} in S^3 (cf. Theorem 5.1).

³This fact is proven in a more general setting in [27].

The main tool we are going to use in order to study the notions defined in this chapter will be a modified version of the τ invariant derived from GH^- . This invariant was first defined for knots in the 3-sphere in the holomorphic setting in [37], and it had proven to be extremely useful since. It is a concordance invariant⁴, and its properties can be exploited *e.g.* to give a proof of the Milnor conjecture and to exhibit infinitely many exotic \mathbb{R}^4 (see [47, Ch. 8]).

The extension to rationally nullhomologous knots in other manifolds, was not present in the original paper of Ozsváth and Szabó, and was first carried out in [46].

DEFINITION 4.9. For $\mathfrak{s} \in \text{spin}^c(L(p, q))$ define the τ -invariants of a knot $(L(p, q), K)$:

$$\tau^{\mathfrak{s}}(K) = -\max\{a \in \mathbb{Q} \mid \exists [x] \in GH^-(K, a, \mathfrak{s}) \text{ such that } \forall d \geq 0, U^d[x] \neq 0\}$$

and

$$\tau(K) = (\tau^0(K), \dots, \tau^{p-1}(K)) \in \mathbb{Q}^p$$

In other words, $\tau^{\mathfrak{s}}(K)$ is (minus) the maximal Alexander degree of generators in $GH^-(K, \mathfrak{s})$ which are not U -torsion.

It will also turn out to be useful to consider a normalized version of these τ -invariants:

$$\tilde{\tau}(K) = (\tilde{\tau}^0(K), \dots, \tilde{\tau}^{p-1}(K)) \in \mathbb{Z}^p$$

where $\tilde{\tau}^{\mathfrak{s}}(K) = \tau^{\mathfrak{s}}(K) - \tau^{\mathfrak{s}}(T_{[K]}^{p,q})$.

Note that by Remark 4.11 these normalized τ invariants are p -tuples of integers.

Clearly the normalized invariants vanish on simple knots. We are going to denote the component of τ of maximal (resp. minimal) value by τ^{\max} (resp. τ^{\min}).

REMARK 4.10. We collect here some facts about these invariants:

- The invariance of the τ p -tuple follows from the fact that the chain homotopy type of GH^- is a knot invariant.
- By Remark 2.25, we can identify $\tau^{\mathfrak{s}}(T_m^{p,q})$ with $-A(x_{\mathfrak{s}})$, minus the Alexander degree of the only generator of $\widehat{GC}(G)$ in spin^c degree \mathfrak{s} , where G is a grid of dimension 1 representing $T_m^{p,q}$ (see also Section 5.1).
- The same invariants (with the filtration of Remark 2.12) were defined by Rasmussen in [50].
- There is also an alternative definition of these τ invariants in term of the *filtered* hat homology⁵: $\tau^{\mathfrak{s}}(K)$ is the minimal

⁴In fact it provides an homomorphism $\tau : \mathcal{C} \rightarrow \mathbb{Z}$, see also Theorem 4.12.

⁵See [47].

rational number r such that the natural inclusion map

$$\iota : \widehat{\mathcal{F}}(L(p, q), K, r, \mathfrak{s}) \longrightarrow \widehat{CF}(L(p, q), \mathfrak{s})$$

is non trivial in homology.

REMARK 4.11. If G and G' are two grids representing two knots $K, K' \subset L(p, q)$, and they differ by a crossing change, then the Alexander degrees of the generators in the same spin^c structure differ by integers. To see why this is the case fix a generator on the grid and think of it as living on G and G' . It is easy to show that the difference of its Alexander degrees in the two grids is an integer, using Equation (14).

The following Theorem was proved for knots in S^3 in [37], building on [39, Theorem 7.1] (which instead works for general 3-manifolds). We reformulate it here as follows:

THEOREM 4.12 ([37]). *Let (S^3, K) and $(L(p, q), K')$ be two knots; then the τ -invariants satisfy this additivity formula:*

$$\tau^{\mathfrak{s}}(K' \# K) = \tau^{\mathfrak{s}}(K') + \tau(K)$$

In other words, the action of \mathcal{C} shifts the τ -invariants of $(L(p, q), K')$ in a uniform manner in each spin^c structure.

EXAMPLE 4.13. We can now continue Example 3.0.1, adding the computations for the τ invariants. The tower of $GH^-(K, 0)$ is generated by the element $x_0^0 = \mathbb{Z}_{[\frac{3}{2}, 1]}$ so $\tau^0(K) = -1$, while in the other two cases the Alexander degree of the only generator is 0, so $\tau^1(K) = \tau^2(K) = 0$. Note that since K is nullhomologous $\tilde{\tau}(K) = \tau(K) = (-1, 0, 0)$.

4.2. Genus bounds

The following Theorem is a generalization of a well known result for knots in the 3-sphere, first proven for knots in S^3 by Sarkar in [52] in a purely combinatorial setting. In the same paper it is used to give an elementary proof of the Milnor Conjecture, first proven by Kronheimer and Mrowka in [26] using gauge theoretic techniques.

THEOREM 4.14. *Let Σ be a smooth cobordism of genus $g(\Sigma)$ in $L(p, q) \times [0, 1]$ between the knots K_0 and K_1 . Then $\forall \mathfrak{s} \in \text{spin}^c(L(p, q))$:*

$$|\tau^{\mathfrak{s}}(K_0) - \tau^{\mathfrak{s}}(K_1)| = |\tilde{\tau}^{\mathfrak{s}}(K_0) - \tilde{\tau}^{\mathfrak{s}}(K_1)| \leq g(\Sigma)$$

The proof of this theorem will occupy the rest of the section; it will substantially follow its S^3 analogue as detailed in [47], highlighting the parts in which the two approaches differ.

But first we show some useful and immediate consequences of Theorem 4.14:

COROLLARY 4.15. *Suppose $(L(p, q), K_0) \sim (L(p, q), K_1)$. Then, for all $\mathfrak{s} \in \text{spin}^c(L(p, q))$*

$$\tau^{\mathfrak{s}}(K_0) = \tau^{\mathfrak{s}}(K_1)$$

that is the τ (and thus $\tilde{\tau}$) invariants are in fact concordance invariants.

PROOF. By hypothesis there is a genus-0 surface Σ connecting K_0 and K_1 in $L(p, q) \times [0, 1]$, so for each $\mathfrak{s} \in \text{spin}^c(L(p, q))$:

$$0 \leq |\tau^{\mathfrak{s}}(K_0) - \tau^{\mathfrak{s}}(K_1)| \leq g(\Sigma) = 0$$

□

REMARK 4.16. The previous Theorem implies that:

$$|\tau^{\mathfrak{s}}(K_1) - \tau^{\mathfrak{s}}(T_{[K]}^{p,q})| = |\tilde{\tau}^{\mathfrak{s}}(K)| \leq |\tilde{\tau}^{\text{max}}(K)| \leq \tilde{g}(K)$$

for all $\mathfrak{s} \in \text{spin}^c(L(p, q))$.

COROLLARY 4.17. *If K is tilde-slice, that is $\tilde{g}(K) = 0$, then*

$$\tilde{\tau}^{\mathfrak{s}}(K) = 0 \quad \forall \mathfrak{s} \in \text{spin}^c(L(p, q))$$

So these τ -invariants provide obstructions to the tilde-sliceness; it would be interesting to tie them to the $W_{p,q}$ genus too (see Definition 4.41 Conjecture 4.45).

Since to prove Theorem 4.14 we will use the normal form for cobordisms developed in the introduction, we will necessarily have to deal with the extension of the grid homology to links.

DEFINITION 4.18. *Consider a grid G of dimension n representing an m -component link $L \subset L(p, q)$; the (uncollapsed) link grid homology of L is the homology of the complex $GC^-(G)$, freely generated over $\mathbb{F}[V_1, \dots, V_n]$ by $S(G)$ with the same differential as the single component theory (Equation (16)).*

The only difference with the grid homology for knots resides in a shift of the Alexander grading:

$$(26) \quad A(x) = \frac{1}{2p} \left[\mathcal{I}(\tilde{\mathbb{O}}, \tilde{\mathbb{O}}) - \mathcal{I}(\tilde{\mathbb{X}}, \tilde{\mathbb{X}}) + 2\mathcal{I}(\tilde{\mathbb{X}}, \tilde{x}) - 2\mathcal{I}(\tilde{\mathbb{O}}, \tilde{x}) \right] + \frac{m-n}{2}$$

THEOREM 4.19 ([47]). *The homology of this complex, which we will denote again by $GH^-(L(p, q), L)$ is an invariant of the link $(L(p, q), L)$.*

Now, one key fact is that in the multi-component case, the action of the V_i variables depends solely on the component where the corresponding \mathbb{O} marking lies:

PROPOSITION 4.20 ([47]). *If \mathbb{O}_i and \mathbb{O}_j belong to the same component of L , then the action of V_i is chain homotopic to the action of V_j .*

This Proposition is then a straightforward generalization to links of Proposition 2.19; in particular the homology $GH^-(L(p, q), L) = H_*(CC^-(G), \partial^-)$ is a (finitely generated) $\mathbb{F}[U_1, \dots, U_m]$ -module.

Now we can define yet another version of the grid homology for links, in which this disparity between variables belonging to different components is algebraically democratized:

DEFINITION 4.21. *With the notation of the previous definition, choose an \mathbb{O} marking $\mathbb{O}_{i_1}, \dots, \mathbb{O}_{i_m}$ from each component. Then the collapsed grid homology for links is the homology of the complex defined as*

$$cGC^-(G) = GC^-(G) / \{V_{i_1} = \dots = V_{i_m}\}$$

endowed with the usual Maslov and $spin^c$ degrees (Equations (13) and (15)), differential (Equation (16)), and Alexander degree as in Equation (26). We denote the homology $H_(cGC^-(G), \partial^-)$ by $cGH^-(G)$. As the uncollapsed grid homology for knots, it is chain homotopic to a finitely generated $\mathbb{F}[U]$ module, since we equalized the action of variables corresponding to different components.*

THEOREM 4.22 ([47]). *Let G represent the link $L \subset L(p, q)$; then the homology $cGH^-(L(p, q), L) = H_*(cGC^-(G), \partial^-)$ is a finitely generated $\mathbb{F}[U]$ module, which is an invariant of $(L(p, q), L)$.*

We will use this following result to define the analogue of the τ invariants in the multi-component case.

PROPOSITION 4.23. *In each $spin^c$ degree \mathfrak{s} there is an isomorphism*

$$cGH^-(G, \mathfrak{s}) \otimes \mathbb{F}[U, U^{-1}] \cong \bigoplus_{2^{m-1}} \mathbb{F}[U, U^{-1}]$$

PROOF. This is a direct consequence of [47, Sec. 8.2.1], together with the fact that lens spaces are L -spaces. \square

DEFINITION 4.24. *In analogy with the previous definition we can derive the collapsed hat homology as the homology of the complex*

$$\widehat{cGC} = CG^-(G) / \{V_{i_1} = \dots = V_{i_m} = 0\}$$

where G represents an m -component link $(L(p, q), L)$, and the \mathbb{O}_{i_j} are m markings belonging to different components of L .

We can generalize Definition 4.9, by introducing the τ -set for the collapsed grid homology of links:

DEFINITION 4.25. *Again, suppose that G is a grid of parameters (n, p, q) , representing an m -component link L . In each spin^c degree \mathfrak{s} consider the 2^{m-1} rational numbers*

$$\tau_{min}^{\mathfrak{s}} = \tau_1^{\mathfrak{s}} \leq \dots \leq \tau_{2^{m-1}}^{\mathfrak{s}} = \tau_{max}^{\mathfrak{s}}$$

given by minus the Alexander degrees of 2^{m-1} homogeneous elements generating $cGH^-(L)/UTor(cGH^-(L))$.

Here $UTor(cGH^-(L))$ is the subcomplex of the U torsion elements, that is elements of the homology that become trivial after multiplication by a suitable power of U . The same considerations of Remark 4.11 show that all the $\tau_i^{\mathfrak{s}}$ s differ by integers, so as in Definition 4.9 we can shift them by the appropriate correction term, and we call $\tilde{\tau}_i^{\mathfrak{s}}$ the integer valued version.

So given an m -component link we are associating $2^{m-1}p$ τ -invariants to it. Studying how these change under oriented saddles and disjoint union of unknots will allow us to prove Theorem 4.14. A proof of the well definiteness of the τ -set can be found in [47, Cor. 8.2.10].

THEOREM 4.26. *Let G represent a link $L \subset L(p, q)$, and suppose that G' is a grid representing $L \sqcup \bigcirc \subset L(p, q)$. Then there is an isomorphism:*

$$(27) \quad cGH^-(G', \mathfrak{s}) \cong cGH^-(G, \mathfrak{s}) \oplus cGH^-(G, \mathfrak{s})_{[-1,0]}$$

Where the last summand denotes $cGH^-(G, \mathfrak{s})$ shifted by -1 in the Maslov degree.

PROOF. A more general version of this Theorem was proved in the holomorphic setting in [39]; alternatively the combinatorial proof of the same statement in the three sphere of [47, Sec. 8.4] works in the exact same way (in each spin^c degree) for lens spaces. \square

The next Lemma follows easily from the previous theorem, noting that the isomorphism it provides preserves the Alexander grading:

LEMMA 4.27. *If G represents $K \sqcup \bigcirc^m$ for a knot $K \subset L(p, q)$, then for each $\mathfrak{s} \in \text{spin}^c(L(p, q))$*

$$\tau_{min}^{\mathfrak{s}}(G) = \tau_{max}^{\mathfrak{s}}(G) = \tau^{\mathfrak{s}}(K)$$

Now we examine how the τ -sets change under oriented saddle moves. Again W denotes the module $\mathbb{F}_{[0,0]} \oplus \mathbb{F}_{[-1,-1]}$.

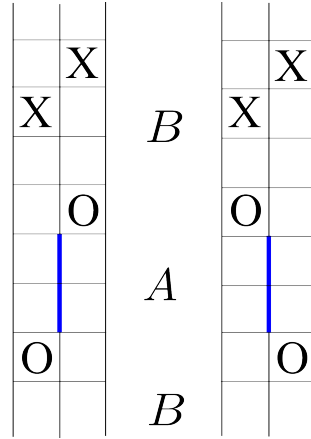


FIGURE 4.3. The two possibilities for a generator on both grids.

PROPOSITION 4.28 ([47]). *Suppose that the two links L_0 and L_1 differ by an oriented saddle move, as in Remark 1.4, and that $|L_1| = |L_0| + 1$. Then there are $\mathbb{F}[U]$ -module tri-graded maps*

$$\sigma : cGH^-(L_0) \otimes W \longrightarrow cGH^-(L_1)$$

$$\mu : cGH^-(L_1) \longrightarrow cGH^-(L_0) \otimes W$$

with grading shifts respectively $(-1, 0, 0)$ and $(-1, -1, 0)$ on the tri-degree (M, A, S) , and such that both $\mu \circ \sigma$, $\sigma \circ \mu$ are multiplication by U on their respective domains.

PROOF. The proof follows immediately from its analogue for links in S^3 (Prop. 8.3.1 of [47]), by noting that the maps σ and μ can be defined in the same way for lens space too, and in this case they respect the spin^c degree.

For completeness we sketch their construction here; first we define the maps μ and σ on the chain complex, prove the stated properties and show that they are chain maps. The result will follow by considering the induced maps in homology.

The generators can be identified in the two grids G_0, G_1 representing L_0 and L_1 respectively. Divide them into two groups, A and B according to whether there is a component of the generator on the red region shown in Figure 4.3.

By assumption, the two markings $\mathbb{O}_1, \mathbb{O}_2$ of G_0 in Figure 4.3 belong to the same component; hence by [47, Lemma 8.3.4]

$$H \left(cGC^-(G_0) / \{V_1 = V_2\} \right) \cong cGH^-(G_0) \otimes W$$

So in both $\frac{cGC^-(G_0)}{\{V_1=V_2\}}$ and $cGC^-(G_1)$ we can think of the two variables V_1, V_2 as identified, and we collectively denote them by U .

The two maps are then defined as follows: $\sigma(x) = U \cdot x$ and $\mu(x) = x$ if $x \in A$, and $\sigma(x) = x$, $\mu(x) = U \cdot x$ otherwise. It is easy to check that these maps satisfy the stated composition property, so we just need to prove that they are chain maps. In other words we want to verify that $\partial^- \circ f = f \circ \partial^-$, with $f = \sigma, \mu$.

We do this for σ , since the same result for μ follows easily. Consider two generators $x, y \in cGC^-(G)$, where G is equivalently G_0 or G_1 . Then if both elements are in A or B , any rectangle connecting x and y will intersect the same \mathbb{X} and \mathbb{O} markings in the two grids.

If $x \in A$ and $y \in B$, then the component of x in the region between the two \mathbb{O} markings is necessarily an edge of any rectangle $r \in \text{Rect}^\circ(x, y)$. This means that going from G_0 to G_1 it acquires an extra \mathbb{O} marking, as in Figure 4.3. In the last case, $x \in B$ and $y \in A$, the result instead is opposite, that is, a rectangle loses an \mathbb{O} marking going from G_0 to G_1 ; in both these two last cases, by definition σ compensates the difference. For example, if $x \in A$ and $y \in B$, then $\partial^-(\sigma(x)) = U \cdot \partial^-(x) = \sigma(\partial^-(x))$. \square

THEOREM 4.29 ([47]). *Suppose $L_0, L_1 \subset L(p, q)$ differ by an oriented saddle move, and $|L_1| = |L_0| + 1$; then for all $\mathfrak{s} \in \text{spin}^c(L(p, q))$:*

$$(28) \quad \tau_{\min}^{\mathfrak{s}}(L_0) - 1 \leq \tau_{\min}^{\mathfrak{s}}(L_1) \leq \tau_{\min}^{\mathfrak{s}}(L_0)$$

$$(29) \quad \tau_{\max}^{\mathfrak{s}}(L_0) \leq \tau_{\max}^{\mathfrak{s}}(L_1) \leq \tau_{\max}^{\mathfrak{s}}(L_0) + 1$$

PROOF. As in Theorem 8.3.2 of [47], applied in each spin^c structure. \square

PROPOSITION 4.30 ([47]). *If $K_0, K_1 \subset L(p, q)$ are two knots connected by $2g$ saddle moves, then $|\tau^{\mathfrak{s}}(K_0) - \tau^{\mathfrak{s}}(K_1)| \leq g$*

PROOF. Since we are dealing with knots, there must be an equal number g of splits and merges; by iterating Theorem 4.29, we get:

$$\begin{aligned} \tau_{\max}^{\mathfrak{s}}(K_1) &\leq \tau_{\max}^{\mathfrak{s}}(K_0) + g \\ \tau_{\min}^{\mathfrak{s}}(K_0) - g &\leq \tau_{\min}^{\mathfrak{s}}(K_1) \end{aligned}$$

But by Definition 4.25, in the case of knots $\tau_{\min}^{\mathfrak{s}} = \tau_{\max}^{\mathfrak{s}} = \tau^{\mathfrak{s}}$, so rearranging the inequalities we obtain the result. \square

PROPOSITION 4.31 ([47]). *Consider two knots $K_0, K_1 \subset L(p, q)$, and suppose that $(L(p, q), K_0)$ can be obtained from $(L(p, q), K_1 \sqcup \mathbb{O}^m)$ by m saddle moves. Then for each $\mathfrak{s} \in \text{spin}^c(L(p, q))$:*

$$\tau^{\mathfrak{s}}(K_0) = \tau^{\mathfrak{s}}(K_1)$$

PROOF. By Theorem 4.29, performing a merge on a link with $\tau_{max}^s = \tau_{min}^s \forall \mathfrak{s} \in \text{spin}^c(L(p, q))$ gives a new link with the same property. Note that both $K_1 \sqcup \bigcirc^m$ and K_0 have this property (the first one by Lemma 4.27, and the second one because it is a knot). The proof then follows by induction on the number of saddle moves from $K_1 \sqcup \bigcirc^m$ to K_0 . \square

PROOF OF THM. 4.14. Refer to the cobordism normal form displayed in Figure 1.6 for the notation. By Lemma 4.27 each τ^s is unchanged under the unknot disjoint union from K_0 to $K_0 \sqcup \bigcirc^b$, and from $K_1 \sqcup \bigcirc^d$ to K_1 ; then Proposition 4.31 takes care of the parts of the cobordism from $K_0 \sqcup \bigcirc^b$ to K'_0 , and from K'_1 to $K_1 \sqcup \bigcirc^d$.

Lastly, we can apply Proposition 4.30 to the part of Σ going from K'_0 to K'_1 to obtain the desired bound. \square

4.3. Related constructions

In this section we present some other relevant applications of the interplay between τ and 4-dimensional aspects of knot theory in lens spaces. We also collect here some Conjectures relating the objects defined in the previous sections.

Consider a mixed diagram for a knot $K \subset L(p, q)$ as on the left of Figure 4.4; we can fix a disk Δ bounded by the trivial surgered component and (after a suitable perturbation by a small isotopy) count the intersections $K \pitchfork \Delta$. Suppose there are l of them; we can perform a move called the *snatch* of K , which consists in attaching l saddles as shown in Figure 4.4, allowing one to rip the knot away from the surgery torus. After the snatch we are left with an $l + 1$ component link. l components are meridians μ_i of $\partial\Delta$, and the other component is a local knot K' in $L(p, q)$. The orientations $\epsilon_i \in \{-1, 1\}$ for $i = 1, \dots, l$ of the l meridians are such that $\sum_{i=1}^l \epsilon_i \equiv [K] \pmod{p}$.

We can interpret this process from a 4-dimensional point of view: as shown in Figure 4.5, these saddle moves induce a genus 0 cobordism in $L(p, q) \times [0, 1]$. Now the snatched component K' can be capped off with a surface of genus $g_*(K')$ (this denotes the usual 4-dimensional slice genus of a knot in S^3). We can merge any pair of meridians with opposite orientations with a saddle as in Figure 4.6. This produces a trivial knot, which can be capped off with a disk. We can iterate this process until we are left with exactly $m = [K]$ meridians with the same orientation. For notational simplicity, suppose the meridians left are the first m . This produces a cobordism $\widehat{\Sigma}$ between K and $\bigsqcup_{i=1}^m \mu_i$, of

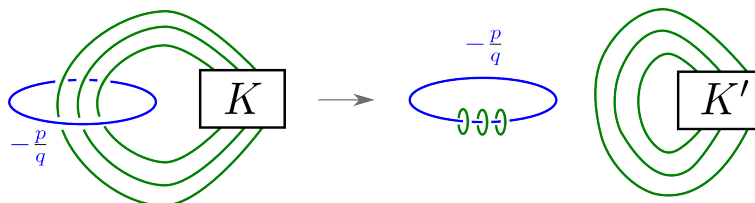


FIGURE 4.4. A description of the snatch cobordism between K and $K' \sqcup_{i=1}^l \mu_i$.

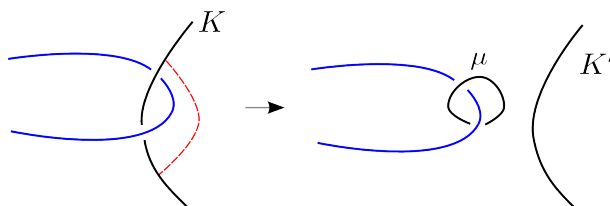


FIGURE 4.5. Detail of the snatch for a single strand.

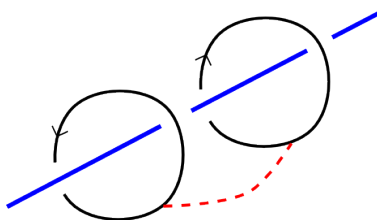


FIGURE 4.6. Killing opposite saddles.

genus

$$g(\widehat{\Sigma}) = \frac{l - m}{2} + g_*(K')$$

In specific cases we can recover a good estimate for the smooth 4-genus of a knot in S^3 through this construction. In principle, since they are not homomorphisms, the τ -invariants of the resulting knot might obstruct finite concordance order, or give bounds on the slice genus which can not be obtained with the usual τ -invariant.

As an example, we might try to use the lens space τ -invariants to prove that the figure eight knot is not slice. Although it is not hard to prove this fact⁶, it can not be done using τ , since the amphichirality of 4_1 implies that $\tau(4_1) = 0$. However, we can apply the previous snatching procedure to the family of knots K_p in Figure 4.7.

⁶*e.g.* its Alexander polynomial does not satisfy the Fox-Milnor condition.

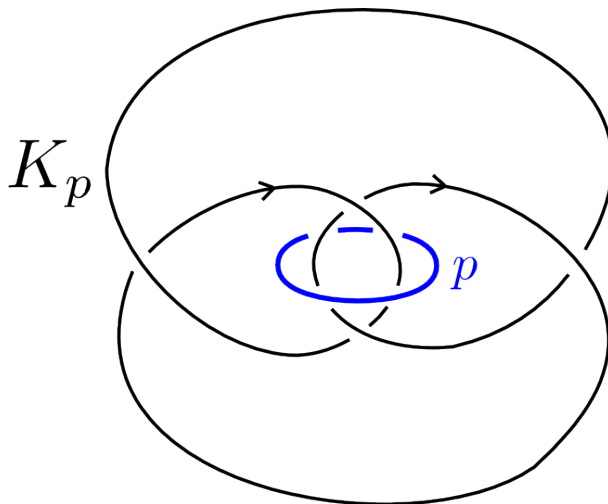


FIGURE 4.7. Snatching out the knots K_p .

This procedure gives a cobordism of genus $2 = 1 + g_*(4_1)$ from K_p to \bigcirc ; if there is at least the $\tau^\mathfrak{s}$ for $\mathfrak{s} \in \text{spin}^c(L(p, 1))$ such that $|\tau^\mathfrak{s}(K_p)| > 1$, then $g_*(4_1) > 0$.

Unfortunately, at the time of writing, the computations for $\tau^\mathfrak{s}(K_p)$ still remains to be done, mainly due to the huge computational power needed (see Chapter 6).

The set of concordances and weak concordances on a general 3-manifold Y is an invariant of Y , which can be also specialized as an invariant of the couple (Y, m) with $m \in H_1(Y; \mathbb{Z})$.

In the following we collect some results and conjectures aimed to better understand these invariants.

The following question arises:

QUESTION 4.32. *Can a local knot be concordant to a non local knot?*

The answer is positive: the easiest way to prove it was suggested by Marco Golla; take a non-local knot (Y, K) and a ribbon pattern $P \subset S^1 \times \mathbb{D}^2$, as in Figure 4.8. Then consider K_P , the satellite of K with pattern P , embedded in $Y \times \{0\} \subset Y \times [0, 1]$. Note that K_P bounds a ribbon disk, and it is nullhomologous in Y . Push the ribbon disk inwards, and remove a small disk from its interior. Tubing the boundary of the removed disk to $Y \times \{1\}$ provides the needed concordance from K_P to (Y, \bigcirc) .

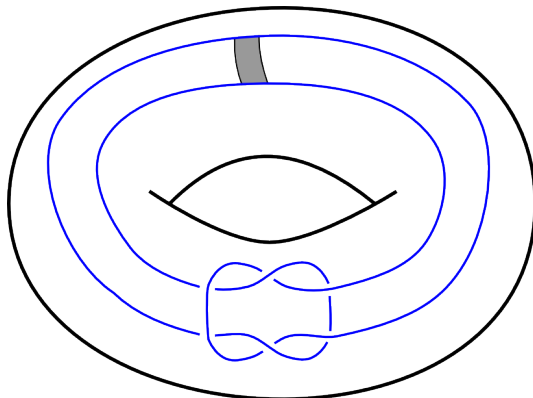


FIGURE 4.8. The band attachment shown produces a concordance in $S^1 \times \mathbb{D}^2 \times [0, 1]$ between P and a pair of unknots.

Now we need to argue the non-locality of K_P ; suppose there existed an embedded 2-sphere $S \subset Y$ bounding a ball containing K_P . If the sphere does not intersect $\partial\nu(K)$, then either it is contained in $\nu(K)$ or it contains it. The first case can be easily dismissed by looking at the pattern P^7 . In the second case we would have found a sphere containing K , which is absurd. Then we just need to argue, similarly to what was done in Theorem 4.7, that all intersections between S and $\partial\nu(K)$ can be removed up to isotopy.

There are two possible kinds of intersections between S and $\partial\nu(K)$; the ones which are nullhomologous in $\partial\nu(K)$, and the ones which are not. The first kind can be eliminated with isotopies. There can not be any of the second kind which is parallel to a meridian of $\partial\nu(K)$, since the existence of such an intersection would produce a disk in $\nu(K)$ bounding a meridian and not intersecting K_P , which is absurd. Lastly, there can not be any other kind of non-homologically trivial (on $\partial\nu(K)$) intersections: if there was only one, then it would bound a disk on S , which would be contained in $\nu(K)$. If there were more than one intersections, consecutive pairs would bound annuli, half of which would be contained in $\nu(K)$, and could be eliminated by an isotopy. The argument follows by induction on the number of this last kind of intersection, after deleting all the other kinds by isotopies.

⁷It can be proved that there can not be any such sphere if the minimal number of intersections with a disk bounding a meridian is $\neq 0$.

REMARK 4.33. From what we have seen so far it should be clear that the quantity

$$\max_{i,j \in \mathbb{Z}_p} |\tau^i - \tau^j|$$

can be interpreted as an obstruction to locality for knots in $L(p, q)$, *i.e.* if it is nonzero the knot can not be local.

We make the following conjecture:

CONJECTURE 4.34. Denote by $\mathcal{C}_{loc}^{p,q}$ the set (it is actually a group) of knots in $L(p, q)$ which are concordant to a local one. Then

$$|\mathcal{C}_0^{p,q} \setminus \mathcal{C}_{loc}^{p,q}| = +\infty$$

We can now study the almost concordance classes of knots in $L(p, q)$. The key fact that will allow us to distinguish several inequivalent classes is Theorem 4.12:

DEFINITION 4.35. Let $(L(p, q), K)$ be a knot; define the shifted τ invariant as the p -tuple

$$\tau_{sh}(K) = (\tilde{\tau}^1(K) + t, \dots, \tilde{\tau}^p(K) + t)$$

where t is the only integer such that $\min_{s \in \mathbb{Z}_p} \{\tilde{\tau}^s(K) + t\} = 0$.

PROPOSITION 4.36. If K is a local knot in $L(p, q)$, then

$$\tau_{sh}(K) = (0, \dots, 0)$$

PROOF. It follows immediately from Theorem 4.12 and the fact that the unknot has trivial τ_{sh} invariant. \square

Now, using Theorem 4.12, it is immediate to show that two almost concordant knots in $L(p, q)$ have the same τ_{sh} invariant. In particular, considering again the knot K of examples 3.11 and 4.13, we see that $\tau_{sh} = (0, 1, 1)$, so we have the following:

PROPOSITION 4.37. The knot $K \subset L(3, 1)$ from example 3.11 is not almost-concordant to a local knot. Furthermore, since it has trivial grid homology in $spin^c$ degree 1, by Remark 4.8 it can not be the connected sum with a knot in S^3 , hence it is also genuine.

PROOF. It is a direct consequence of the computations made in Example 4.13 coupled with Proposition 4.36. \square

COROLLARY 4.38. The equivalence relation induced by almost concordance of knots is nontrivial in general.

PROOF. The previous proposition provides two nullhomologous (K and the unknot) knots in $L(3, 1)$ which are not almost-concordant. \square

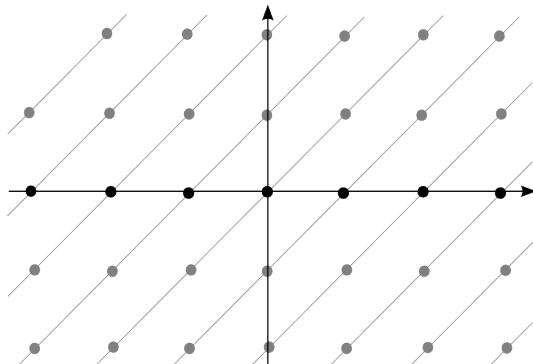


FIGURE 4.9. A representation of the behaviour of τ in $L(2, 1)$; the lines represent the \mathcal{C} -action.

Motivated by several examples and computations, we are led to the following:

CONJECTURE 4.39. *In each lens space there are infinitely many inequivalent almost concordance classes, that is $\forall m \in H_1(L(p, q); \mathbb{Z})$:*

$$\left| \mathcal{C}_m^{p,q} / \sim \right| = \infty$$

One could try to attack the last two conjectures by using cabling techniques; there is an algorithm which produces a grid for the (a, b) -cable of a knot. Using the approach from [23] adapted in this context might yield the result.

However, we suspect that even more is true; the following Conjecture 4.40 actually implies Conjecture 4.39.

CONJECTURE 4.40. *The τ -invariant for knots in $L(p, q)$, seen as a map*

$$\tau : \mathcal{K}(L(p, q)) \longrightarrow \mathbb{Z}^p$$

is surjective.

Note that by considering the \mathcal{C} -action in conjunction with Theorem 4.12, the conjecture is equivalent to requiring that τ is surjective on $\mathbb{Z}^{p-1} \times \{0\}$, as shown in Figure 4.9.

DEFINITION 4.41.

$$g^{W_{p,q}}(K) = \min\{g(F) \mid \iota : (F, \partial F) \hookrightarrow (W_{p,q}, L(p, q)) \text{ and } \partial F = K\}$$

where $W_{p,q}$ is the standard plumbing for $L(p, q)$, as described in Section 1.1. We want the map ι to be a smooth proper embedding of F . This is well defined since $H_1(W_{p,q}; \mathbb{Z}) = 0$.

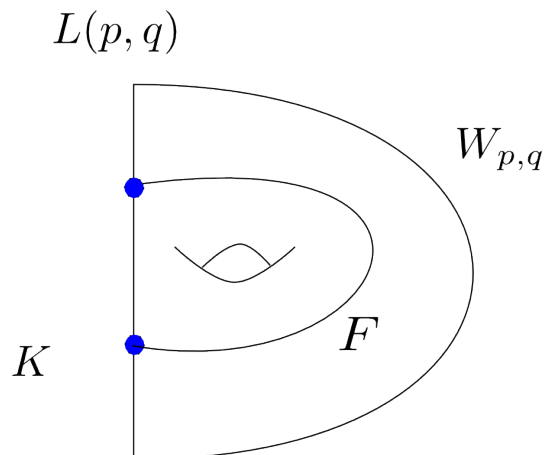


FIGURE 4.10. A visual aid to picture $g^{W_{p,q}}(K)$.

REMARK 4.42. These two notions of genera we have defined coincide in the case of knots in S^3 , since $\mathbb{D}^4 \setminus \mathbb{B}^3 \cong S^3 \times [0, 1]$; so if we have a properly embedded genus g surface in \mathbb{D}^4 bounding a knot $K \subset S^3$, by removing a small 4-ball intersecting the surface in a small disk, we get a genus g cobordism to the unknot. Since removing a 4-ball from $W_{p,q}$ does not produce $L(p, q) \times [0, 1]$, these two notions are a priori distinct.

REMARK 4.43. It is easy to show that $\tilde{g}(K) + g^{W_{p,q}}(T_{[K]}^{p,q}) \geq g^{W_{p,q}}(K)$; just take the cobordism from K to $T_{[K]}^{p,q}$ which realizes $\tilde{g}(K)$ in the product $L(p, q) \times I$, and cap it off with the minimal genus surface bounding $T_{[K]}^{p,q}$ in $W_{p,q}$.

REMARK 4.44. Most of the definitions and results of this Chapter are in no way specific to lens spaces, and can be carried out for general $\mathbb{Q}HS^3$ s; so, the notions of concordances, action of S^3 concordances, weak concordances and genuinity have an obvious extension to all rational homology 3-spheres.

There is however no well defined generalization of the genus \tilde{g} (or $g^{W_{p,q}}$), since for a general $\mathbb{Q}HS^3$ there is no notion of simple knot or standard filling.

In this Chapter we introduced two genera for knots in lens spaces, which are obtained with different definitions. However we were not able to find examples of knots for which they differ. Thus we ask the following:

QUESTION 4.45. *Is it always true that*

$$g^{W_{p,q}}(K) = \tilde{g}(K) ?$$

A negative answer to this question might be found e.g. by exhibiting a $W_{p,q}$ -slice knot $K \subset L(p, q)$ such that $\tilde{g}(K) > 0$.

CHAPTER 5

Applications

In this chapter we collect some results relating the grid homology of knots in lens spaces to other known invariants and constructions; more specifically we compute Turaev's Θ function on $H_1(L(p, 1); \mathbb{Z})$ and in a few other cases in Section 5.1.

In Section 5.2 we compare the decategorification of \widehat{GH} with a generalization of the HOMFLYPT polynomial in lens spaces, and show that, up to certain choices, they produce the same generalization of the Alexander polynomial.

Recently [24] and [50] independently reformulated in similar ways the Berge Conjecture [5] in terms of the Knot Floer homology of knots in $L(p, q)$ (see Section 5.3). In Section 5.3 we verify that the Conjecture holds in a few cases.

5.1. Turaev's Θ function for $L(p, q)$

Knot Floer homology is known to detect the 3-dimensional Seifert genus of knots and, more generally the Thurston seminorm of link complements and fiberdeness of knots in the 3-sphere.

THEOREM 5.1 ([38], [18], [33]). *Let $K \subset S^3$ be a knot. Then*

$$\max\{a \in \mathbb{Z} \mid \widehat{HFK}(K, a) \neq 0\} = g(K)$$

Moreover,

$$rk\left(\widehat{HFK}(K, g(K))\right) = 1 \iff K \text{ is fibered}$$

It is thus natural to ask what kind of quantity associated to a knot in a lens space can be detected by \widehat{GH} . Since such a knot might be only rationally nullhomologous, there is no hope for it to bound an embedded surface.

There are however at least two ways to generalize the notion of Seifert genus for knots in $\mathbb{Q}HS^3$ s; in [34, Thm. 2.2] and [50, Thm. 4.3], the detection of these new genera by \widehat{HFK} was proven¹. As it turns out, the two genera are detected by the two versions of \widehat{GH} which

¹Building on the paper containing the previously stated Theorem [33].

differ by the target space of the Alexander filtration. So, by Remark 2.12, despite their different definitions these two genera coincide up to a factor. The following definitions will be given for knots in lens spaces, but they can be used in general $\mathbb{Q}HS^3$ (see also [50]).

DEFINITION 5.2. *Consider an oriented knot $K \subset L(p, q)$, and call Y the closure of $L(p, q) \setminus \nu(K)$; there is a uniquely defined oriented meridian $\mu \in H_1(Y; \mathbb{Z})$. Choose a simple closed curve $\lambda \subset \nu(K)$ such that $\mu \cdot \lambda = 1$. There is an essential curve $\alpha \in \partial Y$ bounding a surface in Y ; write $\alpha = a\mu + b\lambda$ (up to orientation reversal on α we can suppose $b > 0$). We can define:*

$$g_r(K) = \min\{g(\Sigma) \mid (\Sigma, \partial\Sigma) \hookrightarrow (Y, \partial Y)\}$$

such that $\partial\Sigma$ is non homologically trivial on $\partial\nu(K)$.

REMARK 5.3. The quantity $K \cdot K = \frac{a}{p} \in \mathbb{Q}/\mathbb{Z}$ is the *self linking number* of K . It is well defined, since any two longitudes differ by addition of some meridians, and choosing $\lambda + \mu$ changes $\frac{a}{p}$ to $\frac{a-p}{p}$. There is also a geometric interpretation of $K \cdot K$: if t is the order of $[K]$ in $H_1(L(p, q); \mathbb{Z})$, a link on $\partial\nu(K)$ representing the class $t[K]$ will bound an embedded surface Σ . Then $K \cdot K$ is given by the (normalized) intersection $\frac{\lambda \cdot \Sigma}{p}$.

There is another related definition of genus for rationally nullhomologous knots in $\mathbb{Q}HS^3$ s introduced by Calegari and Gordon in [6].

DEFINITION 5.4. *A rational Seifert surface² for a knot $K \subset L(p, q)$ is a connected, properly embedded incompressible oriented surface*

$$(F, \partial F) \hookrightarrow (L(p, q), L(p, q) \setminus \nu(K))$$

whose boundary is composed by parallel curves on $\partial\nu(K)$ with orientations matching K 's. We also say that such a knot K is rationally fibered if the complement of K fibers over S^1 , with rational Seifert surfaces for K as fibers.

If $K \subset Y$ is a knot in a $\mathbb{Q}HS^3$, the rational genus $g_{\mathbb{Q}}(K)$ is defined as:

$$g_{\mathbb{Q}}(K) = \min_F \frac{\chi_-(F)}{2|[\mu] \cdot [\partial F]|}$$

where F is a rational Seifert surface for K , $\chi_-(F) = \max\{0, -\chi(F)\}$ and μ is the meridian of K .

²These are called *good p -Seifert surfaces* in [6].

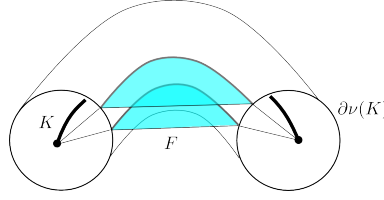


FIGURE 5.1. A portion of a folded surface bounding a knot.

This definition closely resembles the one of *complexity* for surfaces given by Thurston in [54]. Under this point of view, $g_{\mathbb{Q}}$ is a normalized measure of the complexity of folded surfaces (see Figure 5.1) bounding a given knot.

In the nullhomologous case, by taking the minimum of the complexity over all surfaces representing a given homology class, we get what is known as the *Thurston seminorm* on the homology.

Using the same procedure in $\mathbb{Q}HS^3$ s one obtains a function Θ on the first homology. This task was carried out by Turaev in [56]. This section will exploit the knot detection of the previously defined genera by \widehat{HFK} to compute explicitly some values of Θ in lens spaces.

REMARK 5.5. In the rational homology case, this measure of complexity does not produce a seminorm, since every element has a finite order.

An adaptation of Theorem 5.1 contained in [34], shows that $g_{\mathbb{Q}}$ is detected by \widehat{HFK} :

THEOREM 5.6 ([33]). *Given $K \subset L(p, q)$ denote by A_{max} and A_{min} the maximum (minimum respectively) of the Alexander degrees of $\widehat{GH}(L(p, q), K)$. Let also F be a rational genus minimizing Seifert surface. Then*

$$(30) \quad \frac{-\chi(F) + |[\mu] \cdot [\partial F]|}{|[\mu] \cdot [\partial F]|} = A_{max} - A_{min}.$$

Moreover, K is rationally fibered iff the homology supported in Alexander degree A_{max} has rank 1.

Note that this Theorem implies that

$$(31) \quad g_{\mathbb{Q}}(K) = \begin{cases} \frac{A_{max} - A_{min} - 1}{2} & \text{if } A_{max} - A_{min} \geq 1 \\ 0 & \text{otherwise.} \end{cases}$$

REMARK 5.7. The two notions of 3-dimensional genus we have given here, are actually a measure of the same quantity, scaled by an appropriate factor; since $A_{max}^{\mathbb{Z}} - A_{min}^{\mathbb{Z}} = p(A_{max} - A_{min})$, an easy Euler

characteristic argument implies that $pg_{\mathbb{Q}}(K) = g_r(K) + \frac{1}{2}$. Hence, using the rational genus detection described in Theorem 5.6 for the grid homology defined in 2.4.1, it is easy to argue that the complex \widehat{GC} , endowed with the Alexander degree defined in Remark 2.12 detects g_r , as stated in [50, Thm. 4.3].

In [34] Ni and Wu proved that Floer simple knots in $\mathbb{Q}HS^3$ s minimize the rational genus in their homology classes:

THEOREM 5.8 ([34]). *If K is a Floer simple knot in a L -space Y , then for all $K' \subset Y$ such that $[K'] = [K]$:*

$$g_{\mathbb{Q}}(K) \leq g_{\mathbb{Q}}(K')$$

This Theorem answers positively a question of Rasmussen. In [50] Rasmussen also asked if simple knots could be the *only* rational genus minimizers. This question, which would imply the Berge conjecture (see Section 5.3) was answered negatively by Greene and Ni in [21], where they exhibited an infinite family of non-simple minimizers.

We can now define Turaev's Theta function:

$$(32) \quad \begin{aligned} \Theta &: H_1(Y; \mathbb{Z}) \longrightarrow \mathbb{Q} \\ \Theta(a) &= \min_{[K]=a} 2g_{\mathbb{Q}}(K) \end{aligned}$$

In order to find explicit bounds to Θ in lens spaces, we can use Theorem 5.6, and the genus minimizing property of simple knots. In particular, we compute \widehat{GH} for some classes of simple knots in the remaining part of this section.

Recall that by Remark 2.25, in order to compute $\widehat{GH}(L(p, q), T_m^{p,q})$, it is sufficient to compute the Alexander degree of the only generator of $\widehat{GC}(L(p, q), T_m^{p,q})$ in each spin^c degree.

REMARK 5.9. It is proven in [25],[50] that the knot Floer homology groups of simple knots encompass all possible knot Floer homologies of S^3 -dual knots. The computation of the knot Floer homology of simple knots was first produced in [50], but that construction is based on a recursive method, while in some cases we are able to give an explicit answer.

REMARK 5.10. In [34] the authors also prove the existence of a lower bound for Θ , using the difference of suitably shifted correction terms:

$$(33) \quad 1 + \Theta([K]) \geq \max_{\mathfrak{s} \in \text{spin}^c(Y)} \{d(Y, \mathfrak{s} + PD[K]) - d(Y, \mathfrak{s})\}$$

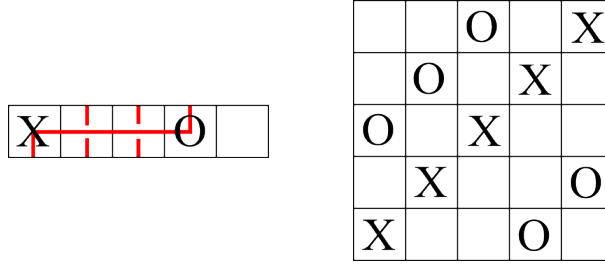


FIGURE 5.2. The simple knot $T_3^{5,1}$ and its lift to S^3 (which is the trefoil).

The following results imply that this bound is in fact sharp for the cases we compute. The sharpness of their bound for lens spaces was apparently already known to Ni and Wu (see [57]), but our calculation has the advantage of being elementary and combinatorial. A complete computation of the values of Θ for an arbitrary homology class in a lens space will be carried out in a future work.

We start with the simple knots $T_m^{p,1} \subset L(p, 1)$; call $x_{\mathfrak{s}}$ the only generator in spin^c degree \mathfrak{s} . It is then an easy albeit tedious computation to find the values of $A(x_{\mathfrak{s}})$ for the generators of the homologies $GH^-(L(p, 1), T_m^{p,1}, \mathfrak{s})$.

Consider the 1-dimensional grid representing $T_m^{p,1}$ where the \mathbb{X} marking is in the leftmost box, and the \mathbb{O} marking in the m -th box from the left (as in Figure 5.2); then call x_t the generator lying on the SW corner of the t -th box. Then $S(x_t) \equiv t - m \pmod{p}$, and if we denote by $\Sigma(n) = \frac{n(n-1)}{2}$, we get:

$$\mathcal{I}(\tilde{\mathbb{O}}, \tilde{\mathbb{O}}) = \Sigma(m) + \Sigma(p - m)$$

$$\mathcal{I}(\tilde{\mathbb{X}}, \tilde{\mathbb{X}}) = \Sigma(p)$$

$$\mathcal{I}(\tilde{\mathbb{X}}, \tilde{x}_t) = \Sigma(p - t) + \Sigma(t)$$

If $t \leq m$:

$$\mathcal{I}(\tilde{\mathbb{O}}, \tilde{x}_t) = \Sigma(p - m) + \Sigma(t) + \Sigma(m - t)$$

while if $t > m$:

$$\mathcal{I}(\tilde{\mathbb{O}}, \tilde{x}_t) = \Sigma(p - t) + \Sigma(m) + \Sigma(t - m)$$

After a substitution³ in Equation (14) we obtain the following:

³We have used the value of the Maslov degree $d(p, 1, \mathfrak{s})$ from Section 2.1.

PROPOSITION 5.11.

$$\widehat{GH}(L(p, 1), T_m^{p,1}, \mathfrak{s}) = \mathbb{Z}_{\left[\frac{p-(2\mathfrak{s}-p)^2}{4p}, A(x_{\mathfrak{s}})\right]}$$

where $A(x_{\mathfrak{s}})$ is given by

$$(34) \quad A(x_{\mathfrak{s}}) = \begin{cases} \frac{m(2\mathfrak{s}+m-p)}{2p} & \text{if } 0 \leq \mathfrak{s} \leq p-m \\ \frac{(2p-m-2\mathfrak{s})(p-m)}{2p} & \text{if } p-m \leq \mathfrak{s} < p \end{cases}$$

The corresponding values of Θ can then be obtained using Equation (31).

It is easy to check that $A_{max} = A(x_{p-m})$ and $A_{min} = A(x_0)$, so by Equation (31) the rational genus is:

$$(35) \quad g_{\mathbb{Q}}(T_m^{p,1}) = \begin{cases} 0 & \text{if } p \leq \frac{m^2}{m-1} \\ \frac{mp-m^2-p}{p} & \text{otherwise.} \end{cases}$$

Using similar techniques we can compute explicitly the homology of another family of simple knots; these are the ones in which the homology class represented by the knot is $1 \in H_1(L(p, q); \mathbb{Z})$.

PROPOSITION 5.12.

$$\widehat{GH}(L(p, q), T_1^{p,q}, \mathfrak{s}) = \widehat{GH}(L(p, 1), T_1^{p,1}, \mathfrak{s})$$

Using the previous results we can determine rational genus and fiberedness for two families of simple knots:

COROLLARY 5.13. *The simple knots $T_1^{p,q}$ are rationally fibered for all coprime p, q , and they bound a rational Seifert surface of genus 0. Likewise, $T_m^{p,1}$ is rationally fibered for all $m \in H_1(L(p, q); \mathbb{Z})$. The rational genus of the fibers is given by Equation (35).*

PROOF. By the computations for $T_m^{p,1}$ and Theorem 5.6 we obtain the statement for $L(p, 1)$. Applying Proposition 5.12 gives the result for $q \neq 1$ and $m = 1$. \square

The proof of Proposition 5.12 relies on the following two Lemmas:

LEMMA 5.14. *For the grid of dimension 1 for $T_1^{p,q}$ described before we have:*

$$\mathcal{I}(\tilde{\mathbb{X}}, \tilde{\mathbb{X}}) - \mathcal{I}(\tilde{\mathbb{O}}, \tilde{\mathbb{O}}) = p - 1$$

PROOF. Consider the lift⁴ of the grid to S^3 . In the case at hand, the \mathbb{O} markers are right below the \mathbb{X} markings, as shown in Figure 5.3; so if we delete the leftmost column the contribution of the remaining markings cancel each other out. We then have to add the contribution of the lowest \mathbb{X} marking, which is just $p - 1$. \square

⁴As described in Section 2.4.1.

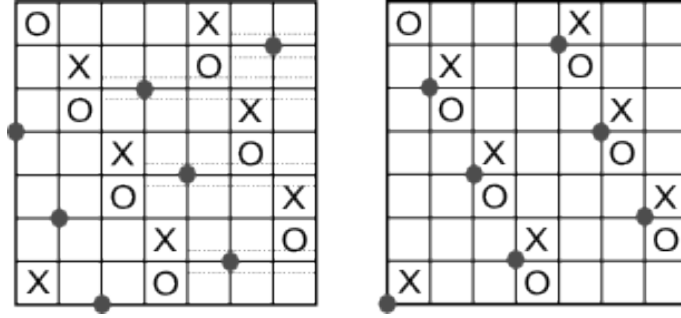


FIGURE 5.3. The lift to S^3 for a 1-dimensional grid of $T_1^{p,q}$. On the left the dotted lines mark the components of the generator on the right of the coupled markings; on the right the case $t = 0$.

LEMMA 5.15. *With the same hypotheses as in Lemma 5.14,*

$$\mathcal{I}(\tilde{\mathbb{X}}, \tilde{x}_s) - \mathcal{I}(\tilde{\mathbb{O}}, \tilde{x}_s) = \mathfrak{s}$$

PROOF. Note that in the lift of the grid in S^3 , we get one \mathbb{X} marking immediately above each \mathbb{O} , with the exception of the first column containing the markings \mathbb{X}_1 and \mathbb{O}_p , which we discard for the moment. Then the only contributions to the difference $\mathcal{I}(\tilde{\mathbb{O}}, \tilde{x}_s) - \mathcal{I}(\tilde{\mathbb{X}}, \tilde{x}_s)$ comes from components of the lifted generators placed on the right of the coupled markings (as in the left part of Figure 5.3). In the notation used before Proposition 5.11, by the spin^c degree formula we have $\mathfrak{s} = S(x_t) \equiv t - 1 \pmod{p}$, and we divide the cases according to the value of t .

If $t = 0$ then on each α -curve the corresponding component of \tilde{x}_t is on the left of the coupled markings, hence $\mathcal{I}(\tilde{\mathbb{O}}, \tilde{x}_t) - \mathcal{I}(\tilde{\mathbb{X}}, \tilde{x}_t) = \mathcal{I}(\tilde{\mathbb{O}}_1, \tilde{x}_t) - \mathcal{I}(\tilde{\mathbb{X}}_1, \tilde{x}_t) = 1 - p$.

If instead $0 < t < p$, let $\omega = \sum_{i=2}^p \mathcal{I}(\tilde{\mathbb{X}}_i, \tilde{x}_t)$. Then, adding up the contribution of the first column we obtain $\mathcal{I}(\tilde{\mathbb{X}}, \tilde{x}_t) = p - 2 + \omega$ (since $t \neq 0$ there are two marking on the lower and left edges of the lifted square, as in the left portion of Figure 5.3). There is no contribution to $\mathcal{I}(\tilde{\mathbb{O}}, \tilde{x}_t)$ from the first column, so as noted before, the difference $\mathcal{I}(\tilde{\mathbb{O}}, \tilde{x}_t) - \omega$ is given by the number of components of \tilde{x}_t on the right of the coupled markings, which is just $p - t - 1$.

So if $t \neq 0$ we have:

$$\mathcal{I}(\tilde{\mathbb{O}}, \tilde{x}_t) - \mathcal{I}(\tilde{\mathbb{X}}, \tilde{x}_t) = \omega + p - t - 1 - \omega - p + 2 = 1 - t = -\mathfrak{s}$$

A comparison with the computation of $\widehat{GH}(T_1^{p,1})$ yields the result. \square

PROP. 5.12. By Equation (14), the two previous Lemmas provide a proof of Proposition 5.12. \square

Now the computations for $T_1^{p,q}$, combined with Lemma 1.16, give the Alexander degrees of $\widehat{GH}(T_{\pm q'}^{p,q'})$ when $qq' \equiv 1 \pmod{p}$ as well. Again, by using part (1) of Lemma 1.16 and Proposition 2.27, these results hold for the opposite knots $T_{p-1}^{p,q}$ as well.

As an example, we can compare our computations with the estimates on $\Theta_{L(5,1)}$ given by Turaev in [56, Sec. 1]:

- $\Theta_{L(5,1)}(m) = 0$ for $m = 0, \pm 1$
- $\Theta_{L(5,1)}(m) \geq \frac{1}{5}$ for $m = \pm 2$

The computation of $\widehat{GH}(L(5,1), T_m^{5,1})$ in these cases yields the following results for the difference $A_{max} - A_{min}$:

$$(36) \quad A_{max} - A_{min} = \begin{cases} 0 & \text{if } m = 0 \\ \frac{4}{5} & \text{if } m = \pm 1 \\ \frac{6}{5} & \text{if } m = \pm 2 \end{cases}$$

So, using Equation (31) we see that Turaev's and Ni-Wu's bounds (Equation (33)) are sharp for $L(5,1)$.

It is worth noting that the difference between Turaev's estimate for Θ and the actual value can be arbitrarily big. For example, if $p \gg 1$ and $m \sim \frac{p}{2}$, the knots $T_m^{p,1}$ have rational genus $g_{\mathbb{Q}}(T_m^{p,1}) \sim \frac{p}{4}$, while the bound given in [56] is always ≤ 1 .

5.2. Cornwell's polynomial and decategorification

As shown in Section 2.2, the Alexander polynomial $\Delta_K(t)$ is obtained as the decategorification of $\widehat{GH}(K)$. In a similar vein, we might want to define a generalization of Δ to lens spaces as the decategorification $\chi_t(\widehat{GH}(L(p,q), K))$.

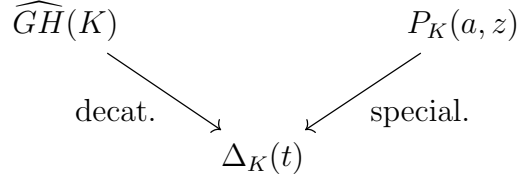
There is a well known two-variable generalization of the Alexander polynomial, due to several authors, known as the HOMFLYPT polynomial $P(a, z)$. $\Delta_K(t)$ can be recovered⁵ by specializing P :

$$(37) \quad \Delta_K(t) = P\left(1, \sqrt{t} - \frac{1}{\sqrt{t}}\right)$$

It is thus natural to ask if this relations also holds in the context of lens spaces. A recent paper of Cornwell [10] gives a candidate for the HOMFLYPT polynomial of links in lens spaces. We will give the

⁵Note that there are several equivalent definitions of P , and the relation with Δ changes accordingly.

precise statement in a moment, mentioning that his definition relies on a choice of normalizations on an infinite family of *trivial links*, which generalize simple knots.



In the following we are going to prove that, after a suitable choice of these normalizations, the relations in the diagram above hold for lens spaces too.

There are however some issues regarding the Alexander degrees of \widehat{GH} and the splitting in spin^c components that give several possible candidates satisfying these relations.

According to [10, Prop. 4.6], a knot K in a lens space can be *monotonically simplified*, that is changed into a simple knot by applying a sequence of column commutations (interleaving and non-interleaving) followed by a destabilization. Each time we destabilize the dimension of the grid decreases by one.

In particular, this means that up to skein and grid moves every knot $(L(p, q), K)$ can be reduced to the unique trivial knot $(L(p, q), T_{[K]}^{p,q})$ in its homology class:

PROPOSITION 5.16 ([10]). *Every knot $K \subset L(p, q)$ is equivalent to the unique trivial knot $T_{[K]}^{p,q}$, up to destabilizations and both interleaving and non-interleaving column commutations.*

The HOMFLYPT skein basis for $L(p, q)$ can be explicitly defined in terms of grid diagrams; it is composed of links made up of grid number 1 knots. They will be uniquely determined by a string of p natural numbers which records how many components there are in each homology class.

DEFINITION 5.17. *Choose a string $I = (m_0, \dots, m_{p-1}) \in \mathbb{N}^p$ such that $\sum_{i=0}^p m_i = n > 0$. The trivial link $T_I^{p,q} \subset L(p, q)$ is the n -component link represented by a grid G_I of parameters (n, p, q) described as follows: the \mathbb{X} markings are placed along the antidiagonal of the first box⁶; the \mathbb{O} markings are placed in such a way that there are (starting from the top) exactly m_i grid number 1 components in the i -th homology class, as in Figure 5.4. If $m_0 > 0$, we represent these*

⁶This convention is the opposite of the one used in [10]; see also Remark 1.11.

				⊗										
			X				O							
		X				O								
	X									O				
X										O				

FIGURE 5.4. The simple link in $L(3, 1)$ corresponding to $I = (1, 2, 2)$. The first 1 corresponds to the nullhomologous component in the top row of the grid.

$$\begin{array}{|c|c|} \hline & \\ \hline \otimes & \\ \hline & \\ \hline \end{array} = \begin{array}{|c|c|} \hline & \\ \hline \text{O} & \text{X} \\ \hline \text{X} & \text{O} \\ \hline & \\ \hline \end{array}$$

FIGURE 5.5. How to convert a singular grid to a regular one, increasing the dimension of the grid by 1.

m_0 trivial components as a couple of markings of different kind in the same square⁷, as in Figure 5.5.

Simple knots are just one component trivial links, and correspond thus to strings $I \in \mathbb{N}^p$ with 1 as the only non-zero entry.

THEOREM 5.18 ([10]). Choose a polynomial $p_I \in \mathbb{Z}[a^{\pm 1}, z^{\pm 1}]$ for each trivial link $T_I^{p,q}$. Then there is a unique map

$$P : \mathcal{L}_{p,q} \longrightarrow \mathbb{Z}[a^{\pm 1}, z^{\pm 1}]$$

such that:

- $P_{\bigcirc}(a, z) = a^{1-p}$ (trivial knot normalization)
- $P_{T_I^{p,q}}(a, z) = p_I(a, z)$ (trivial link normalization)
- $a^{-p}P_{G_+}(a, z) - a^pP_{G_-}(a, z) = zP_{G_0}(a, z)$ (skein relation)
- $P_{\bigcirc \sqcup L}(a, z) = \frac{a^{-p}-a^p}{z}P_L(a, z)$ (disjoint unknot union)

There is a grid homology version of the skein exact triangle satisfied by $HF\mathcal{K}^\circ$ given in Chapter 2.2:

⁷The theory for grids with markings in the same squares is developed *e.g.* in [10] and [47]; with this convention the trivial knot \bigcirc has grid number 1, as the other trivial knots.

THEOREM 5.19. *Suppose G_+ , G_- and G_0 are three grids related by grid skein moves, as in Figure 1.11. Then if the two strands in the crossing of G_+ belong to the same component:*

$$\rightarrow cGH_m^-(G_+, a, \mathfrak{s}) \rightarrow cGH_m^-(G_-, a, \mathfrak{s}) \rightarrow cGH_{m-1}^-(G_0, a, \mathfrak{s}) \rightarrow$$

Otherwise:

$$\rightarrow cGH_m^-(G_+, a, \mathfrak{s}) \rightarrow cGH_m^-(G_-, a, \mathfrak{s}) \rightarrow (cGH^-(G_0, \mathfrak{s}) \otimes Z)_{m-1, a} \rightarrow$$

where Z is the 4-dimensional graded vector space of Theorem 2.7.

In analogy with Definition 4.9, we can give two distinct variants for the decategorification of \widehat{GH} , depending on the choice of the Alexander degree. We denote by $\mathbb{Z}[t^{\mathbb{Q}}]$ the ring of polynomials in t with rational exponents.

DEFINITION 5.20. *Given a link $(L(p, q), L)$, call $\chi^{\mathfrak{s}} \in \mathbb{Z}[t^{\mathbb{Q}}]$ the decategorification of $\widehat{GH}(L(p, q), L)$ in spin^c degree \mathfrak{s} :*

$$(38) \quad \chi_L^{\mathfrak{s}}(t) = \sum_{m \in \mathbb{Z}} \sum_{a \in \mathbb{Q}} (-1)^m rk \left(\widehat{GH}_{m+d(p, q, \mathfrak{s})}(L(p, q), L, a, \mathfrak{s}) \right) t^a \in \mathbb{Z}[t^{\mathbb{Q}}]$$

We can also consider the other version of \widehat{GH} (as in Remark 2.12), and define:

$$(39) \quad \tilde{\chi}_L^{\mathfrak{s}}(t) = \sum_{m, a \in \mathbb{Z}} (-1)^m rk \left(\widehat{GH}_{m+d(p, q, \mathfrak{s})}(L(p, q), L, a, \mathfrak{s}) \right) t^a \in \mathbb{Z}[t^{\pm 1}]$$

We can also consider the sum over all spin^c degrees:

$$\tilde{\chi}_L(t) = \sum_{\mathfrak{s} \in \text{spin}^c(L(p, q))} \tilde{\chi}_L^{\mathfrak{s}}(t), \quad \chi_L(t) = \sum_{\mathfrak{s} \in \text{spin}^c(L(p, q))} \chi_L^{\mathfrak{s}}(t)$$

LEMMA 5.21. *Each decategorification $\chi_L^{\mathfrak{s}}(t) = \chi_t(\widehat{GH}(L(p, q), L, \mathfrak{s}))$ satisfies the skein exact sequence:*

$$(40) \quad \chi_{L_+}^{\mathfrak{s}}(t) - \chi_{L_-}^{\mathfrak{s}}(t) = \left(\sqrt{t} - \frac{1}{\sqrt{t}} \right) \chi_{L_0}^{\mathfrak{s}}(t)$$

Where the links involved are represented by grids related by the skein moves of Figure 1.11.

PROOF. Follows from the exact triangle, as in [47, Ch. 9]. \square

Note that the same relation is satisfied by the sum of the decategorifications over all spin^c structures.

There are several other properties of the classical Alexander polynomial which are shared by its generalizations; here we list some.

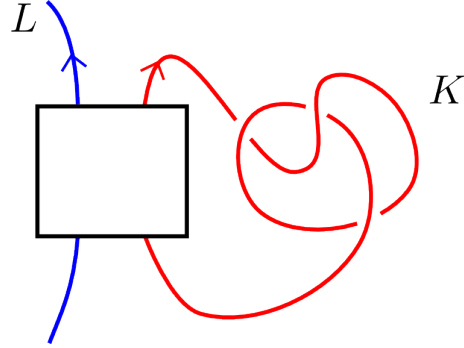


FIGURE 5.6. Substitute the skein relation in the box; L_{\pm} are $L\#K$, while L_0 is $L\sqcup K$.

PROPOSITION 5.22. *The decategorification χ_K^{\natural} enjoys the following properties:*

- (1) *If K is a knot, the evaluation of $\chi_K^{\natural}(t)$ in $t = 1$ is 1.*
- (2) *$\chi_L^{\natural}(t) = 0$ if $L = L_1\sqcup K$ is a disjoint sum of a link with a local knot.*
- (3) *$\chi_K(t) = \chi_{-K}(t)$*
- (4) *If $(L(p, q), K) = (S^3, K_0)\#(L(p, q), K_1)$ then*

$$\chi_K^{\natural}(t) = \chi_{K_0}^{\natural}(t) \cdot \chi_{K_1}^{\natural}(t)$$

- (5) *The span of χ_K is a lower bound for the rational genus:*

$$\text{Amp}(\chi_K(t)) \leq 2g_{\mathbb{Q}}(K) + 1$$

PROOF. (1) is a simple consequence of the skein relation; evaluating in $t = 1$ gives the relation $\chi_{G_+}(1) = \chi_{G_-}(1)$, so the evaluations in 1 are insensitive to crossing changes. Since K is a knot, then it is equivalent to $T_{[K]}^{p,q}$ up to crossing changes; the statement follows from Proposition 5.16 and the computations in Remark 2.25.

Part (2) is again due to the skein relation, as shown in Figure 5.6. (3) follows from Proposition 2.27, (4) from the connected sum formula (Proposition (11)) for \widehat{GH} , and (5) from Equation (31). \square

REMARK 5.23. Appealing to [40, Prop. 5.1], and the correspondence⁸ between m -component links and knots in $\#^{m-1}S^1 \times S^2$, it is also possible to prove that $\chi_L^{\natural}(1) = 0$ when $|L| \geq 2$. Note also that it follows easily from the definitions that $\chi_K(1) = \tilde{\chi}_K(1) = p$.

⁸See Section 2.2, or [39, Prop. 2.1].

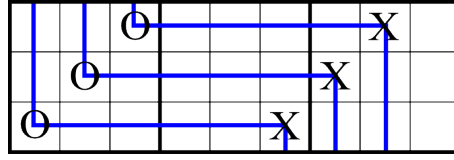


FIGURE 5.7. The smallest knot (in $L(3,1)$) with non symmetric decategorifications.

PROPOSITION 5.24. *If $(L(p, q), K) = (S^3, K') \# (L(p, q), \bigcirc)$ is a local knot, then:*

$$\chi_K(t) = p\Delta_{K'}(t)$$

PROOF. As mentioned in Remark 2.24 the grid homology of $(L(p, q), K)$ is given by p copies of $\widehat{GH}(K')$, one for each $\mathfrak{s} \in \text{spin}^c(L(p, q))$, without any shift in the Alexander degree. \square

REMARK 5.25. It is a well known fact that the Alexander polynomial is symmetric, *i.e.* it is unchanged under the substitution $t \mapsto t^{-1}$. As shown in Proposition 5.22, this is also true for the polynomials $\chi_K(t)$ and $\tilde{\chi}_K(t)$, but not for the single spin^c summands; the smallest example is given by the knot in Figure 5.7, where the computations yield:

$$\chi_K^{\mathfrak{s}}(t) = \begin{cases} +t^{\frac{2}{3}} - t^{-\frac{4}{3}} + t^{-\frac{7}{3}} & \text{if } \mathfrak{s} = 0 \\ +t - 1 + t^{-1} & \text{if } \mathfrak{s} = 1 \\ +t^{\frac{7}{3}} - t^{\frac{4}{3}} + t^{-\frac{2}{3}} & \text{if } \mathfrak{s} = 2 \end{cases}$$

It is also possible to find knots for which none of the polynomials $\chi_K^{\mathfrak{s}}(t)$ are symmetric. One small example is given by the knot in $L(4,1)$ represented by the 4-dimensional grid $\mathbb{X} = [0, 1, 2]$ and $\mathbb{O} = [5, 6, 7]$, in the notation explained in Section 6.1.1.

Cornwell's polynomial depends upon a choice of infinitely many polynomials, one for each trivial link. We can pin down one particular choice of normalization by prescribing that the value of the normalization on the trivial link $T_I^{p,q}$ coincides with the decategorification of $\widehat{GH}(L(p, q), T_I^{p,q})$, which we denote by $\chi_I(t)$.

Note that in each case we obtain a generalization of the Alexander polynomial to links in lens spaces as both decategorification of \widehat{GH} and specialization of an HOMFLYPT polynomial.

PROPOSITION 5.26. *There is only one function*

$$\widehat{P} : \mathcal{L}(L(p, q)) \longrightarrow \mathbb{Z}[a^{\pm 1}, z^{\mathbb{Q}}]$$

such that:

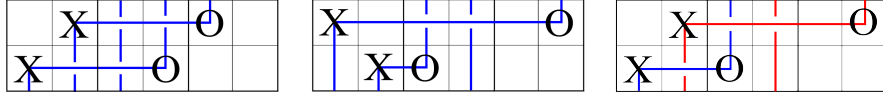


FIGURE 5.8. The skein triple from the example; on the left $G_+ = K$, in the center $G_- = \bigcirc$, and on the right a two component link.

- $\widehat{P}_{\bigcirc}(a, z) = p$ (trivial knot normalization)
- $\widehat{P}_{T^{p,q}}(z, t^{\frac{1}{2}} - t^{-\frac{1}{2}}) = \chi_I(t)$ (trivial links normalization)
- $a^{-p}\widehat{P}_{G_+}(a, z) - a^p\widehat{P}_{G_-}(a, z) = z\widehat{P}_{G_0}(a, z)$ (skein relation)
- $\widehat{P}_{\bigcirc \sqcup L}(a, z) = \frac{a^{-p}-a^p}{z}\widehat{P}_L(a, z)$ (disjoint unknot union)

Moreover this function satisfies the following equality:

$$(41) \quad \widehat{P}_K \left(1, \sqrt{t} - \frac{1}{\sqrt{t}} \right) = \chi_t(\widehat{GH}(L(p, q), K))$$

PROOF. The existence and uniqueness of \widehat{P} are a corollary of Theorem 5.18. The second statement follows the skein relation (Corollary 5.21) satisfied by χ . Both invariants satisfy the same skein relation, and have the same value on all trivial links by construction, hence are the same. \square

REMARK 5.27. Changing the normalizations yields several other polynomials: if we choose the value of \widehat{P} on the unknot to be 1, and fix the value of the trivial links to be $\chi_I^{\mathfrak{s}}(t)$, we get another polynomial, which is the decategorification of the grid homology $\widehat{GH}(L(p, q), K, \mathfrak{s})$.

Yet again, if we choose 1 as the value on the unknot, and $\widetilde{\chi}_I^{\mathfrak{s}}$ on the trivial links, we get a decategorification of $\widehat{GH}(L(p, q), K, \mathfrak{s})$ with Alexander degree as in Remark 2.12, so it belongs to $\mathbb{Z}[t^{\pm 1}]$.

EXAMPLE 5.28. We give here a sample computation of $\chi^{\mathfrak{s}}$ for the 2-component link represented by the grid G_0 in Figure 5.8. From Example 3.11, we can compute:

$$(\chi_{G_+}^0(t), \chi_{G_+}^1(t), \chi_{G_+}^2(t)) = \left(t - 1 + \frac{1}{t}, 1, 1 \right).$$

It is easy to show that the grid G_- represents the unknot $\bigcirc \subset L(3, 1)$. So, using the skein relation of Lemma 5.21, the decategorification of the homology for the link L represented by G_0 is:

$$(\chi_{G_0}^0(t), \chi_{G_0}^1(t), \chi_{G_0}^2(t)) = \left(\sqrt{t} - \frac{1}{\sqrt{t}}, 0, 0 \right)$$

5.3. Some restrictions on the Berge Conjecture

The celebrated Berge conjecture aims to classify the knots in S^3 on which Dehn surgery can produce a lens space. It was known since 1971 (see [31]) that $pq \pm 1$ surgery on the torus knot $T_{p,q}$ yields the lens space $L(pq \pm 1, p^2)$.

In the following years Bayer and Rolfsen provided several non torus knots which admit lens space surgeries, and Finthusel and Stern showed that, among others, the pretzel knot $P(-2, 3, 7)$ has two distinct lens space surgeries.

In an unpublished note, J. Berge defined a class of knots, the *doubly primitive knots*, which admit a lens space surgery by construction. Later on Gordon conjectured that besides torus knots, the knots in Berge's list were the only knots which could produce lens spaces by Dehn surgery.

A *doubly primitive* knot is a knot embedded on a genus 2 surface induced by an Heegaard splitting of S^3 ; moreover its pushoff in either of the handlebodies has to represent a generator of the fundamental group. It is easy to show that performing Dehn surgery on such a knot with the framing induced by the surface produces a lens space.

In [20], Greene proved that the lens spaces realizable by surgeries on knots in S^3 coincide with the ones that can be obtained by a surgery on a Berge or torus knot.

There are several obstructions on knots admitting an L -space surgery arising from HFK^c ; most notably, in [36] Ozsváth and Szabó gave strong restrictions on the Alexander polynomial of such knots.

Using Ni's Theorem from [32], it is immediate to show that all knots admitting a lens space surgery (or more generally a L -space surgery) need to be fibered. A thorough investigation of several families of Berge knots was conducted by Baker in [1] and [2].

In 2007 Rasmussen and Hedden⁹ independently reformulated the Berge Conjecture in terms of the knot Floer homology of the dual knot. In particular, they were able to prove that this conjecture is equivalent to the following pair of conjectures:

CONJECTURE 5.29. *A knot K in $L(p, q)$ with simple knot Floer homology¹⁰ is simple.*

CONJECTURE 5.30. *There are exactly two knots T_i $i = 0, 1$ in $L(p, q)$ which satisfy*

$$rk_{\mathbb{F}}(\widehat{GH}(L(p, q), T_i)) = p + 2$$

⁹See [50] and [24].

¹⁰The definition can be found in Remark 2.25.

In particular, Conjecture 5.29 could be shown to hold by showing that knots whose grid number is greater than 1 have non-simple Floer homologies. This approach is closely related to the unknot detection of \widehat{HFK} in S^3 .

REMARK 5.31. Remark 2.24 together with the unknot recognition of Knot Floer homology in S^3 , shows that a connected sum

$$(L(p, q), K) = (L(p, q), K_1) \# (S^3, K_2)$$

with K_2 nontrivial has non simple Floer homology.

Moreover, one can use the $\tilde{\tau}$ invariants to obstruct knots from having a minimal rank grid homology. Basically if a knot has at least one nonzero $\tilde{\tau}^{\mathfrak{s}}$ invariant, then its homology in the \mathfrak{s} -th spin^c structure has rank greater than 1.

These sections are devoted to prove special cases of Conjecture 5.29.

5.3.1. Grid number 2. Conjecture 5.29 can be solved for almost all grid number 2 knots in $L(p, 1)$ as follows: we show that any such knot has at least one spin^c structure \mathfrak{s} for which $rk(\widehat{GH}(L(p, 1), K, \mathfrak{s})) > 1$. Since it is easier to work with the tilde flavor, using Proposition 2.26 we can equivalently rewrite this statement as

$$\exists \mathfrak{s} \in \text{spin}^c(L(p, 1)) \text{ such that } rk(\widetilde{GH}(L(p, 1), K, \mathfrak{s})) > 2$$

In the case of a grid number 2 knot, we can apply strong constraints to its diagram, putting it in a standard form.

REMARK 5.32. A knot admitting a grid diagram of dimension 2 can always be described¹¹ by giving the number of the boxes containing the markings¹²:

$$\mathbb{X} = [0, 2a + 1], \mathbb{O} = [2b + 1, 2c] \quad a, b, c \in \{0, p - 1\}$$

As an example, the knot considered in example 3.11 can be written as $\mathbb{X} = [0, 1]$ and $\mathbb{O} = [3, 4]$.

DEFINITION 5.33. *The skein number $sk(K)$ of a knot K with grid number 2 is the minimal number of skein moves that need to be applied to each grid number 2 grid diagram of K to obtain the only grid number 1 knot in its homology class.*

Given a 2-dimensional grid for a knot, call \mathbb{X}_1 the \mathbb{X} marking in the lower left corner of the grid¹³. Now call \mathbb{X}_2 the remaining \mathbb{X} marking,

¹¹See also Sec. 6.1.1.

¹²Boxes are ordered from left to right, starting from 0, and markings from bottom to top.

¹³It can be made sure \mathbb{X}_1 exists after applying some row translations.

and \mathbb{O}_i the \mathbb{O} markings on the same column of \mathbb{X}_i , $i = 1, 2$. Define $l(\mathbb{X}_i, \mathbb{O}_{i+1})$ ($i \in \mathbb{Z}_2$), the distance of two markings on the same row, as the minimum of the differences of the x coordinates of the two markings. By Remark 5.32:

$$l(\mathbb{X}_2, \mathbb{O}_1) = \min\{|2a + 1 - 2c|, 2p - |2a + 1 - 2c|\}$$

Call $l(K)$ the minimum of these numbers among all grid number 2 diagrams of K . If $l(K) = 1$ the knot is in fact a stabilization of a grid number 1 knot (see [10, Sec. 4.2]).

A skein move decreases the row distance by at most 2, so

$$sk(K) \leq \frac{l(K) - 1}{2}$$

We say that a grid number 2 diagram of K is in standard form if:

- \mathbb{X}_1 is in the bottom/left-most square
- \mathbb{O}_2 is in the $l(K)$ -th square of the lowest row
- \mathbb{O}_1 is at the right of \mathbb{O}_2
- \mathbb{X}_2 is either in the second square (from the left) in the highest row (Case 1), or on the right of \mathbb{O}_1 (Case 2)
- $l(\mathbb{X}_2, \mathbb{O}_1) \geq l(\mathbb{X}_1, \mathbb{O}_2) = l(K)$
- There is a non-interleaving commutation between the two columns

PROPOSITION 5.34. *Every grid number 2 knot K has a standard form diagram, up orientation reversal.*

PROOF. Consider a grid number 2 grid for K which minimizes $l(K)$. Up to row/columns translations we can place an \mathbb{X} marking in the lower-bottom square, and choose the distance between the markings in the bottom row to be minimal, as in the top part of Figure 5.9; we can achieve this configuration up to orientation reversal.

Next we place the \mathbb{O} marking on the bottom row. It can not be in the square on the immediate right of the one containing \mathbb{X}_1 , otherwise K would be a stabilization of a grid number one knot. So \mathbb{O}_2 is in the $(2b + 1)$ -th square of the lowest row (with $b \in \{1, \dots, \lceil \frac{p-1}{2} \rceil\}$, by minimality of $l(\mathbb{X}_1, \mathbb{O}_2)$), and $sk(K) \leq b$.

Then we place the \mathbb{O} marking on the same column as \mathbb{X}_1 . There are two possible choices according to the position of \mathbb{O}_2 : \mathbb{O}_1 can be above or below \mathbb{O}_2 (as shown in case a and b in Figure 5.9).

We can discard case a . In fact, by assumption the distance from \mathbb{X}_1 to \mathbb{O}_2 is minimal. The two columns must comprise a skein crossing change, and in case a this is possible only if \mathbb{X}_2 is between \mathbb{X}_1 and \mathbb{O}_1 (as shown in the vertical grid denoted by a'). But this would imply that $l(\mathbb{X}_2, \mathbb{O}_1) < l(\mathbb{X}_1, \mathbb{O}_2)$, which is impossible by assumption.

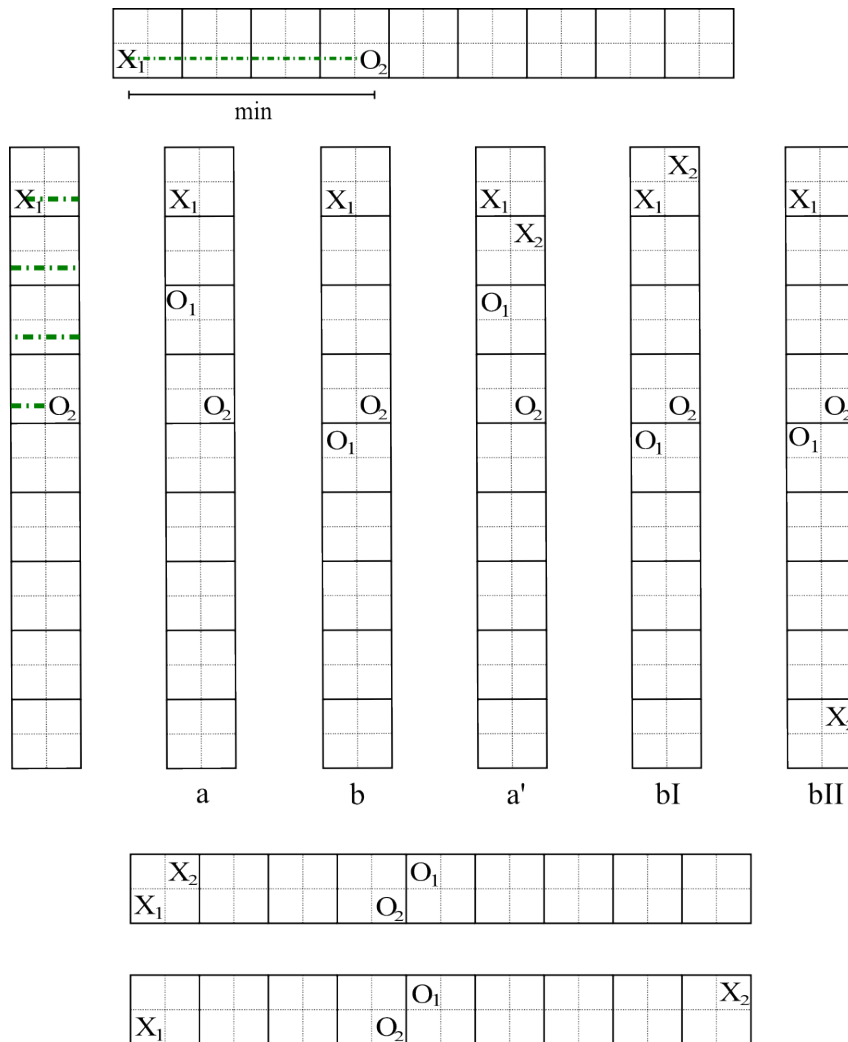


FIGURE 5.9. An example showing the possible cases of the proof. The vertical representations are obtained from the usual one by cutting along α_1 and β_1 , and regluing the (now disconnected) boxes according to their top-bottom identifications.

We are left with two (very similar) subcases of case b , indicated in Figure 5.9 as bI and bII . These are precisely the two possible configurations of Definition 5.33. \square

We can now prove the following statement:

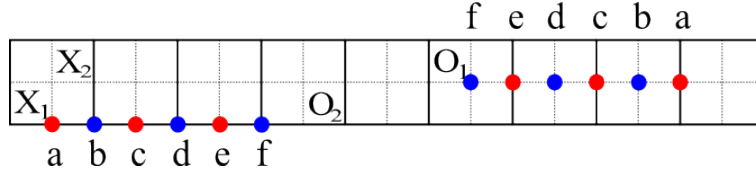


FIGURE 5.10. Some of the possible choices of the components of a lonely generator for a knot in $L(9, 1)$.

PROPOSITION 5.35. All grid number 2 knots $(L(p, 1), K)$ such that $sk(K) > 1$ satisfy

$$rk(\widehat{GH}(L(p, 1), K)) > p$$

In particular, they are not counterexamples to Conjecture 5.29.

PROOF. We are going to show how to find some generators of the (tilde-flavored) grid homology for a grid diagram in standard form. We call an element of a chain complex *lonely* if it has no boundary and it does not appear in the differential of any other element. Clearly such an element produces a non-trivial homology class.

In our case the complex is generated over \mathbb{F} by a set whose elements can be identified with $\mathfrak{S}_2 \times (\mathbb{Z}_p)^2$. Each generator x has two components x_1 and x_2 which lie on the curves α_1 and α_2 respectively. To find a lonely generator, just choose x_1 in the interval $[\mathbb{X}_1 + 1, \mathbb{O}_2 - 1]$ and the second coordinate between \mathbb{O}_1 and \mathbb{X}_2 , as shown in Figure 5.10 for Case 2.

Note that if we label the possible components as in Figure 5.10, then the generators whose components have the same letter all belong to the spin^c structure 0.

REMARK 5.36. All these generators in the 0-th spin^c structure are in fact lonely in the \sim complex: every rectangle starting/ending from/in one of the two components of such a generator is bound to meet an \mathbb{O} or \mathbb{X} marking before it can reach the other component.

REMARK 5.37. All the considerations we made so far, involving the rank of the tilde-flavored groups, are unaffected by an exchange of the \mathbb{X} and \mathbb{O} markings.

Lonely generators in a diagram are still lonely in the tilde complex generated by the knot with the opposite orientation. The only thing that changes is the spin^c structure in which the rank is greater than 2, according to Proposition 2.27.

So for a grid number 2 knot K we have found $2sk(K)$ lonely generators (all belonging to the same spin^c structure). It follows that

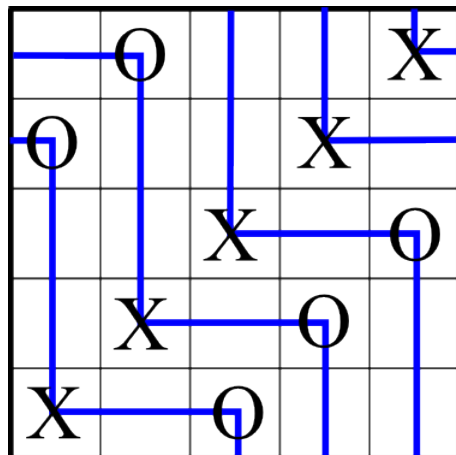


FIGURE 5.11. A torus knot in S^3 ; it admits a grid without crossings.

$rk(\widehat{GH}(L(p, 1), K, 0)) \geq 4 \implies rk(\widehat{GH}(L(p, 1), K, 0)) \geq 2$, which is what we wanted. \square

REMARK 5.38. The same techniques apply to grid number 2 knots in arbitrary lens spaces; however the description of the general standard form is quite cumbersome, so in order to get a clean statement we restricted ourselves to $L(p, 1)$. However, the same approach does not work for grids of dimension greater than 2; it can be shown *e.g.* that the tilde grid complex of the knot $\mathbb{X}, \mathbb{O} = [0, 1, 2], [5, 6, 7]$ in $L(3, 1)$ does not have enough lonely generators.

5.3.2. Generalized torus knots. In this section we exhibit another family of knots in $L(p, 1)$ whose hat grid homology has rank greater than p . For simplicity we restrict ourselves to \mathbb{F} coefficients. In view of the results of Subsection 5.3.1, we will suppose that all knots considered have grid number greater than 2.

It is well known (see *e.g.* [47]) that a torus knot $T(a, b) \subset S^3$ admits a grid diagram in which all markings of one kind lie on the antidiagonal of the grid, while the markings of the other kind are placed at a fixed distance from this diagonal, as shown in Figure 5.11 for $T(3, 2) = 3_1$.

Note that such a grid diagram produces a knot diagram of $T(a, b)$ on the splitting torus of the genus 1 decomposition of S^3 containing no crossings.

DEFINITION 5.39. A generalized torus link is a link in $L(p, q)$ admitting a grid diagram with all the markings of one type placed in the

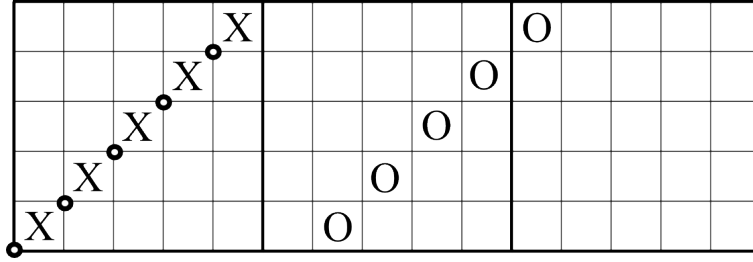


FIGURE 5.12. A generalized torus knot in $L(3,1)$, with the generator x^+ .

(anti)diagonal of the leftmost box, and the markings of the other type placed at fixed distance from them, as in Figure 5.12.

REMARK 5.40. For concreteness, from now on we suppose that the markings on the antidiagonal are all of \mathbb{X} type. In the other case, the following results apply to the link with opposite orientation.

PROPOSITION 5.41. *Let $(L(p,1), K)$ be a generalized torus knot. Then,*

$$rk_{\mathbb{F}} \left(\widehat{GH}(L(p,1), K) \right) > p$$

PROOF. Given a generalized torus knot in S^3 , represented by G , we are going to identify two cycles in $GC^-(G)$, and prove that they are non trivial in homology and distinct. In particular this provides another infinite family of knots which can not produce counterexamples to Conjecture 5.29. We will denote the set of empty rectangles connecting two generators $a, b \in S(G)$ which do not contain any \mathbb{X} marking by $Rect_{\mathbb{X}}^{\circ}(a, b)$.

The first generator we examine is the cycle x^+ which determines the Legendrian invariant¹⁴ of GH^- : its components are placed in the lower left squares containing an \mathbb{X} marking. Each rectangle starting from this generator necessarily contains an \mathbb{X} marking. This means that $\forall y \in S(G)$ no rectangles in $Rect^{\circ}(x^+, y)$ are counted in the differential, so x^+ is in fact a cycle.

To show that it is not a boundary, we could modify the argument of [47, Ch. 6], but instead we prove this directly, since similar considerations will be helpful in what follows. In order to do so, we are going to prove a stronger statement: if $y \in GC^-(G)$ is such that $Rect_{\mathbb{X}}^{\circ}(y, x^+) \neq \emptyset$, then each $r \in Rect_{\mathbb{X}}^{\circ}(y, x^+)$ necessarily contains at least one \mathbb{O} marking. Note that this implies that x^+ is not a boundary:

¹⁴For the definitions and use of these invariants see e.g. [45].

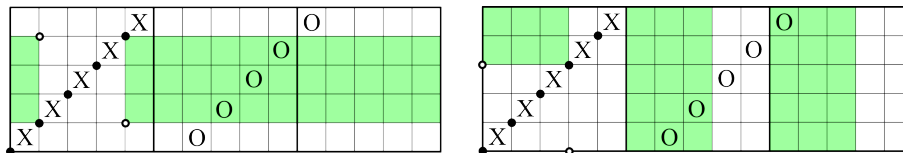


FIGURE 5.13. Two rectangles arriving to x^+ . Only the relevant part of y are drawn.

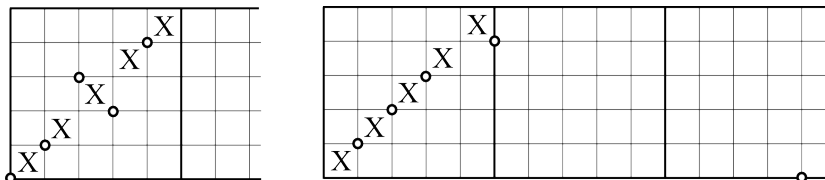


FIGURE 5.14. The generators x_3 (left) and x_n (right), in a grid of dimension 5.

every element containing x^+ in its differential, does so with at least one V_i coefficient.

Consider a rectangle $r \in \text{Rect}_{\mathbb{X}}^{\circ}(y, x^+)$. It must be of one of the types shown in Figure 5.13, which intersect all boxes. Hence, r must contain at least one \circledast marking, so x^+ can not be a boundary.

Now we define the second non trivial cycle. Consider the n elements $\{x_1, \dots, x_n\} \in S(G)$ given by transposing two consecutive components in x^+ , as shown in Figure 5.14.

Each x_i has a non trivial boundary: there are exactly two rectangles starting from each x_i , with height or width equal to 1, and no \mathbb{X} marking in their interior. Moreover, these rectangles connect each x_i to x^+ , and contain an \circledast marking each. Call σ_{\circledast} the permutation describing the positioning of the \circledast markings. Then we can write:

$$\partial^-(x_i) = (V_i + V_{\sigma_{\circledast}(i)}) x^+$$

and, if we define $\bar{x} = \sum_{i=1}^n x_i$, it is immediate to prove that \bar{x} is a cycle¹⁵.

Showing that \bar{x} is not a boundary is slightly more involved than the previous case, but relies on similar considerations.

Choose a generator x_i ; note that if a rectangle r to any x_i does not involve the transposed components of x_i , then r must contain at least one \circledast marking by the same considerations made for x^+ . So we are left

¹⁵With some more work it can be shown that \bar{x} is a cycle also in the sign refined theory.

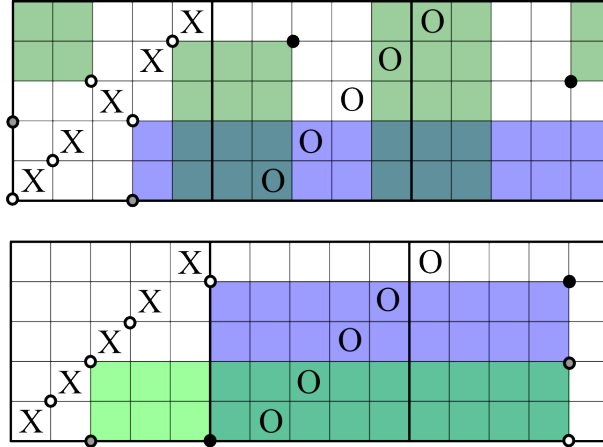


FIGURE 5.15. Some of the possible empty rectangles reaching x_i , for $i = 3, 5$.

with rectangles which have their SE or NW corner on one transposed component of x_i .

There are several possibilities for a rectangle $r \in \text{Rect}_{\mathbb{X}}^{\circ}(y, x_i)$. it is however easy to check that each of these rectangles contains at least one \circ marking. Indeed, it is immediate to see that if $i < n$, r intersects all the boxes. If instead $i = n$, we just need to check those rectangles to x_n which have a corner on the lower component of x_n (as done in the bottom portion of Figure 5.15).

So each x_i can not be the boundary of any other generator, but one of its multiples by some product of V variables is.

Summing up, we have determined two non-trivial elements of the homology $GH^-(K)$, where K is a generalized torus knot in $L(p, 1)$. These elements are necessarily distinct, since their degrees are different: each x_i has x^+ in its boundary, so we can apply the equations determining the behavior of the degrees under multiplication by a V_i variable and the differential (see Section 2.4.1). Since they belong to the same spin^c degree, we have proved the statement. \square

REMARK 5.42. The argument of the proof of Proposition 5.41 does not work for $L(p, q)$ with $q \neq 1$, because in that case the generators x_n and x^+ are not even in the same spin^c degree. However, the same argument works in $L(p, 1)$ for configurations of the \circ markings which are quite more general than the ones considered in Definition 5.39.

CHAPTER 6

Computations

In this last chapter we show that the theory is computable, by exhibiting some computer programs capable of determining the groups \widehat{GH} , and extracting informations and invariants from them.

It was first proved by Droz in [16] that prime knots in the three sphere with less than 12 crossings have torsion-free knot Floer homologies. There is no apparent reason for the lack of torsion in these groups.

Consequently, as suggested to my advisor by András Stipsicz, knot Floer homology of knots in lens spaces is a natural place where to look for possible torsion.

With this motivation I encoded sign assignments (for grids with small parameters) in the program described in Section 6.1.1. With this tool I was able to prove a result (Proposition 6.1) analogous to Droz's for knots in lens spaces, providing empirical evidence for the absence of torsion in the grid homology of lens spaces.

6.1. The programs

It becomes immediately apparent that the work needed to actually compute $\widehat{GH}(G)$ for grids with dimension greater than 3 is not manageable by hand¹. So the author developed several programs in `soqpe` (see [15]) capable of computing the hat flavored grid homology of links in lens spaces.

The programs can be freely used online at my homepage:

<http://poisson.dm.unipi.it/~celoria/#programs>

6.1.1. Grid homology calculator. It is the basic program for the computation of the *hat* grid homology. The input consists of the grid parameters (n, p, q) , followed by two strings of length n determining the positions of the \mathbb{X} and \mathbb{O} markings.

We encode the markings with a string of length n for each kind; to the i -th marking (from the bottom row) we associate the number (from the left, and starting from 0) of the small square containing it.

¹The complex for a grid with parameters (n, p, q) has $n!p^n$ elements!

As an example, the knot in Figure 1.8 is encoded as $\mathbb{X} = [12, 1, 8, 5, 9]$ and $\mathbb{O} = [6, 3, 0, 9, 12]$.

The output consists of the following:

- (Optional) A drawing of the chosen grid
- The hat grid homology² $\widehat{GH}(G, \mathfrak{s}; \mathbb{Z})$ for each $\mathfrak{s} \in \text{spin}^c$ structure, and its decategorification.
- Whether the knot is rationally fibered, the homology class it represents and its rational genus.
- (Optional) A long list of the generators with their tri-grading.
- (Optional) A drawing of the grid for the lift of the knot to S^3 , together with its (univariate) Alexander polynomial and the number of components of the lift.

Basically the program creates the generators $S(G)$ and computes their tri-degree; afterwards it checks for empty rectangles, and creates the matrices of the differentials.

However, rather than computing the module $\widehat{GC}(G)$, we adopt the simpler approach of computing the *tilde* flavored homology $\widetilde{GH}(G)$, defined in Section 2.4.3. We modify the differential to encompass \mathbb{Z} coefficients as explained in Chapter 3:

$$\tilde{\partial}(x) = \sum_{y \in S(G)} \sum_{\substack{r \in \text{Rect}^\circ(x,y) \\ (\mathbb{X} \cup \mathbb{O}) \cap r = \emptyset}} \mathcal{S}(r)y$$

where \mathcal{S} is a sign assignment. Using the amazing group theoretic capabilities of `sojge`, the relations in $\widetilde{\mathfrak{S}}_n$ are encoded in a matrix associated to the differential, and a fixed sign assignment \mathcal{S} is chosen for each $n \leq 5$.

After computing the homology $\widetilde{GH}(G)$, the program “factors out” the tensor product dependent on the size of the grid (see Proposition 2.26), and prints the requested information. The various invariants are obtained from the homology using the equations from the previous chapters of this thesis. If the grid represents a link, some of the features described above (such as rational genus and fiberdeness) are disabled.

Using the program we verified the following:

PROPOSITION 6.1. *All grids with parameters³ (n, p, q) such that*

- $n = 2$ and $p \leq 12$
- $n = 3$ and $p \leq 6$
- $n = 4$ and $p \leq 3$

²If the grid dimension is greater than 5 it returns the \mathbb{F} version.

³These values will be updated.

- $n = 5$ and $p \leq 2$

have grid homologies containing no r -torsion for $r \leq 17$.

6.1.2. The Atlas. The speed of the previous program depends heavily on the parameters; it is painfully slow for $n \geq 6$. Another project I am currently managing is to keep a library of already computed knots; this the Lens Space Knot Atlas *a.k.a.* **LSKA**.

Since it only has to read from existing files its speed is more or less independent from the parameters; **LSKA** encompasses all knots (links soon to come) for parameters in the following ranges⁴:

- $n = 1$ you can choose p up to 20.
- $n = 2$ you can choose p up to 10.
- $n = 3$ you can choose p up to 5.
- $n = 4$ you can choose p up to 2.
- $n > 4$ soon to appear.

In order to further reduce computational time, we used the symmetries (Propositions 2.27 and 2.8) described in Section 2.2; this allows one to approximately cut $\frac{3}{4}$ of the needed work for knots in $L(p, *)$.

A related project consists in encoding the isotopy classes of small-parameter knots into a library, so that **LSKA** first tries to reduce the knot before reading from the library of examples. This improvement would drastically abridge the computational cost for knots with grid dimension ≥ 3 which are in fact stabilizations of smaller knots.

6.1.3. Tech talk. As mentioned above, the programs involved were all developed in **SDGE**. This is a free open source alternative to the usual⁵ mathematical computational tools. Its main strength comes from the presence of a intuitive GUI, a competitive computational speed⁶ and the possibility of programming in mixed languages.

The latter has been used extensively in the creation of the programs; both projects have been encoded into computational cells⁷, embedded in my homepage.

The *interact*⁸ mode allows a user to easily choose the parameters, and the **L^AT_EX** compatibility makes sure that the output is adequately readable and comprehensible.

⁴This values are constantly updated.

⁵Mathematica, Maple, Magma, Matlab...

⁶See <http://www.sagemath.org/tour-benchmarks.html>.

⁷Like <http://aleph.sagemath.org/>

⁸<http://wiki.sagemath.org/interact>

`soqe` is built on top of several existing open source packages and programs; in the writing of the GH-calculator and `ESKA` I primarily used the modules Numpy, Maxima, Ginac, GAP, GMP and MPFR.

The computations were mainly carried out on computers provided by the University of Pisa, with four AMD A8-3850 APU processors, running on a 64-bit Ubuntu 12.04 LTS release.

6.2. Examples

In this Section we display the computations of the grid homology for some small knots, highlighting some peculiarities.

6.2.1. Small knots. Here we list all hat grid homologies (with integer coefficients) for knots in $L(2, 1)$ and $L(3, 1)$ admitting grids with dimension $n \leq 3$, up to orientation reversal.

Before that we present some small refinement on the function f defined in Section 3.0.1; recall that $f : \mathbb{N}_{\geq 1} \rightarrow \mathbb{N}_{\geq 1}$ is defined as the minimal dimension of a grid in $L(p, *)$ representing a non-simple knot. Clearly it can be specialized to encompass the coefficient q too. Furthermore, we can fix the homology class represented by the non-simple knot, obtaining a new function $f(p, q, m)$, which records the minimal grid number of a non-simple knot in $L(p, q)$ representing $m \in H_1(L(p, q); \mathbb{Z})$. The computations below show that in fact f does depend on the choice of m ; in particular $f(2, 1, 0) = 3$, $f(2, 1, 1) = 4$, $f(3, 1, 0) = 2$ and $f(3, 1, 1) = f(3, 1, 2) = 3$. So, from this point of view, the smaller the parameters of the lens spaces are, the more knot theory behaves similarly⁹ to S^3 .

L(2, 1) :

- $\mathbf{n} = 1$: $\bigcirc, T_1^{2,1}$
- $\mathbf{n} = 2$: none
- $\mathbf{n} = 3$: (these last two are mirror images of one another)

★ $(\mathbb{X}, \mathbb{O}) = (012, 234)$ class 0

$$\left(\mathbb{Z}_{[\frac{7}{4}, 1]} \oplus \mathbb{Z}_{[\frac{3}{4}, 0]} \oplus \mathbb{Z}_{[-\frac{1}{4}, -1]}, \mathbb{Z}_{[\frac{1}{4}, 0]} \right)$$

★ $(\mathbb{X}, \mathbb{O}) = (210, 054)$ class 0

$$\left(\mathbb{Z}_{[-\frac{1}{4}, 0]}, \mathbb{Z}_{[\frac{1}{4}, 1]} \oplus \mathbb{Z}_{[-\frac{3}{4}, 0]} \oplus \mathbb{Z}_{[-\frac{7}{4}, -1]} \right)$$

L(3, 1) :

- $\mathbf{n} = 1$: $\bigcirc, T_1^{3,1}, T_2^{3,1}$

⁹Recall that in this case $f(1, 0, 0) = 5$.

- $\mathbf{n} = 2$: $(\mathbb{X}, \mathbb{O}) = (01, 34)$ (fully amphichiral) class 0

$$\left(\mathbb{Z}_{[\frac{3}{2}, 1]} \oplus \mathbb{Z}_{[\frac{1}{2}, 0]} \oplus \mathbb{Z}_{[-\frac{1}{2}, -1]}, \mathbb{Z}_{[\frac{1}{6}, 0]}, \mathbb{Z}_{[\frac{1}{6}, 0]} \right)$$

- $\mathbf{n} = 3$:

- ★ $(\mathbb{X}, \mathbb{O}) = (012, 234)$ class 2

$$\left(\mathbb{Z}_{[\frac{3}{2}, \frac{2}{3}]} \oplus \mathbb{Z}_{[\frac{1}{2}, -\frac{1}{3}]} \oplus \mathbb{Z}_{[-\frac{1}{2}, -\frac{4}{3}]} \oplus \mathbb{Z}_{[\frac{13}{6}, \frac{4}{3}]} \oplus \mathbb{Z}_{[\frac{7}{6}, -\frac{1}{3}]} \oplus \mathbb{Z}_{[\frac{1}{6}, -\frac{2}{3}]} \oplus \mathbb{Z}_{[\frac{1}{6}, 0]} \right)$$

- ★ $(\mathbb{X}, \mathbb{O}) = (012, 456)$ class 1

$$\left(\mathbb{Z}_{[\frac{3}{2}, \frac{2}{3}]} \oplus \mathbb{Z}_{[\frac{1}{2}, -\frac{4}{3}]} \oplus \mathbb{Z}_{[-\frac{1}{2}, -\frac{7}{3}]} \oplus \mathbb{Z}_{[\frac{13}{6}, 1]} \oplus \mathbb{Z}_{[\frac{7}{6}, 0]} \oplus \mathbb{Z}_{[\frac{1}{6}, -1]} \oplus \mathbb{Z}_{[-\frac{25}{6}, \frac{7}{3}]} \oplus \mathbb{Z}_{[\frac{19}{6}, \frac{4}{3}]} \oplus \mathbb{Z}_{[\frac{1}{6}, -\frac{2}{3}]} \right)$$

- ★ $(\mathbb{X}, \mathbb{O}) = (012, 537)$ class 1

$$\left(\mathbb{Z}_{[\frac{3}{2}, \frac{2}{3}]} \oplus \mathbb{Z}_{[\frac{1}{2}, -\frac{1}{3}]} \oplus \mathbb{Z}_{[-\frac{1}{2}, -\frac{4}{3}]} \oplus \mathbb{Z}_{[\frac{1}{6}, 0]} \oplus \mathbb{Z}_{[\frac{13}{6}, \frac{4}{3}]} \oplus \mathbb{Z}_{[\frac{7}{6}, \frac{1}{3}]} \oplus \mathbb{Z}_{[-\frac{1}{6}, -\frac{2}{3}]} \right)$$

- ★ $(\mathbb{X}, \mathbb{O}) = (015, 480)$ class 2

$$\left(\mathbb{Z}_{[-\frac{1}{2}, -\frac{1}{3}]} \oplus \mathbb{Z}_{[\frac{1}{6}, \frac{1}{3}]} \oplus \mathbb{Z}_{[\frac{7}{6}, 1]} \oplus \mathbb{Z}_{[\frac{1}{6}, 0]}^3 \oplus \mathbb{Z}_{[-\frac{5}{6}, -1]} \right)$$

- ★ $(\mathbb{X}, \mathbb{O}) = (018, 264)$ class 1

$$\left(\mathbb{Z}_{[-\frac{1}{2}, -\frac{1}{3}]} \oplus \mathbb{Z}_{[\frac{7}{6}, 1]} \oplus \mathbb{Z}_{[\frac{1}{6}, 0]}^3 \oplus \mathbb{Z}_{[-\frac{5}{6}, -1]} \oplus \mathbb{Z}_{[\frac{1}{6}, \frac{1}{3}]} \right)$$

- ★ $(\mathbb{X}, \mathbb{O}) = (048, 261)$ class 2

$$\left(\mathbb{Z}_{[-\frac{1}{2}, -\frac{1}{3}]} \oplus \mathbb{Z}_{[\frac{1}{6}, \frac{1}{3}]} \oplus \mathbb{Z}_{[\frac{1}{6}, 1]} \oplus \mathbb{Z}_{[-\frac{5}{6}, 0]} \oplus \mathbb{Z}_{[-\frac{11}{6}, -1]} \right)$$

- ★ $(\mathbb{X}, \mathbb{O}) = (048, 726)$ class 1

$$\left(\mathbb{Z}_{[-\frac{1}{2}, -\frac{1}{3}]} \oplus \mathbb{Z}_{[\frac{1}{6}, 1]} \oplus \mathbb{Z}_{[-\frac{5}{6}, 0]} \oplus \mathbb{Z}_{[-\frac{11}{6}, -1]} \oplus \mathbb{Z}_{[\frac{1}{6}, \frac{1}{3}]} \right)$$

- ★ $(\mathbb{X}, \mathbb{O}) = (054, 216)$ class 0

$$\left(\mathbb{Z}_{[-\frac{1}{2}, 0]} \oplus \mathbb{Z}_{[\frac{1}{6}, 1]} \oplus \mathbb{Z}_{[-\frac{5}{6}, 0]} \oplus \mathbb{Z}_{[-\frac{11}{6}, -1]} \oplus \mathbb{Z}_{[\frac{1}{6}, 1]} \oplus \mathbb{Z}_{[-\frac{5}{6}, 0]} \oplus \mathbb{Z}_{[-\frac{11}{6}, -1]} \right)$$

6.2.2. Future work. There are several ways to continue the work brought on in this Thesis; first of all, with more powerful computers one could greatly improve the ranges of computations of $\mathfrak{L}\mathfrak{S}\mathfrak{K}\mathfrak{A}$.

In another direction, one might want to extend the kind of invariants which can be computed from these programs; of particular interest (see *e.g.* [9] and [3]) are for example the contact invariants, both classical (Thurston-Bennequin number, self linking..) and homological (see [22]).

Also, by extending the computations to the filtered hat theory (as in [47, Ch. 13]), one might hope to compute the τ invariants defined in Chapter 4.

Clearly the work on concordances of Chapter 4 can be expanded, and partial answers to the conjecture stated therein will be the subject of future work.

Bibliography

1. Kenneth L Baker, *Surgery descriptions and volumes of Berge knots I: Large volume Berge knots*, Journal of Knot Theory and Its Ramifications **17** (2008), no. 09, 1077–1097.
2. ———, *Surgery descriptions and volumes of Berge knots II: Descriptions on the minimally twisted five chain link*, Journal of Knot Theory and Its Ramifications **17** (2008), no. 09, 1099–1120.
3. Kenneth L Baker and J Elisenda Grigsby, *Grid diagrams and legendrian lens space links*, arXiv preprint arXiv:0804.3048 (2008).
4. Kenneth L Baker, J Elisenda Grigsby, and Matthew Hedden, *Grid diagrams for lens spaces and combinatorial knot Floer homology*, International Mathematics Research Notices (2008).
5. John Berge, *Some knots with surgeries yielding lens spaces*, unpublished manuscript.
6. Danny Calegari and Cameron Gordon, *Knots with small rational genus*, arXiv preprint arXiv:0912.1843 (2009).
7. A. Cattabriga, E. Manfredi, and L. Rigolli, *Equivalence of two diagram representations of links in lens spaces and essential invariants*, ArXiv preprint arXiv:1312.2230 (2013).
8. Alessia Cattabriga, Enrico Manfredi, and Lorenzo Rigolli, *Equivalence of two diagram representations of links in lens spaces and essential invariants*, Acta Mathematica Hungarica **146** (2013), no. 1, 168–201.
9. Christopher R Cornwell, *Bennequin type inequalities in lens spaces*, International Mathematics Research Notices (2011).
10. ———, *A polynomial invariant for links in lens spaces*, Journal of Knot Theory and Its Ramifications **21** (2012), no. 06, 1250060.
11. Peter R Cromwell, *Embedding knots and links in an open book I: Basic properties*, Topology and its Applications **64** (1995), no. 1, 37–58.
12. Celoria Daniele, *A note on grid homology in lens spaces: \mathbb{Z} coefficients and computations*, arXiv preprint arXiv:1510.07141 (2015).
13. ———, *On concordances in 3-manifolds*, preprint, available online. (2016).
14. Yael Degany, Andrew Freimuth, and Edward Trefts, *Some computational results about grid diagrams of knots*, (2008).
15. The Sage Developers, *Sage Mathematics Software (Version 6.7)*, 2015, <http://www.sagemath.org>.
16. Jean-Marie Droz, *Effective computation of knot Floer homology*, arXiv preprint arXiv:0803.2379 (2008).
17. Étienne Gallais, *Sign refinement for combinatorial link Floer homology*, Algebraic & Geometric Topology **8** (2008), no. 3, 1581–1592.

18. Paolo Ghiggini, *Knot Floer homology detects genus-one fibred knots*, American journal of mathematics **130** (2008), no. 5, 1151–1169.
19. R.E. Gompf and A. Stipsicz, *4-manifolds and Kirby calculus*, Graduate studies in mathematics, American Mathematical Soc.
20. Joshua Evan Greene, *The lens space realization problem*, arXiv preprint arXiv:1010.6257 (2010).
21. Joshua Evan Greene and Yi Ni, *Non-simple genus minimizers in lens spaces*, arXiv preprint arXiv:1305.0517 (2013).
22. Matthew Hedden, *An Ozsváth–Szabó Floer homology invariant of knots in a contact manifold*, Advances in Mathematics **219** (2008), no. 1, 89–117.
23. ———, *On knot Floer homology and cabling: 2*, International Mathematics Research Notices **2009** (2009), no. 12, 2248–2274.
24. ———, *On Floer homology and the Berge conjecture on knots admitting lens space surgeries*, Transactions of the American Mathematical Society **363** (2011), no. 2, 949–968.
25. ———, *On Floer homology and the Berge conjecture on knots admitting lens space surgeries*, Transactions of the American Mathematical Society **363** (2011), no. 2, 949–968.
26. Peter B Kronheimer and Tomasz S Mrowka, *Gauge theory for embedded surfaces, i*, Topology **32** (1993), no. 4, 773–826.
27. Charles Livingston, *Homology cobordisms of 3-manifolds, knot concordances, and prime knots*, Pacific Journal of Mathematics **94** (1981), no. 1, 193–206.
28. Charles Livingston and Naik Swatee, *Introduction to Knot Concordance*, available online.
29. Ciprian Manolescu, Peter Ozsváth, and Sucharit Sarkar, *A combinatorial description of knot Floer homology*, Annals of Mathematics (2009), 633–660.
30. Ciprian Manolescu, Peter Ozsváth, Zoltán Szabó, and Dylan P Thurston, *On combinatorial link Floer homology*, Geometry & Topology **11** (2007), no. 4, 2339–2412.
31. Louise Moser, *Elementary surgery along a torus knot*, Pacific Journal of Mathematics **38** (1971), no. 3, 737–745.
32. Yi Ni, *Knot Floer homology detects fibred knots*, Inventiones mathematicae **170** (2007), no. 3, 577–608.
33. ———, *Link Floer homology detects the Thurston norm*, Geometry & Topology **13** (2009), no. 5, 2991–3019.
34. Yi Ni and Zhongtao Wu, *Heegaard Floer correction terms and rational genus bounds*, Advances in Mathematics **267** (2014), 360–380.
35. Peter Ozsváth, András I Stipsicz, and Zoltán Szabó, *Combinatorial Heegaard Floer homology and sign assignments*, Topology and its Applications **166** (2014), 32–65.
36. Peter Ozsváth and Zoltán Szabó, *Absolutely graded Floer homologies and intersection forms for four-manifolds with boundary*, Advances in Mathematics **173** (2003), no. 2, 179–261.
37. ———, *Knot Floer homology and the four-ball genus*, Geometry & Topology **7** (2003), no. 2, 615–639.
38. ———, *Holomorphic disks and genus bounds*, Geometry & Topology **8** (2004), no. 1, 311–334.

39. ———, *Holomorphic disks and knot invariants*, *Advances in Mathematics* **186** (2004), no. 1, 58–116.
40. ———, *Holomorphic disks and three-manifold invariants: properties and applications*, *Annals of Mathematics* (2004), 1159–1245.
41. ———, *Holomorphic disks and topological invariants for closed three-manifolds*, *Annals of Mathematics* (2004), 1027–1158.
42. ———, *On knot Floer homology and lens space surgeries*, *Topology* **44** (2005), no. 6, 1281–1300.
43. ———, *An introduction to Heegaard Floer homology*, *Floer homology, gauge theory, and low-dimensional topology* **5** (2006), 3–27.
44. ———, *Holomorphic disks, link invariants and the multi-variable Alexander polynomial*, *Algebraic & Geometric Topology* **8** (2008), no. 2, 615–692.
45. Peter Ozsváth, Zoltán Szabó, and Dylan P Thurston, *Legendrian knots, transverse knots and combinatorial Floer homology*, *Geometry & Topology* **12** (2008), no. 2, 941–980.
46. Peter S Ozsváth and Zoltán Szabó, *Knot Floer homology and rational surgeries*, *Algebraic & Geometric Topology* **11** (2010), no. 1, 1–68.
47. Zoltán Szabó Peter S. Ozsváth, András I. Stipsicz, *Grid homology for knots and links*, vol. 208, American Mathematical Society, *Mathematical Surveys and Monographs*, 2015.
48. Józef H Przytycki and Akira Yasukhara, *Symmetry of links and classification of lens spaces*, *Geometriae Dedicata* **98** (2003), no. 1, 57–61.
49. Jacob Rasmussen, *Floer homology and knot complements*, arXiv preprint math/0306378 (2003).
50. ———, *Lens space surgeries and L-space homology spheres*, arXiv preprint arXiv:0710.2531 (2007).
51. D. Rolfsen, *Knots and Links*, AMS Chelsea Publishing, 2003.
52. Sucharit Sarkar, *Grid diagrams and the Ozsváth-Szabó tau-invariant*, arXiv preprint arXiv:1011.5265 (2010).
53. Sucharit Sarkar and Jiajun Wang, *An algorithm for computing some Heegaard Floer homologies*, arXiv preprint math/0607777 (2006).
54. William P. Thurston, *A norm for the homology of 3-manifolds*, *Memoirs of the American Mathematical Society* (1986).
55. Vladimir Turaev, *Torsion invariants of spinc-structures on 3-manifolds*, *Mathematical Research Letters* **4** (1997), 679–696.
56. ———, *A function on the homology of 3-manifolds*, *Algebraic & Geometric Topology* **7** (2007), no. 1, 135–156.
57. Zhongtao Wu, *On minimal genus problem*, *Proceedings of the Gokova Geometry-Topology Conference* (2015) (2015), 250–264.